INFORMATION TO USERS

This manuscript has been reproduced from the microfilm master. UMI films the text directly from the original or copy submitted. Thus, some thesis and dissertation copies are in typewriter face, while others may be from any type of computer printer.

The quality of this reproduction is dependent upon the quality of the copy submitted. Broken or indistinct print, colored or poor quality illustrations and photographs, print bleedthrough, substandard margins, and improper alignment can adversely affect reproduction.

In the unlikely event that the author did not send UMI a complete manuscript and there are missing pages, these will be noted. Also, if unauthorized copyright material had to be removed, a note will indicate the deletion.

Oversize materials (e.g., maps, drawings, charts) are reproduced by sectioning the original, beginning at the upper left-hand corner and continuing from left to right in equal sections with small overlaps.

Photographs included in the original manuscript have been reproduced xerographically in this copy. Higher quality 6" x 9" black and white photographic prints are available for any photographs or illustrations appearing in this copy for an additional charge. Contact UMI directly to order.

Bell & Howell Information and Learning
300 North Zeeb Road, Ann Arbor, MI 48106-1346 USA
800-521-0600

FACTORS THAT INFLUENCE THE EXPRESSION OF NEUROTRANSMITTER-GATED ION CHANNELS ON DEVELOPING PERIPHERAL NEURONS

by

Madelaine Rosenberg

Department of Physiology
Faculty of Medicine
McGill University
Montreal, Quebec, Canada

September 1998

A thesis submitted to the
Faculty of Graduate Studies and Research
in partial fulfillment
of the requirements for the degree of
Doctor of Philosophy

© Madelaine Rosenberg, 1998

National Library of Canada
Acquisitions and Bibliographic Services
395 Wellington Street
Ottawa ON K1A 0N4
Canada

Bibliothèque nationale du Canada
Acquisitions et services bibliographiques
395, rue Wellington
Ottawa ON K1A 0N4
Canada

Your file Votre reference

Our file Notre reference

The author has granted a non-exclusive licence allowing the National Library of Canada to reproduce, loan, distribute or sell copies of this thesis in microform, paper or electronic formats.

L'auteur a accordé une licence non exclusive permettant à la Bibliothèque nationale du Canada de reproduire, prêter, distribuer ou vendre des copies de cette thèse sous la forme de microfiche/film, de reproduction sur papier ou sur format électronique.

The author retains ownership of the copyright in this thesis. Neither the thesis nor substantial extracts from it may be printed or otherwise reproduced without the author's permission.

L'auteur conserve la propriété du droit d'auteur qui protège cette thèse. Ni la thèse ni des extraits substantiels de celle-ci ne doivent être imprimés ou autrement reproduits sans son autorisation.

0-612-44563-1

Canada

Preface

This thesis includes the text of original papers that have been or will be published, and therefore in accordance to the "Guidelines for Thesis Preparation" from the Faculty of Graduate Studies and Research, the following must be cited:

"Candidates have the option of including, as part of the thesis, the text of one or more papers submitted or to be submitted for publication, or the clearly-duplicated text of one or more published papers. These texts must be bound as an integral part of the thesis.

If this option is chosen, connecting texts that provide logical bridges between the different papers are mandatory. The thesis must be written in such a way that it is more than a mere collection of manuscripts; in other words, results of a series of papers must be integrated.

The thesis must still conform to all other requirements of the "Guidelines for Thesis Preparation". The thesis must include: A Table of Contents, an abstract in English and French, an introduction which clearly states the rationale and objectives of the study, a review of the literature, a final conclusion and summary, and a thorough bibliography or reference list.

Additional material must be provided where appropriate (e.g. in appendices) and in sufficient detail to allow a clear and precise judgment to be made of the importance and originality of the research reported in the thesis.

In the case of manuscripts co-authored by the candidate and others, the candidate is required to make an explicit statement in the thesis as to who contributed to such work and to what extent. Supervisors must attest to the accuracy of such statements at the doctoral oral defense. Since the task of the examiners is made more difficult in these cases, it is in the candidate's interest to make perfectly clear the responsibilities of all the authors of the co-authored papers."

Abstract

Synapse formation involves multiple coordinated events between the presynaptic and the postsynaptic nerve that ultimately results in the expression of the appropriate neurotransmitters at the presynaptic nerve terminal and the matching neurotransmitter receptors on the opposing postsynaptic membrane. For my thesis research, I investigate different aspects of neurotransmitter receptor gene expression, an early step in the process of synaptogenesis. Specifically, I focus on two different neurotransmitter-gated ion channels that are expressed on neonatal rat peripheral neurons: the serotonin 5-HT_3 receptor (5-HT_3R) and the neuronal nicotinic acetylcholine receptor (nAChR).

The 5-HT_3R is expressed on both nodose sensory neurons and sympathetic neurons. However, little is known about 5-HT_3R expression during neonatal development or about the factors that regulate its expression. To investigate 5-HT_3R gene expression, first I examined 5-HT_3R mRNA levels in nodose and sympathetic neurons as they develop *in vivo* and in culture. My results show that 5-HT_3R gene expression is differentially regulated in these two populations of neurons. In addition, I demonstrate that 5-HT_3R gene expression in nodose neurons depends on target innervation and can be modulated by neurotrophins.

Neonatal sympathetic neurons express five different neuronal nAChR subunit genes. One unresolved issue is the contribution of these five subunits to nAChR function. To investigate this issue, I altered the expression of one nAChR subunit gene, α3, using transient transfection procedures. To do this, first I modified and optimized gene transfer procedures for sympathetic neurons, based on recombinant adenovirus vectors. Using this approach, I overexpressed sense and antisense α3 mRNA and investigated how the changes in α3 subunit expression affect ACh-evoked currents on cultured sympathetic neurons. I show that changes in α3 mRNA levels alter the magnitude of ACh-evoked current densities. My results indicate that α3 gene expression is rate-limiting for the assembly and insertion of nAChRs on sympathetic neurons.

Together, my results show that multiple mechanisms influence the expression neurotransmitter-gated ion channel genes on peripheral neurons.

Résumé

La synaptogénèse implique une multitude d'étapes coordonnées qui mène à l'expression appropriée de neurotransmetteurs à la terminaison présynaptique et de leurs récepteurs dans la membrane postsynaptique. Dans ma thèse, j'étudie divers aspects de l'expression des gènes codant pour des récepteurs de neurotransmetteurs, une étape précoce de la synaptogénèse. J'ai concentré mes études sur deux canaux ioniques activés par des neurotransmetteurs qui sont exprimés dans les neurones périphériques chez le rat nouveau-né: le récepteur de la sérotonine 5-HT_3 (5-HT_3R) et le récepteur nicotinique de l'acétylcholine neuronal (nAChR).

Le 5-HT_3R est exprimé dans les neurones sensoriels provenant du ganglion nodose et dans les neurones sympathiques chez le rat nouveau-né et adulte. Cependant, on connaît peu de chose sur l'expression néonatale du 5-HT_3R et sur les facteurs qui régulent son expression. Pour étudier l'expression du 5-HT_3R, j'ai d'abord examiné le niveau d'ARNm du 5-HT_3R exprimé par les neurones nodose et sympathiques lors de leur développement *in vivo* et en culture. Mes résultats montrent que l'expression du gène 5-HT_3R est régulée différemment dans les neurones nodose et sympathiques. De plus, je démontre que l'expression de ce gène dépend de l'innervation post-ganglionnaire et peut être modulée par la présence de facteurs neurotrophiques.

Les neurones sympathiques du rat nouveau-né expriment cinq sous-unités différentes du nAChR neuronal. Un problème non résolu est le rôle de ces cinq sous-unités dans la fonction du nAChR. Pour aborder ce problème, j'ai modifié l'expression d'une de ces sous-unités, α3, par transfections transitoires. Pour accomplir cela, j'ai adapté aux neurones sympathiques des procédures de transfert de gène avec l'aide de vecteurs adénoviraux. En utilisant ces vecteurs, j'ai surexprimé de l'ARNm sens et antisens de la sous-unité α3 dans les neurones sympathiques en culture et j'ai étudié la contribution de celle-ci au courant activé par l'ACh. Je montre que l'altération du niveau d'ARNm α3 conduit à des modifications de la densité du courant activé par l'ACh. De plus, mes résultats indiquent que l'expression du gène α3 est limitante pour l'assemblage et l'insertion des nAChR dans la membrane neuronale. Ensemble, mes résultats démontrent que de multiples mécanismes influencent l'expression des canaux ioniques activés par des neurotransmetteurs.

Contributions to Publications and Results

The manuscript entitled Developing neonatal rat sympathetic and sensory neurons differ in their regulation of 5-HT_3 receptor expression by **Madelaine Rosenberg**, Brigitte Pié and Ellis Cooper, presented in Chapter 2 of this thesis, was published in *The Journal of Neuroscience* 17:6629-6639, 1997. This manuscript was prepared jointly by myself and my supervisor, Dr. Ellis Cooper. I performed all of the experiments presented in this paper except for (a) the mRNA *in situ* hybridization experiments which were carried out by Brigitte Pié and (b) the electrophysiology experiments which were performed by Dr. Cooper.

The results presented in Chapter 3 describe my experiments and results on optimizing gene delivery procedures for rat sympathetic neurons in culture. I initiated the project on recombinant adenoviruses and established the necessary techniques for building recombinant adenovirus vectors in Dr. Cooper's laboratory. I performed all of the experiments presented in this chapter except for the electrophysiology experiments which were carried out by Dr. Cooper and Ali (Pejmun) Haghighi. Some of the results presented in this chapter were published in a joint paper with Dr. Frieda Miller's laboratory (Montreal Neurological Institute, McGill University) entitled Adenovirus-mediated gene transfer of the tumor suppressor, p53, induces apoptosis in postmitotic neurons by R.S. Slack, D.J. Belliveau, **M. Rosenberg**, J. Atwal, H. Lochmuller, R. Aloyz, A. Haghighi, B. Lach, P. Seth, E. Cooper, F.D. Miller, in *The Journal of Cell Biology*, 135:1085-1096, 1996. Our contribution to this manuscript includes the characterization of sympathetic neuron infection efficiencies by recombinant adenovirus vectors, and the electrophysiological characterization of voltage-gated K currents on adenovirus-infected sympathetic neurons.

In Chapter 4 of this thesis, I describe my results on overexpressing neuronal nicotinic acetylcholine receptor (nAChR) subunits in sympathetic neurons using recombinant adenovirus vectors. I performed all of the experiments described in this chapter except for the electrophysiological experiments which were performed by Dr. Cooper.

Contributions to Original Knowledge

For my thesis research, I have investigated the factors that influence the expression of neurotransmitter-gated ion channels on developing peripheral neurons. Specifically, I have studied different aspects of gene expression for neuronal nAChRs and 5-HT_3Rs on neonatal rat sympathetic and sensory neurons.

In the manuscript presented in Chapter 2, I provide the first quantitative investigation of 5-HT_3R mRNA levels in neonatal sensory nodose and sympathetic SCG neurons as they develop *in vivo* and in culture. I demonstrate that 5-HT_3R gene expression in nodose and SCG neurons is differentially regulated. In addition, I show, for the first time, that 5-HT_3R gene expression in nodose neurons depends on target innervation and can be modulated by neurotrophins. Lastly, I show that 5-HT_3R mRNA levels in both SCG and nodose neurons correlate directly with the appearance of 5-HT-evoked current densities.

In Chapter 3, I present my study on optimizing gene delivery procedures for rat sympathetic neurons in culture. First, I show that Ca^{2+}phosphate- and liposome-mediated gene transfer techniques are not efficient methods for transfecting cultured sympathetic neurons. I demonstrate that recombinant adenovirus vectors are efficient gene delivery vehicles for sympathetic neurons. Moreover, I show that adenovirus vectors do not affect sympathetic neuron survival or growth and do not interfere with the expression of endogenous ACh-evoked currents or voltage-gated outward K currents on sympathetic neurons.

Finally, in Chapter 4, I investigate the contribution of specific nAChR subunits to functional nAChRs expressed on the cell surface of neonatal rat sympathetic neurons. For this study, I use adenovirus-mediated gene transfer to alter the expression of α3 subunits. I provide the first demonstration that recombinant adenovirus vectors can be used

augment nAChR subunit expression in neurons. I show that manipulating α3 expression alters the magnitude of ACh-evoked current densities on cultured sympathetic neurons. Together, my results demonstrate that α3 subunits are an important component of the receptors that mediate ACh-evoked currents on cultured sympathetic neurons. Lastly, my results show that recombinant adenovirus vectors are an effective tool for studying protein function in primary cultures of sympathetic neurons. The development of viral vectors opens new avenues for the investigation of multiple cellular and molecular aspects of neuronal function.

Table of Contents

Abbreviations

aa	amino acid
AAV	adeno-associated virus
ACh	acetylcholine
Ad	adenovirus
α-BTX	alpha bungarotoxin
Ara-C	cytosine-arabinofuranoside
β-gal	β-galactosidase
bp	basepair
C-terminus	carboxy terminus
CGN	ciliary ganglion neuron
CNTF	ciliary neurotrophic factor
CNS	central nervous system
Cys	cysteine
E8	embryonic day 8
ER	endoplasmic reticulum
FLAG	artificial peptide epitope
$GABA_AR$	γ-amino butyric acid type A receptor
GFP	green fluorescent protein
GlyR	glycine receptor
HSV	herpes simplex virus
$5\text{-}HT_3R$	5-hydroxytrypamine type 3 receptor
kb	kilobasepair
kDa	kilodalton
M	membrane spanning domain
mAb	monoclonal antibody
nAChR	nicotinic acetylcholine receptor
n-BTX	neuronal bungarotoxin
NMDA	N-methyl-D-aspartate
N-terminus	amino terminus
P1	postnatal day 1
PAGE	polyacrylamide gel electrophoresis
PCR	polymerase chain reaction
PNS	peripheral nervous system
rAAV	recombinant adeno-associated virus
SEM	standard error of the mean
SCG	superior cervical ganglion
SFV	Semliki forest virus
TTX	tetrodotoxin
UTR	untranslated region
X-gal	5-bromo-4-chloro-3-indolyl-β-D-galactoside

Acknowledgments

First and foremost, I wish to thank my mentor and friend, Dr. Ellis Cooper, to whom I owe a lot. Ellis, thank you for teaching me to love science and how to ask the right questions. Thank you for giving me the freedom to try new things and for trusting and believing in my abilities.

I owe a huge thank you to all the members of the "Cooper Lab" who made this lab a great and happy place to learn, work, and play. Andrew, Brigitte, Damian, Isabelle, Paul, Pejmun, and Tom, thanks for all the advice, discussions, and good times. Many thanks to Brigitte for the *in situ* hybridization experiments. I wish to thank Paul for teaching me how to prepare neuronal cultures and how to do RNase protection assays. Tom, thanks for your help in preparing many of my figures. Pejmun, thank you for the oocyte experiments.

I am very grateful to Drs. John Orlowski and John White for their expert molecular biology advice, and for sharing their equipment and reagents. I wish to thank Dr. Phil Branton for his help when I began building recombinant adenoviruses. I am also indebted to Dr. Alvin Shrier for his help, advise, and friendship throughout my studies.

I also wish to thank all the members of Shrier's lab for many helpful discussion, many laughs, and for sharing equipment and reagents.

I am very grateful to my parents, my brother and my parents-in-law for their untiring support and encouragement. Lastly and most importantly, I wish to thank the most important person in my life, Andrew, for so many things. Andrew, thank you for your help, encouragement, and patience.

I will miss this place! Thanks everyone!

Chapter 1

Introduction

Introduction

Neurons communicate with one another at synapses, specialized structures formed between the axon terminal of one neuron and the dendrite of another neuron. To ensure efficient synaptic function, the presynaptic neuron must release neurotransmitters that can be recognized by neurotransmitter receptors in the postsynaptic membrane. During synapse formation, the postsynaptic neuron expresses the appropriate neurotransmitter receptor genes, synthesizes and assembles neurotransmitter receptor subunit proteins, and then targets these receptors to the postsynaptic membrane where they are anchored to the cytoskeleton. Work on nerve-muscle synapses has revealed that these events involve both factors released from the presynaptic nerve as well as intrinsic developmental programs. Little is known, however, about the cellular and molecular mechanisms that govern these processes at nerve-nerve synapses. My long term research goal is to learn more about the various factors and mechanisms that promote the formation and the maintenance of interneuronal synapses.

For my thesis research, I investigate different aspects of neurotransmitter receptor gene expression, an early step in the process of synapse formation. Specifically, I focus on two different neurotransmitter-gated ion channels that are expressed on neonatal rat peripheral neurons: the serotonin 5-HT_3 receptor (5-HT_3R) and the neuronal nicotinic acetylcholine receptor (nAChR). Because rat peripheral neurons express both 5-HT_3Rs and neuronal nAChRs, one of my interests is to compare the mechanisms that influence the gene expression of these two receptors in order to gain a better understanding of neurotransmitter-gated ion channel expression.

Peripheral 5-HT_3Rs modulate many peripheral functions including nociception, gastrointestinal motility, and a variety of reflexes. However, little is known about the expression of 5-HT_3Rs on peripheral neurons during early postnatal development or the

factors that regulate its expression. In the first part of this dissertation, I present my investigation on the factors that influence the expression of 5-HT_3Rs on developing rat sympathetic and sensory neurons.

The second part of my thesis focuses on neuronal nAChRs, the principal mediators of fast synaptic transmission on autonomic ganglia. Sympathetic neurons express several nAChR subunit genes. An unresolved issue is the contribution of specific subunits to the appearance of functional nAChRs on the cell surface. One approach to investigate this problem is to manipulate nAChR subunit gene expression and study how these changes influence the physiological properties of functional receptors. In order to manipulate nAChR gene expression, I adapted and optimized gene transfer techniques for sympathetic neurons, based on adenovirus vectors. I then used recombinant adenoviruses to investigate the contributions of nAChR subunits to the receptors that mediate ACh-evoked currents on neonatal rat sympathetic neurons.

Before describing my results, I review the structure and function of neurotransmitter-gated ion channels and the expression and physiological functions of neuronal nAChRs and 5-HT_3Rs. In addition, I review several current gene transfer techniques and discuss their usefulness as gene delivery methods for neurons.

A) Neurotransmitter-gated ion channels

Neurotransmitter receptors exist in the postsynaptic membrane where they function to bind neurotransmitters released from the presynaptic nerve. The term "receptor" was first coined by Langley, in 1906, in his pioneering studies on the binding of nicotine and curare to a "receptive substance" on muscle cells (Changeux et al., 1984). This "receptive substance" is now known to be the muscle acetylcholine receptor. Over the last 90 years,

there has been an enormous increase in the understanding of the structure and the physiology of neurotransmitter receptors. In general, neurotransmitter receptors can be divided into two broad categories: those that activate G-proteins and second messenger systems, and those that are ion channels. Serotonin 5-HT_3Rs and neuronal nAChRs, on which I focus in my thesis, are of the second type and are referred to as neurotransmitter-gated ion channels.

Neurotransmitter-gated ion channels are ion channels that open rapidly upon agonist binding, allowing the flow of ions across the membrane, and then desensitize or close in the presence of agonist. These channels are highly permeable, typically passing more than 10^4 ions per ms, and are highly selective for either cations or anions (Unwin, 1993). Molecular studies have revealed the existence of a large superfamily of neurotransmitter-gated ion channels that bear a strong homology to one another in their overall structure. Included in this superfamily are: the muscle nAChRs, neuronal nAChRs, 5-HT_3Rs, glycine receptors (GlyRs), and γ-aminobutyric acid A receptors ($GABA_A$Rs). Muscle nAChRs, neuronal nAChRs and 5-HT_3Rs are selective for cations and when activated under normal physiological conditions allow the inward flow of cations, primarily Na^+ or Ca^{2+}, leading to cellular depolarization and excitation. In contrast, $GABA_A$Rs and GlyRs are selective for anions: upon agonist binding these receptors allow the passive flow of Cl^- down its electrochemical gradient into the neuron, thereby hyperpolarizing the neuron's membrane and inhibiting the action of other excitatory stimuli.

Neurotransmitter-gated ion channels share a large number of sequence and structural characteristics. All of these receptors are oligomeric complexes composed of five membrane spanning protein subunits that form a pseudosymetric ring around an aqueous ion channel (Fig. 1.1). They all share a high degree of amino acid sequence similarity, particularly in their membrane spanning domains, and are presumed to have

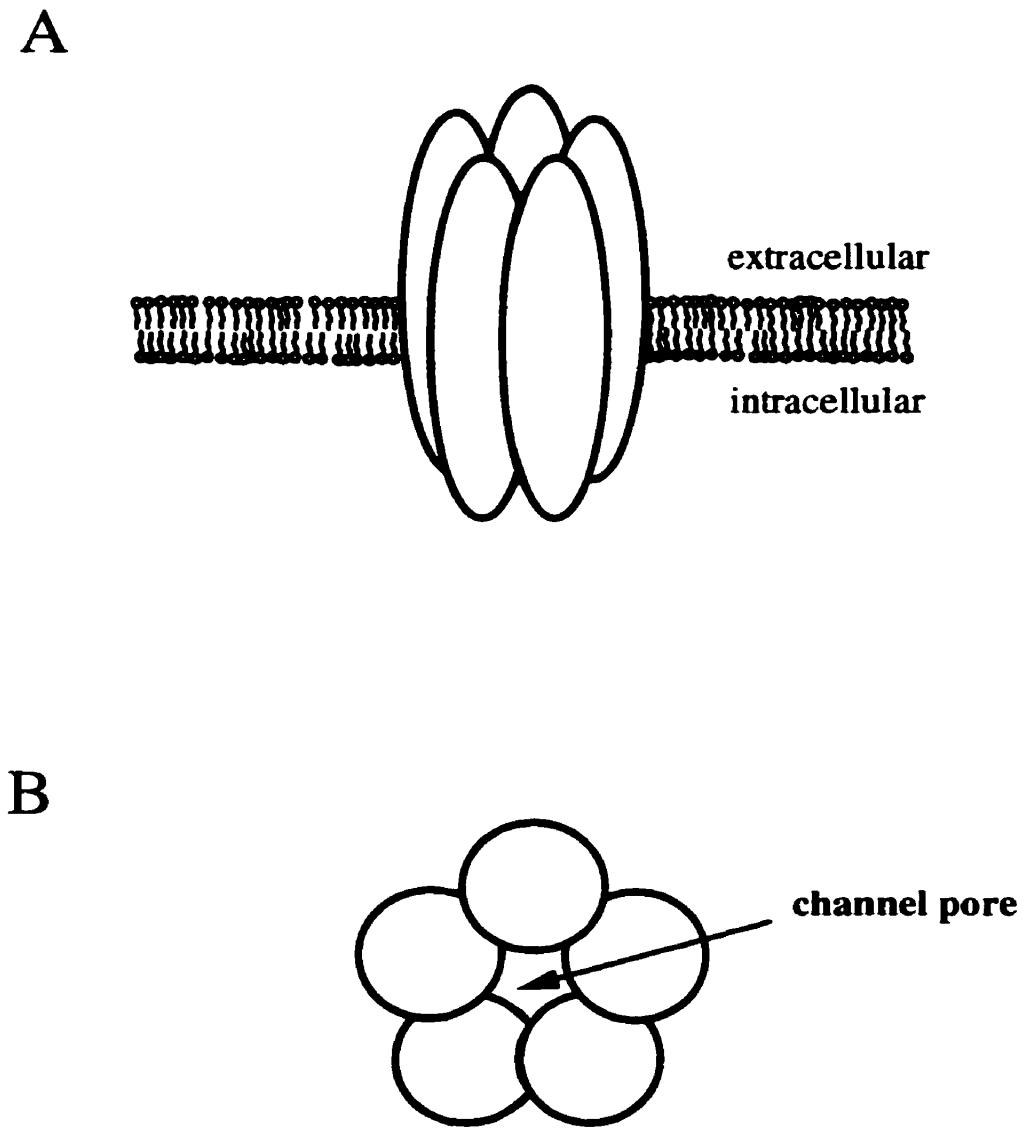

Figure 1.1. Cartoon of a typical neurotransmitter-gated ion channel receptor inserted into the cell membrane. All neurotransmitter-gated ion channels are composed of five membrane spanning protein subunits arranged in a pseudosymetric ring around the channel pore. Neurotransmitter-gated ion channel viewed from ***A,*** side and ***B,*** above.

evolved through gene duplication and divergent evolution from a common ancestor (Le Novère and Changeux, 1993; Ortells and Lunt, 1995).

So far, well over 100 different neurotransmitter-gated ion channel subunit cDNAs have been sequenced from numerous species ranging from nematodes and insects to mammals, revealing a high degree of conservation as well as subunit diversity among family members (Ortells and Lunt, 1995). I have restricted the focus of this introduction to neuronal nAChRs and 5-HT_3Rs. The general principals about these two receptors also apply for $GABA_A$Rs and GlyRs, however, a complete review of $GABA_A$R and GlyR biology is outside the scope of this thesis (for reviews see Whiting et al., 1995, Rajendra et al., 1997; Vannier and Triller, 1997).

Muscle nACh Receptor: the prototype

The muscle nAChR has long served as the prototype of neurotransmitter-gated ion channel receptors because it is the best characterized member of this superfamily. I will briefly review the main structural features of the muscle nAChR to provide a framework for the discussion of the structure of neuronal nAChRs and 5-HT_3Rs, for which much less is known.

Structure of muscle nAChRs subunits

Cloning of nAChR cDNAs

The nAChR was the first neurotransmitter receptor to be isolated and sequenced (Noda et al., 1982; Noda et al., 1983a,b). Its purification and cloning were facilitated by two factors: (1) the existence of high densities of nAChR proteins in the electric organ of

the electric eel (*Electrophorus electricus*), a tissue rich in cholinergic synapses, and (2) the availability of α-bungarotoxin (α-BTX), a neurotoxin from the venom of the snake *Bungarus multicinctus* that binds to and blocks nAChRs with high affinity and specificity (Changeux et al., 1984; Loring and Zigmond, 1988). During the 1970's, biochemical investigations of purified electric organ nAChRs showed that it is composed of five proteins chains: 2 copies of an α protein, and three proteins of different molecular weight called β, γ, and δ (reviewed by Changeux et al., 1984). In 1980, Raftery's group succeeded in microsequencing the first 54 amino acids of the four different nAChR subunits found in the electric organ of the Californian electric ray (*Torpedo Californica*) (Raftery et al., 1980). To their surprise, the four different subunits shared between 35-50% sequence homology, suggesting that the four subunits were related evolutionarily (Raftery et al., 1980). Armed with new molecular biology techniques, Numa and colleagues cloned and sequenced the cDNA sequences coding for all four *T. Californica* nAChR subunits in 1982-83 (Noda et al., 1982; Noda et al., 1983a,b).

Through low stringency screens for homologous sequences to *Torpedo* nAChRs, the cDNAs of the four muscle nAChR subunits were cloned from many species including rat, mouse, chicken, bovine, and *Xenopus* (Ortells and Lunt, 1993). An additional subunit, ε, was identified in vertebrates; this subunit is expressed during embryonic development and apparently replaces the γ subunit in the nAChR pentamer (reviewed in Murray et al., 1995). In a given species, the amino acid sequences of the different nAChR cDNAs share ≈ 30% sequence identity to one another (Lukas, 1995). When one compares the homology of a given subunit in different species, significantly higher homologies are found (Boulter et al., 1985, 1986b).

Analysis of the genomic structures of these genes in several vertebrate species including human, chick and mouse, reveals that the overall exon organization of muscle nAChR subunit genes differ from one another: α subunit genes contain 9 protein coding exons, β subunit genes contain 11 exons, while γ, ε , and δ subunit genes each contain 12

exons (reviewed in Le Novère and Changeux, 1995). Of the five genes, γ, ε , and δ share the highest sequence identity ranging from 42-52% (Lukas, 1995) and contain an identical genomic organization (Buoanno et al., 1989). Moreover, the γ and δ subunit genes are physically linked on the same chromosome; the ε subunit is not found on the same chromosome as these two genes (reviewed in Buoanno et al., 1989; Beeson et al., 1993).

Primary structure

The primary structures of the muscle nAChR subunits have been deduced from hydropathy analyses of the predicted amino acid sequences, and from several mutational and biochemical studies (Karlin and Akabas, 1995). Each subunit is comprised of a cleavable signal sequence, a large extracellular N-terminal domain, four membrane spanning domains (termed M1-M4), and a short extracellular C-terminal domain (Fig. 1.2). The mature subunits range from ≈430-520 amino acids in length (Le Novère and Changeux, 1997). A conserved 15 amino acid loop formed by disulfide bonding between two cysteine residues is found in the N-terminal domain of all muscle nAChR subunits and is conserved in all neurotransmitter-gated ion channel subunits. Lastly, a long intracellular loop is found between M3 and M4 and is the least conserved domain among the different subunits. In several subunits, this domain contains phosphorylation consensus sequences for protein kinases (Lindstrom, 1995), suggesting that it may be involved in intracellular signaling, modulation of receptor function, or receptor anchoring.

Traditionally, the four membrane spanning domains have been thought to be α-helices (Ortells and Lunt, 1995). However, recent studies using electron microscopy, cysteine scanning mutagenesis, and Fourier-transformation infrared spectroscopy, indicate that only the M2 domain is a true α-helix and that the other membrane spanning

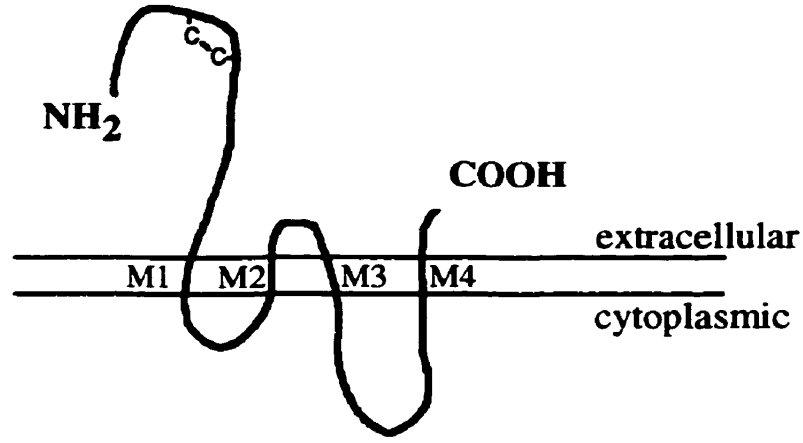

Figure 1.2. Predicted membrane topology of muscle nAChR subunits. Each subunit contains a large extracellular N-terminal domain, four membrane spanning domains, termed M1-M4, and a short extracellular C-terminal domain. Similar topologies are predicted for all neurotransmitter-gated ion channel subunits.

domains are in part non-helical and possibly form β-sheets (Unwin, 1993b, 1995; Akabas et al., 1994, 1995; Görne-Tschelnokow et al., 1994).

The ACh binding site

Photoaffinity labeling and mutagenesis studies show that the ACh-binding site is near two cysteine residues at position 192 and 193 on the extracellular N-terminal domain of the α subunit. These cysteines are critical for ligand binding and are conserved in all species of muscle α subunits studied so far (Lindstrom, 1995). The ACh-binding site also involves additional residues within the N-terminus as well as the interface between the α subunit and its neighboring subunit (Czajkowski and Karlin, 1991; Lindstrom, 1995).

The nAChR pore

The M2 domain of each nAChR subunit in the pentamer is believed to line the pore of the ion channel (Fig. 1.3)(Unwin, 1989; Unwin, 1993a). This domain, which is the most highly conserved domain among the different neurotransmitter-gated ion channel subunits, has a number of features that give insight into how the channel works. Firstly, evidence from combined mutagenesis and single channel recording experiments indicates that three critical sets of negatively charged amino acids at either end of the M2 domain function as ion selectivity filters (Fig. 1.3B; Imoto et al., 1988). These residues are conserved at the same position in all five nAChR subunits: a Glu residue at the extracellular end of M2 and an Asp and a Glu residue on the cytoplasmic end of M2 (Karlin and Akabas, 1995). These residues are postulated to form negatively charged rings around the entrances of the channel pore that function to draw positively charged ions into the pore (Imoto et al., 1988; Karlin and Akabas, 1995).

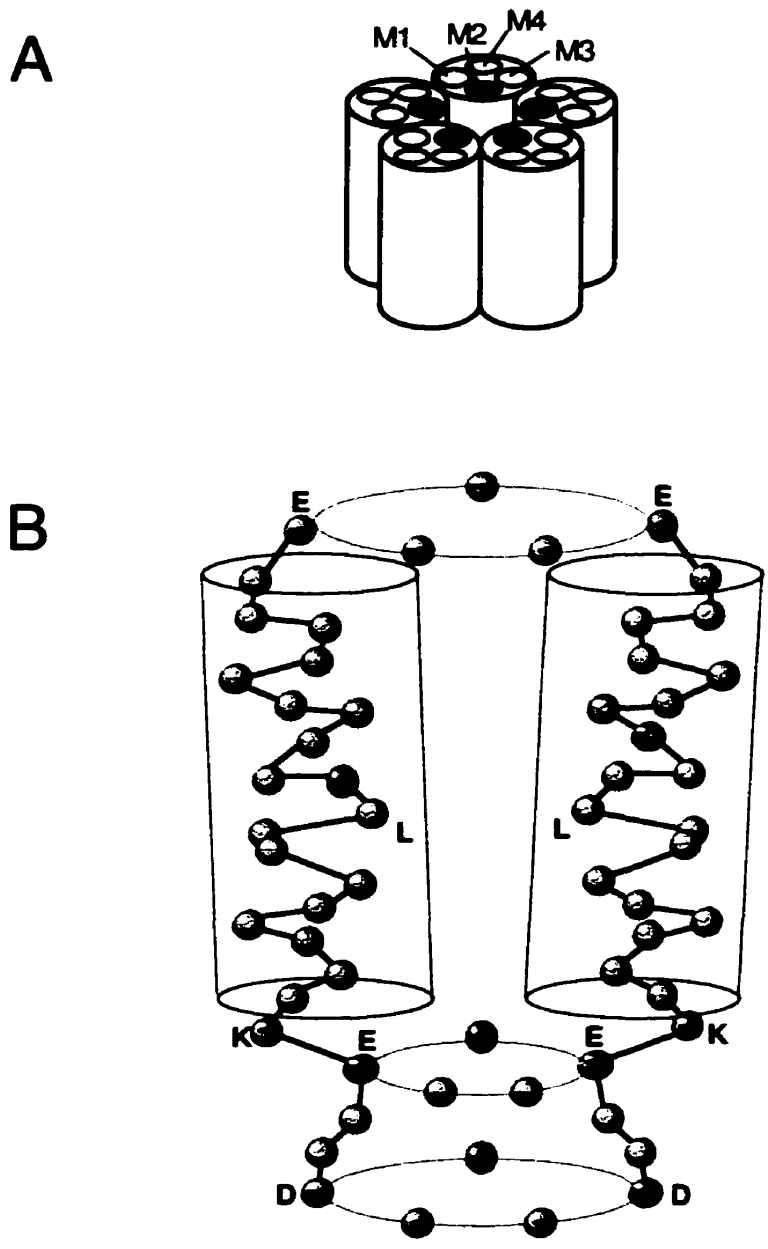

Figure 1.3. Cartoon depicting the M2 domain of the muscle nAChR. ***A***, The M2 domain lines the pore of the channel. ***B***, Image showing some features of the M2 domain: α-helical structure; the charged amino acid residues that may form negatively charged rings at both entrances of the pore; and the leucine residues that may form the channel gate.

Secondly, the M2 contains several serine and threonine residues that are thought to line the side of the α-helix that faces the lumen of the aqueous pore (Guy and Hucho, 1987; Lindstrom, 1995). The hydroxyl sidechains of these residues may provide a hydrophilic environment that could facilitate the passage of hydrated ions through the channel (Lindstrom, 1995).

Lastly, the location of the channel gate, which either stops or allows the flow of ions across the pore, is controversial. Evidence from electron microscopy experiments by Unwin suggests that the narrowest point in the pore is formed by a conserved leucine residue found roughly in the middle of the M2 domain in all nAChR subunits (Unwin, 1993a,b). This uncharged leucine is thought to form a kink in the α-helical structure of M2 that would rotate to the side during channel opening (Unwin, 1993a,b). However, based on their results using cysteine scanning mutagenesis to detect exposed residues in the channel pore, Karlin and colleagues suggest that the narrowest point of the channel and the channel gate are located much closer to the intracellular end of the pore (Karlin and Akabas, 1995).

While much is known about the ACh-binding pocket and the channel pore, less is known about how ligand-binding leads to channel gating. Channel opening, desensitization and closing presumably involve complex conformational changes in all five subunits of the receptor (for a review on neurotransmitter-gated ion channel gating, see Karlin and Akabas, 1995).

B) Neuronal nAChRs

Nicotinic AChRs are widely expressed on peripheral and central neurons. Classical studies have demonstrated that nAChRs are the principal mediators of fast synaptic

transmission on autonomic ganglia and on adrenal chromaffin cells (Langley and Anderson, 1892; Paton and Zaimis, 1952; Dale, 1954). Recent studies show that most nAChRs in the CNS are located presynaptically (Role and Berg, 1996). For a long time, it was thought that central neurons did not express nAChRs because fast nicotinic synapses are generally absent in the CNS (Role and Berg, 1996). The widespread expression of nAChRs on central neurons was discovered only in the mid 1980's with the development of high specific activity [^{3}H]nicotine which was used to identify nAChRs in brain tissues (Clarke, 1995).

Cloning and Characterization of Neuronal nAChRs

While nAChRs expressed on neurons resemble those found on muscle in a number of properties such as ion selectivity and gating, they differ in their ion permeabilities and agonist and antagonist potencies (Sargent, 1993). Experiments by Patrick and Stallcup (1977a,b) showed that antibodies against muscle nAChRs could block neuronal-type nAChRs on cells from the sympatho-adrenal PC12 cell line, indicating that some structural similarities exist between neuronal and muscle nAChRs. This observation plus the finding that muscle nAChR subunits share a high degree of sequence homology among themselves suggested to researchers that it may be possible to isolate neuronal nAChR cDNAs using low stringency cDNA library screening with muscle nAChR cDNA probes (Sargent, 1993).

Prior to the cloning of neuronal nAChRs, it was generally believed that there were only two types of nAChRs: one in muscle and one in the nervous system. Therefore, researchers were surprised by the results from molecular cloning which identified eleven vertebrate genes that encode distinct neuronal nAChR subunits: eight α subunits (α2-α9) and three β (β2-β4) (Sargent, 1993; Elgoyhen et al., 1994). The chick and rat nAChR

subunits are predicted to be between 424-600 amino acids in length (Sargent, 1993; Le Novère and Changeux, 1997). All of these subunits have a similar primary structure to muscle nAChR subunits with an extracellular N-terminal domain, four membrane spanning domains and an extracellular C-terminal domain. All of the α subunits possess adjacent cysteine residues equivalent to those found at amino acid positions 192 and 193 of the muscle α subunit (α1); they are similarly postulated to form part of ACh-binding pocket (Sargent, 1993). The β subunits lack these cysteines but retain numerous other muscle nAChR features (Sargent, 1993).

Genomic analyses of neuronal nAChR subunit genes in several species reveal that these genes share a similar exon organization that differs from those of muscle nAChRs. The α2-α6 and β2-β4 subunit genes all contain 6 protein coding exons (reviewed in Le Novère and Changeux, 1995). An exception is the α7 gene which contains 10 exons; the genomic structure of α8 and α9 are not known (Le Novère and Changeux, 1995).

Neuronal nAChRs are pentamers

In 1991, using very different approaches, two research groups demonstrated that neuronal nAChRs are pentamers. Cooper and colleagues co-expressed different chick α4 and β2 conductance mutants with wild-type α4 and β2 nAChR subunits in *Xenopus* oocytes (Cooper et al., 1991). This gave rise receptors with wild-type, mutant, and hybrid conductances. Using single-channel analysis, they deduced that neuronal nAChRs are pentamers composed of two α and three β subunits. Lindstrom's team obtained identical results by measuring the subunit stoichiometry of assembled neuronal nAChRs (Anand et al., 1991). They labeled chick α4 and β2 nAChR subunits expressed in *X.* oocytes with ^{35}S-methionine, quantified the amount of radioactivity of individual subunits in

assembled receptors, and determined that nAChRs are pentamers composed of two α and three β subunits.

Diversity of nAChR subtypes

The discovery of such a large number of different subunits suggested that different subunits may co-assemble to form a large diversity of different receptor subtypes. Indeed, expression studies in *X.* oocytes revealed that numerous subunit combinations can form functional nAChRs but that there are some constraints (Sargent, 1993). Specifically, pair-wise combinations of either α2, α3, α4 with either β2 or β4 are sufficient to produce ACh-gated ion channels in *X.* oocytes (Sargent, 1993). However, when expressed alone, none of these subunits gives rise to functional receptors (Sargent, 1993). In *X.* oocytes, the α5 subunit does not form functional receptors when expressed pair-wise with any of the other subunits (Sargent, 1993). However, when co-expressed with α3 and β4, α5 appears to co-assemble into functional receptors (Ramirez-Latorre et al., 1996; Fucile et al., 1997; Sivilotti et al., 1997). Such complex subunit combinations with more than one type of α or β subunit per receptor can form functional receptors in heterologous systems (Colquhoun et al., 1993; Ramirez-Latorre et al, 1996; Forsayeth and Kobrin, 1997; Sivilotti et al., 1997) and likely exist *in vivo* (Conroy et al., 1992; Role and Berg, 1996).

The α7, α8, and α9 subunits differ from the other neuronal nAChR subunits in that they do not co-assemble with β subunits but rather form homomeric receptors when expressed in *X.* oocytes (Sargent, 1993). These three subunits are quite distantly related from all other nAChRs subunits, each having less than 40% sequence identity with all other nAChRs; however they have high identity among themselves.

α-BTX-sensitive and -insensitive nAChR subtypes

The nAChRs formed by different subunit combinations can be divided into two classes based on their sensitivity to the neurotoxin α-bungarotoxin (α-BTX), one of the best known antagonists of muscle nAChRs that also blocks some but not all neuronal nAChRs (Loring and Zigmond, 1984; Role and Berg, 1996). The α-BTX-sensitive receptors contain α7, αδ, or α9 subunits. Of these receptors, α7 is expressed at the highest levels and forms the majority of α-BTX-binding sites in the peripheral nervous system (PNS) and central nervous system (CNS) (Role and Berg; 1996). Less is known about α8 and α9 subunits. So far, α8 subunits have been found only in chick brain where they either form homomeric receptors or are associated with α7 subunits (Gotti et al., 1994). α9 expression is absent from the CNS and is found primarily in rat cochlear hair cells and some endocrine cells (Elgoyhen et al., 1994).

In contrast, receptors formed by combinations of α2, α3, α4, α5, β2, and β4 are insensitive to α-BTX but are blocked by neuronal bungarotoxin (n-BTX), a very minor component of the same snake venom from which α-BTX is purified (Luetje et al., 1990; Sargent, 1993). These subunits are all expressed in the PNS and CNS with the exception of α2 which is found only in the CNS (Wada et al., 1989; Daubas et al., 1990; McGehee and Role, 1995).

α6 and β3: orphan subunits

Lastly, α6 and β3 are orphan subunits that have been largely ignored. They do not assemble with other subunits when expressed in pair-wise combinations in *X.* oocytes (Sargent, 1993). However, chick and rat α6 subunits can form functional heteromeric nAChR when expressed with human β4 in *X.* oocytes (Gerzanich et al., 1997) while β3 co-assembles into functional receptors when co-expressed with α4, β2, and β4 subunits in *X.* oocytes (Forsayeth and Kobrin, 1997). The functional roles of α6 and β3 are unclear.

Physiological Significance of nAChR Subtype Diversity

There is ample evidence that ACh-gated channels expressed on different neurons are physiologically distinct: they differ in their kinetics, ion permeability, pharmacological profiles and in their cellular and subcellular localization (see below; McGehee and Role, 1995; Role and Berg, 1996). It is probable that different receptor subtypes underlie these differences. The existence of a large diversity of nAChR subtypes therefore has important functional implications. For example, expression studies in *X.* oocytes show that receptors with different subunit combinations have different pharmacological properties and disensitization kinetics (Sargent, 1993). In addition, different receptor subtypes are likely to be targeted to different locations in the neurons. Therefore, during synaptogenesis and in mature neurons, there is a large potential to modulate receptor function by altering subunit expression which in turn may alter the subunit composition of nAChRs.

Two different approaches have been used to understand the functional relevance of nAChR subtype diversity. One approach has focused on characterizing the regulation of nAChR gene transcription in order to understand the different factors that govern subunit expression. Another approach has been to study the expression patterns and physiological functions of different receptor subunits.

a) Transcriptional Regulation of nAChR Gene Expression

Regulatory elements of the β4, α3 and α5 nAChR genes

The genes coding for the subunits α3, α5, and β4 form a tightly linked gene cluster in both mammals and birds (Lukas, 1995). In mouse and human, the cluster is found on

syntenic regions of chromosome 9 and 15 respectively (Bessis et al., 1990; Eng et al., 1991; Anand and Lindstrom, 1992). While the chromosome locations of this cluster in chick and rat have not been determined (Anand and Lindstrom, 1992), in these two species, the cluster is known to span approximately 60 kilobases and is arranged in the following order: β4→ α3→ α5← (Boulter et al., 1990; Couturier et al., 1990b). This curious genomic organization suggests that these three genes may have arisen through tandem gene duplication and that their expression may be co-regulated (Boulter et al., 1990). Indeed, there is ample evidence that α3, α5 and β4 are co-expressed in many neurons including autonomic neurons (Mandelzys et al., 1994; Conroy and Berg, 1995), however the expression of these three genes does not always overlap (Sargent, 1993). One likely explanation is that these genes may each have their own transcriptional regulation but share some common regulatory features that are active in specific cellular and developmental contexts (Du et al., 1997).

The transcriptional regulatory elements that govern the expression of this gene cluster are currently being dissected. So far, in the promoter region of the rat β4 gene, researchers have found a binding site for each of the transcription factors Sp1, Sp3, and AP1 (Bigger et al., 1996; 1997), and a novel regulatory element that binds to the transcription factor Purα (Du et al., 1997). Analysis of the α3 promoter region reveals numerous potential transcription factor consensus sequences (Boyd, 1994; Yang et al., 1994; Yang et al., 1995); only Sp1, the POU domain factors SCIP/Tst-1 and Brn-3a, have been shown to drive α3 promoter activity *in vitro* (Yang et al., 1994; 1995; Milton et al., 1996). So far, Sp1-binding sites are the only identified common regulatory elements for both β4 and α3 that have been concretely shown to be important for transcription of these two genes (Du et al., 1997). Interestingly, a novel neural specific α3 gene enhancer has been found in the 3'-untranslated region of the β4 gene (McDonough and Deneris, 1997). The location of this enhancer may serve as selective pressure to ensure linkage of these two genes (McDonough and Deneris, 1997).

Regulatory elements of other nAChR genes

The promoters of several other neuronal nAChR genes are also in the process of being characterized. Regulation of chick α2 gene expression involves a silencer element found within its promoter (Bessis et al., 1993) and the POU homeodomain transcription factor Brn-3b (Milton et al., 1995). A functional E-box, a repressor element, and a neuron-restrictive silencer element (NRSE) appear to regulate β2 promoter activity (Bessis et al., 1995; 1997). A potential Sp1-binding site is also found in the β2 promoter (Bessis et al., 1995). Lastly, promoter analysis of the bovine α7 gene reveals the existence of three potential binding sites for each Sp1 and Egr-1, one for Myc-Max, and one E-box (Campos-Caro et al., 1997; Criado et al., 1997). In addition, it has been shown that Egr-1-binding is important for α7 transcriptional activation in adrenal chromaffin cells and neural cells lines (Campos-Caro et al., 1997; Criado et al., 1997). The significance of the presence of potential Sp1-binding sites in several nAChR genes is not clear. Because the Sp1 transcription factor is expressed ubiquitously and because Sp1 consensus sites are found in numerous different genes, additional elements must be involved in nAChR gene expression (Yang et al., 1995).

b) Expression and Physiological Function of neuronal nAChRs

Another approach to investigate the functional implications of neuronal nAChR diversity is to determine the expression patterns of specific subunits and their contribution to nAChR functions. It is clear that neurons in the CNS and PNS express a variety of ACh-gated channels that differ in their kinetics, pharmacological profiles and in both their cellular and subcellular localization (Role and Berg, 1996). The exact subunit composition of most nAChR receptors expressed on neurons has not been clearly established. Numerous attempts to match the electrophysiological and pharmacological

properties of native nAChRs with specific combinations of nAChR subunits expressed in heterologous systems have failed (Sargent, 1993; Silviotti and Colquhoun, 1995). The reasons for this failure are unclear. One possibility is that nAChR subunits expressed on neurons may consist of subunit combinations not yet tested in *X.* oocytes (Sargent, 1993). Alternatively, the *X.* oocyte expression system may impart different postranslational modifications to nAChR subunits that make pharmacological and electrophysiological comparisons difficult (Sargent, 1993).

Over the last decade, much progress have been made in understanding the expression patterns of nAChR subunits in the CNS and the PNS which has helped to narrow down the number of possible receptor subtypes that are expressed on different populations of neurons. However, in many cases, it is not known whether all cells in a given neuronal population express the same subunits or if certain subunits are expressed by a subset of neurons within the population.

i) Central nAChRs

There are several reports that document fast synaptic signaling by central nAChRs (Elgoyhen et al., 1994; Sivilotti and Colquhoun, 1995; Zhang et al., 1993; Roerig et al., 1997). However, the majority of nAChRs in the CNS do not appear to mediate synaptic transmission directly (Clarke, 1993; Role and Berg, 1996). Rather, emerging evidence strongly suggests that the principal function of central neuronal nAChRs is to modulate neurotransmitter release at presynaptic sites (Role and Berg, 1996; Wonnacott, 1997).

Support for this hypothesis comes from several lines of evidence. Neuronal nAChRs are found on the nerve terminals of many central neurons including terminals in the retinal tectum, dopaminergic terminals in the striatum, in thalamic terminals in the

cortex and in medial-habenula terminals in the interpenduncular nucleus (reviewed in Léna and Changeux, 1997). In addition, nicotinic agonists have been shown to stimulate the release of various neurotransmitters from synaptosomes prepared from different CNS regions (reviewed in Wonnacott et al., 1989).

Because neuronal nAChRs are highly permeable to Ca^{2+}, their activation at presynaptic sites likely leads to increased intracellular Ca^{2+} in the terminals that in turn may enhance neurotransmitter release and synaptic transmission (Role and Berg, 1996). In particular, α7 homomeric channels are far more Ca^{2+} permeable than other nAChRs or even N-methyl-D-aspartate (NMDA) receptors and can provide a route of Ca^{2+} entry at normal resting potentials or even at hyperpolarized potentials (Role and Berg, 1996). Several recent studies demonstrate that nicotine acting on presynaptic sites can enhance synaptic transmission and neurotransmitter release on a variety of CNS neurons (McGehee et al., 1995; Alkondon et al., 1996; Gray et al., 1996; Léna and Changeux, 1997). In the absence of external Ca^{2+}, nicotine induced synaptic enhancement does not occur, indicating that Ca^{2+} influx through presynaptic nAChRs is essential to stimulate or facilitate neurotransmitter release (McGehee et al., 1995).

Distribution of neuronal nAChR subunits in the CNS

All neuronal nAChR subunits are expressed in the vertebrate CNS except for α8 which is found only in the chick CNS and α9 whose expression is limited to cochlear hair cells (Sargent, 1993; Elgoyhen et al., 1994). By far, β2 is the most widely expressed subunit and is detected in most parts of the brain (Sargent, 1993). α4 expression correlates with that of β2 in many areas; however, not all neurons that express β2 also express α4 (Sargent, 1993). α7 is expressed in many regions of the brain with high levels found in the cerebellum and the sensory and motor nuclei of the brain stem (Del Toro et al., 1994). In contrast, the expression of α2, α3, α6, β3 and β4 is more restricted: α2

subunits are found uniquely in the interpenduncular nucleus in mammals and in the lateral spiriform nucleus in the chick, α3 and α6 appear to have a similar distribution and are found in the thalamus and parts of the brain stem, while β3 and β4 appear to be expressed mainly in the striatum and cerebellum (Wada et al., 1989; Lamar et al., 1990; Sargent, 1993; Hernandez et al., 1995; Morley and Happes, 1995; Forsayeth and Kobrin, 1997; Gerzanich et al., 1997). Extensive expression of multiple subunits is found in various regions, suggesting that more than one nAChR subtype may be expressed on certain neurons (Wada et al., 1989). Little is known, however, about the distribution of these subunits within specific nuclei or whether all cells within a nuclei express the same subunits.

The chick lateral spiriform nucleus

The difficulty in deciphering the subunit composition of nAChRs expressed by neurons within individual CNS nuclei is well exemplified by studies on the chick lateral spiriform nucleus (SpL), a discrete population of thalamic cells that receive cholinergic innervation from the basal ganglia and project to the optic tectum (Reiner et al., 1982; Sorrenson et al., 1989). Approximately 70% of late embryonic SpL neurons display immunoreactivity for the subunits α2, α5 and β2 while an additional 20% express only α5 and β2 (Ullian and Sargent, 1995). An overlapping subset of these chick neurons express α-BTX-binding sites with 20% and 15% positive for α7 and α8 immunoreactivity respectively (Ullian ant Sargent, 1995). However, α5 is never found in the same cells as α8 while α5 is co-expressed with α7 in some cells but not in others. This complex pattern of nAChRs subunit expression suggests that multiple receptor subtypes are likely to exist in these neurons.

Physiological roles of CNS receptors

To learn more about the physiological functions of CNS nAChRs, researchers have focused on two major receptor species that are found on central neurons: the α4β2-containing receptor that binds nicotine and ACh with high affinity and is not blocked by α-BTX, and the α7-containing receptor that is sensitive to α-BTX but has a much lower affinity for nicotine and ACh (Role and Berg, 1996). Using [^{3}H]nicotine, [^{3}H]ACh, and [^{125}I]α-BTX, Clarke et al. (1985) showed that high affinity nicotine- and ACh-binding sites are distinct from α-BTX-binding sites, indicating that the expression of these two receptor subtypes does not generally overlap. These findings are corroborated by immunostaining experiments that show that nAChRs recognized by anti-α7 antibodies are distinct from those recognized by anti-β2 antibodies (Britto et al., 1992).

The α4β2 nAChR and nicotine addiction

The most abundant nAChR species in the CNS is composed of α4 and β2 subunits (Role and Berg, 1996) and is found at high levels in the thalamus and at lower levels in the basal ganglia and brain stem (Hill et al., 1993). This receptor forms the high affinity nicotine-binding site in rats, chickens and humans (Role and Berg, 1996). Its interactions with nicotine are responsible for our pathological addition to smoking tobacco products. Nicotine is a stimulant that lowers anxiety, provides mild analgesia, and helps to acquire and retain short term memories (Role and Berg, 1996). Using mice lacking the β2 subunit, Changeux's laboratory showed that β2 subunits are an integral part of the brain's high affinity nicotine-binding sites (Picciotto et al., 1995). These β2 "knockout" mice lack the high affinity nicotine-binding sites, but have normal mRNA levels for all other nAChR subunits. Surprisingly, these mice are normal in all aspects except they are insensitive to nicotine and do not exhibit nicotine induced increases in learning in

passive-avoidance tests (Picciotto et al., 1995). Interestingly, chronic exposure to nicotine, such as in heavy smoking, causes an increase in α4β2 receptors that is not due to increased mRNA expression but rather to a slowdown in receptor turnover at the cell surface (Flores et al., 1992; Marks et al., 1992; Peng et al., 1994).

Recently, Changeux and colleagues showed that nicotine acting on presynaptic β2 nAChRs stimulates the release of dopamine from the mesolimbic dopamine system (Picciotto et al., 1998). Because dopamine release from the mesolimbic dopamine system mediates the reinforcing properties of drugs of abuse such as cocaine, ethanol, amphetamines and nicotine (Koob, 1992), this study directly implicates α4β2 receptors in nicotine addiction.

The α7-containing nAChR

The second major nAChR subtype found in the CNS is an α7-containing receptor. This receptor accounts for most of the α-BTX-binding sites in the brain (Role and Berg, 1996). Recent reports show that presynaptic α7-containing receptors can enhance synaptic transmission. The first demonstration was provided by Role and colleagues who showed that presynaptic α-BTX-sensitive nAChRs can enhance glutaminergic synaptic transmission in medial habenula-interpenduncular system (McGehee et al., 1995). Dani's team recently reported similar α-BTX-sensitive nicotine enhancement of synaptic activity among cultured neonatal rat hippocampal neurons (Gray et al., 1996).

Mice lacking the α7 subunit have been generated, and are viable and anatomically normal (Orr-Urtreger et al., 1997). They show no signs of neurological dysfunction, have normal levels of high-affinity nicotine-binding sites and, as expected, lack high-affinity α-BTX-binding sites. It is hoped that these α7 knockouts will help to define the functional role of α7 nAChRs in both the CNS and PNS (Orr-Urtreger et al., 1997).

Other minor nAChR species also exist in the CNS such as α3β4, α4β2α5, and α7α8 (Wada et al., 1989; Sargent, 1993; Lindstrom et al., 1995; Conroy and Berg, 1998). The pattern of nAChR subunit expression in the CNS reveals that most neurons that do express nAChRs are likely to express more than just one or two types of subunits (Sargent, 1993). However, deciphering the exact composition of nAChRs expressed by central neurons has been hampered by the complex structures and circuitry of the CNS.

ii) Peripheral nAChRs

Because of the complexity of determining the subunit composition of nAChRs species on CNS neurons, researchers have turned to simpler and better defined systems in the periphery to investigate the regulation of neuronal nAChR expression. Neuronal nAChRs are the principal mediators of synaptic transmission in both sympathetic and parasympathetic ganglia and as such have been studied on many different autonomic ganglia in rats, cats, chickens, mice, and frogs. Two well developed models for investigating peripheral neuronal nAChRs are the chick parasympathetic ciliary ganglion neuron (CGN) and the rat sympathetic superior cervical ganglion (SCG) neuron.

Chick Parasympathetic Neurons

The chick parasympathetic ciliary ganglion contains two types of neurons: ciliary neurons that innervate muscle cells in the iris and ciliary body, and choroid neurons that innervate muscles in the choroid layer of the eye; both populations express α-BTX-insensitive and α-BTX-sensitive receptors (Jacob and Berg, 1983; Jacob et al., 1984;

Boyd et al., 1991). The α-BTX-insensitive nAChRs mediate synaptic transmission through the ciliary ganglion (Jacob et al., 1984; Halvorsen and Berg, 1986; Loring and Zigmond, 1987). These receptors can be identified by their binding to mAb35, a monoclonal antibody raised originally against electric eel nAChRs (Jacob et al., 1984; Smith et al., 1985, 1986; Halvorsen and Berg, 1986). mAb35 recognizes neuronal nAChRs containing α5 subunits and has been used extensively to characterize synaptic nAChRs in CGNs (Conroy et al., 1992; Vernallis et al., 1993). Several reports show that most mAb35 nAChRs are found at synaptic sites and occasionally on pseudodendrites, small processes adjacent to synaptic sites (Jacob et al., 1984; Jacob and Berg, 1983; Loring and Zigmond, 1987; Jacob, 1991). However, recent results of a detailed study by Wilson Horch and Sargent (1995) indicate that most surface mAb35-binding sites are in fact perisynaptic. Additional evidence indicates that a large intracellular pool of mAb35 nAChRs exists and is several fold larger than the population of surface receptors (Jacob and Berg, 1987; Margiotta et al., 1987; Stollberg and Berg, 1987). In contrast, the α-BTX-sensitive receptor is found extrasynaptically (Loring and Zigmond, 1987), more precisely at perisynaptic sites (Wilson Horch and Sargent, 1995) and does not bind mAb35 (Jacob and Berg, 1983; Smith et al., 1985; Vijayaraghavan et al., 1990).

CGNs express five nAChR subunits

Ciliary ganglion neurons express five nAChR subunit transcripts: α3, α5, α7, β2 and β4 (Boyd et al., 1988; Corriveau and Berg, 1993). The most abundant subunit mRNA is α7 and it is expressed at levels that are 2 fold higher than α3 and 6-9 fold higher than α5, β2, β4 in embryonic day 18 (E18) neurons (Corriveau and Berg, 1993). The synaptic-type nAChRs on CGNs are thought to be composed of the subunits α3, α5, β4 and possibly β2 (Role and Berg, 1996). The role of the β2 subunit is unclear as its mRNA

levels are comparable to those of α5 and β4, but it is found in only 20% of synaptic receptors (Corriveau and Berg, 1993; Conroy and Berg, 1995). Most ciliary and choroid neurons co-express α3, α5, β2, β4 and α7 gene products indicating that most neurons express both classes of neuronal nAChRs, the α-BTX-sensitive and α-BTX-insensitive nAChRs (Corriveau and Berg, 1993; Vernallis et al., 1993; Conroy and Berg, 1995).

The α-BTX receptor contains the α7 gene product but not α3, α5, β2, or β4 subunits (Vernallis et al., 1993). Berg and colleagues provided the first demonstration of α-BTX-sensitive ACh-evoked currents on peripheral neurons using an ultra-rapid method of agonist application (Zhang et al., 1994): this current activates and desensitizes much more rapidly than α-BTX-insensitive currents. Recently, Sargent's laboratory has shown that synaptic transmission through the ciliary ganglion may be mediated, in part, by α-BTX-sensitive nAChRs (Ullian et al., 1997). Additional evidence reveals that α7-containing receptors are also found on the presynaptic nerve terminals of accessory motor neurons that innervate ciliary neurons; their presynaptic localization suggests that α7-containing receptors may serve to modulate transmitter release (Coggan et al., 1997).

Changes in nAChR subunit expression during CGN development

Neuronal nAChR subunit expression is developmentally regulated in CGNs. Traditionally, neuronal nAChRs have been studied on CGNs between the embryonic stages E8-9 when synapse formation begins and stages E11-18, mid-to-late embryonic stages when the synapses are maturing (Landmesser and Pilar, 1972). At E8, α3 and α7 transcripts are expressed at modest levels while those of α5, β2, β4 are barely detectable (Corriveau and Berg, 1993). Between E8 and E18, α3 mRNA levels increase 5 fold while β2 and β4 levels increase 4-6 fold (Corriveau and Berg, 1993). The increases in α3, β2, and β4 correlate with increases in ACh-evoked currents (Margiotta and Gurantz, 1989;

Engisch and Fishbach, 1990). Interestingly, α5 is lowest expressed subunit at both time points and shows the greatest changes: α5 mRNA levels increase 13 fold during this time period; this correlates very well with the 14 fold increase in mAb35-binding between E8 and E18 (Smith et al., 1985). In addition, α7 mRNA levels also increase 4 fold during this same time period, and this increase is similar to the observed 6 fold increase in α-BTX-binding sites (Corriveau and Berg, 1993).

When E8 CGN neurons develop in culture for 1 week, α7 mRNA levels drop 4 fold while the levels of α3, α5, β2, and β4 do not change (Corriveau and Berg, 1994). However, the expression of surface mAb35- and α-BTX-binding sites are ≈ 3 fold greater in these cultured neurons as compared to neurons at the time of plating, suggesting that postranscriptional mechanisms regulate nAChR abundance on surface of these neurons (Corriveau and Berg, 1994). The differences between subunit mRNA expression *in vivo* and in culture suggest that nAChR mRNA expression in CGN may depend on innervation and/or target tissue interactions or other factors that may be absent in tissue culture.

Innervation and target tissue interactions regulate nAChR expression

The role of presynaptic and postsynaptic contacts in the expression of neuronal nAChRs on chick CGN has been extensively characterized. Both CGN development in the absence of innervation (by ablation *in ovo* of inputs prior to innervation) and denervation of mature CGNs in posthatch chicks reduces total mAb35 and α-BTX-binding (Jacob and Berg, 1987; Arenella et al., 1993), as well as α3, α5 and β4 transcripts levels (β2 and α7 levels have not been examined)(Boyd et al., 1988; Levey et al., 1995; Levey and Jacob, 1996). Surprisingly, surface mAb35-binding and ACh sensitivity are not affected by denervation or input deprivation (McEachern et al., 1989;

Engisch and Fishbach, 1990; Levey et al., 1995). These results strongly suggest that the maintenance of surface nAChRs on CGN occurs independently of innervation.

Axotomy of newly hatched chick CGN decreases total and as well as surface mAb35-binding, the mRNA levels of α3, α5, and β4, and ACh sensitivity (Jacob and Berg, 1987; Boyd et al., 1988; McEachern et al., 1989; Levey and Jacob, 1996). When CGN develop *in ovo* in the absence of peripheral targets (by ablation of target muscle tissue prior to synaptogenesis), α3 and β4, but not α5 mRNA levels are significantly lower than in control age-matched neurons (Levey et al., 1995). In these target-deprived CGN, ACh-evoked currents are also decreased in comparison to age-matched controls, suggesting that α3 and/or β4 but not α5 are important for the expression of surface nAChRs (Levey et al., 1995). These studies show that either factors or cell-cell contacts with target tissues are essential for nAChR expression in chick parasympathetic neurons.

Through these studies on chick CGN, much has been learned about the factors and mechanisms that regulate the expression of several different nAChR subunits. In particular, these studies reveal that nAChR expression on developing CGN depends on as yet unidentified signals from pre- and postsynaptic tissues.

Rat Sympathetic Neurons

Rat sympathetic neurons from the superior cervical ganglion (SCG) have several features that make them ideal to investigate nAChR expression in mammalian neurons. These neurons are located in discrete ganglia and receive relatively simple excitatory cholinergic innervation from preganglionic neurons (Black, 1978). Both the incoming preganglionic nerve and the outgoing postganglionic sympathetic trunk are accessible for experimental manipulation. Cholinergic synapses on sympathetic neurons have long

served as a model for the investigation of synaptic transmission and neurotransmitter release at neuron-neuron synapses (Hall et al., 1974). Concerning synapse formation, most synapses on SCG neurons form during the first three weeks of postnatal life (Smolen and Raisman, 1980), and consequently one can perturb the system during this period of synaptogenesis in ways that would be much more difficult to do in embryonic rats (Purves and Lichtman, 1984). In addition, neonatal SCG neurons differentiate well in pure neuronal cultures: in the absence of other cell types, these neurons extend extensive neurites, develop their *in vivo* polarity and extend dendrites (Furshpan et al., 1980-81). Over the past few years, Cooper and colleagues have investigated the factors that influence the expression of postsynaptic neuronal nAChRs on developing sympathetic neurons. There are both similarities and differences in the regulation of nAChRs expression between neonatal rat sympathetic neurons and chick ciliary ganglion neurons. Below is a review of some of the work on rat sympathetic neurons.

Rat SCG express the same five nAChR subunits as chick CGN

Rat sympathetic SCG neurons express both α-BTX-insensitive and α-BTX-sensitive nAChRs (Fumagali et al., 1976; Loring et al., 1988). The α-BTX-insensitive receptors are highly localized to synapses (Loring et al., 1988) whereas α-BTX-sensitive receptors are extrasynaptic and more uniformly distributed over the soma and dendrites (Fumagali and DeRenzis, 1984). As a first step to determine the subunit composition of nAChRs on SCG neurons, Mandelzys et al. (1994) previously used RNase protection assays to determine which nAChR subunits are expressed by these neurons. They found that neonatal rat SCG neurons express the same five nAChR transcripts as chick CGNs: α3, α5, α7, β2 and β4 (Mandelzys et al., 1994). However, the mRNA levels of these subunits differ from CGNs: α3 in postnatal day 1 (P1) neurons are comparable to α7, and

are 5 fold greater than α5, 2 fold greater than β2, and 30% less than β4 (Fig 1.4A; Mandelzys et al., 1994, 1995).

In a combined electrophysiological and pharmacological study using various nicotinic agonists and antagonists, Mandelzys et al. (1995) demonstrated that most, if not all, functional nAChRs on SCG neurons are likely to contain α3, β2 and β4 in the same receptor complex. These receptors are blocked by n-BTX and likely form the synaptic nAChRs. While the α5 subunit is expressed at very low levels, it may form part of this receptor or other receptor species.

The α7 nAChRs form the α-BTX-binding sites that are detected on the surface of SCG neurons (Schoepfer et al., 1990; Couturier et al., 1990a; Séguéla et al., 1993). However, De Koninck and Cooper (1995) were unable to detect any α-BTX-sensitive currents on SCG neurons, even using an ultra fast agonist application method, suggesting that the density of functional α7-type receptors is too low to resolve. The functional role of α7 receptors on sympathetic neurons is not known.

nAChR subunit expression increases during *in vivo* SCG development

Developmental changes in nAChR subunit gene expression were measured during the first three postnatal weeks, a time when the number of synapses formed by the preganglionic nerve increases several fold (Mandelzys et al., 1994). α3 mRNA levels increase ≈ 4 fold during this period while α7 levels increased ≈ 3 fold; no significant changes were found in the mRNA levels of the other three subunits (Fig. 1.4B; Mandelzys et al., 1994). Using whole-cell patch clamp techniques, Mandelzys et al. (1994) detected that a 2 fold increase in α-BTX-insensitive ACh-evoked current densities on these neurons during the first three postnatal weeks. This increase in ACh-evoked current densities correlates well with the increase in α3 mRNA levels. I hypothesize

Figure 1.4. Rat sympathetic neurons express five neuronal nAChR subunits: α3, α5, α7, β2, and β4. ***A***, mRNA levels of nAChR subunits expressed by postnatal day 1 (P1) SCG neurons relative to α3 mRNA levels; taken from Mandelzys et al., 1994. ***B***, mRNA levels of nAChR subunits in SCG neurons during *in vivo* development expressed relative to α3 transcript levels; adapted from Mandelzys et al., 1994. ***C***, nAChR subunit mRNA levels in SCG neurons during development *in vitro* relative to α3 mRNA levels; from De Koninck and Cooper, 1995. Error bars represent the standard error of the mean (SEM).

A

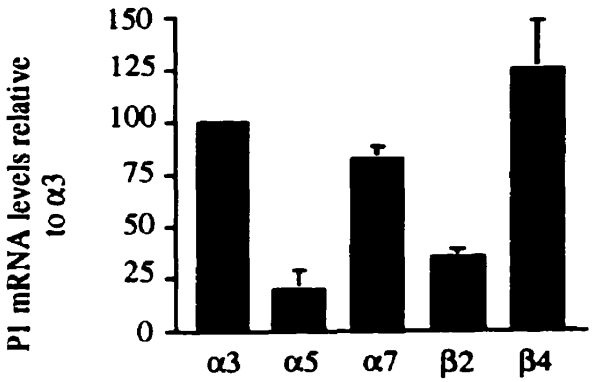
P1 mRNA levels relative to α3
150
125
100
75
50
25
0
α3
α5
α7
β2
β4

B

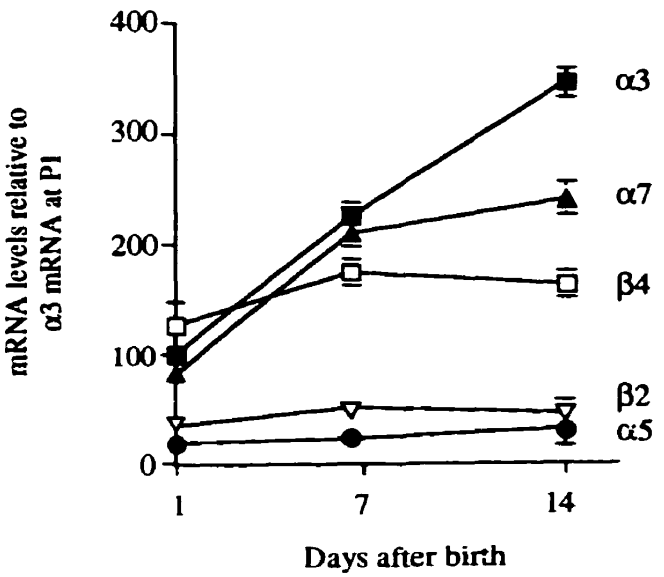
mRNA levels relative to α3 mRNA at P1
400
300
200
100
0
α3
α7
β4
β2
α5
1
7
14
Days after birth

C

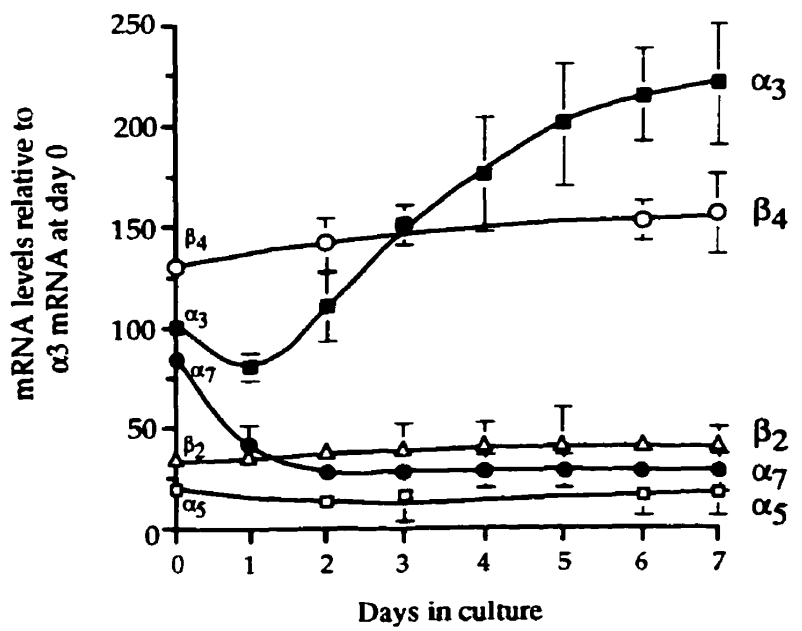
mRNA levels relative to α3 mRNA at day 0
250
200
150
100
50
0
α3
β4
β2
α7
α5
0
1
2
3
4
5
6
7
Days in culture

that α3 may be rate limiting for the assembly and insertion of functional nAChRs during development.

By denervating SCG neurons at postnatal day 1, Mandelzys et al. (1994) showed that much of the increase in α3 gene expression and ACh-evoked current densities occurs independently of preganglionic innervation. Axotomy experiments were not performed because it is difficult to access the ganglionic outputs and because the neurons do not survive this treatment.

nAChR subunit expression during SCG development in culture

To learn more about the factors that regulate nAChR gene expression, De Koninck and Cooper (1995) investigated P1 SCG neurons developing in culture. Of the five transcripts, α3, α5, β2, and β4 are expressed in a very similar fashion to their expression *in vivo*. Briefly, α3 mRNA levels increase 2-3 fold during the first week in culture whereas α5, β2 and β4 do not change (Fig. 1.4C). Furthermore, as *in vivo*, a good correlation exists between α3 mRNA levels and ACh-evoked current densities. This adds further support to my hypothesis that receptors incorporating α3 subunits are responsible for the ACh-evoked currents on these neurons. In addition, as neither the mRNA levels for β2 or β4 change, these findings suggest that α3 subunits are rate-limiting for the assembly and insertion of new functional nAChR in the cell membrane.

Experiments with antisense oligonucleotides

Role and colleagues previously examined the contribution of α3 subunits to functional nAChRs expressed on chick lumbar sympathetic neurons using antisense oligonucleotides to block α3 mRNA translation (Listerud et al., 1991); these neurons express the same five nAChR subunits as rat SCG neurons as well as α4 subunits. To

eliminate pre-existing functional receptors at the cell surface, they first treated the neurons with bromoacetylcholine (BAC) which covalently binds to and inactivates surface nAChRs, and then incubated the neurons with antisense α3 oligonucleotides for 2 days, the estimated time for complete receptor turnover. Chick sympathetic neurons treated with α3 antisense oligonucleotides had decreased ACh-evoked currents in comparison to controls. Mandelzys et al (1995) performed similar experiments on cultured SCG neurons using similar antisense α3 oligonucleotides and found no significant difference between treated neurons and controls. Interestingly, functional recovery after BAC treatment was observed within 45 hr, consistent with a turnover rate of 1-2 days. To examine the contribution of β2 and β4 subunits to the receptors that mediate ACh-evoked currents, SCG neurons were treated with antisense β2 and β4 oligonucleotides both separately and together: no effect on current densities or amplitudes was found (Mandelzys et al., 1995). The reasons for this lack of effect by these antisense oligonucleotides are not clear, but may be due to inefficient oligonucleotide uptake into the nucleus (Wagner, 1994).

The role of CaM kinase in α7 gene expression

In contrast to *in vivo*, when SCG neurons develop in culture α7 mRNA levels drop 75% during the first 2 days and remain low for at least 3 weeks (De Koninck and Cooper, 1995; see Fig. 1.4). A similar decrease in α7 mRNA levels is found for chick CGNs developing in culture (Corriveau and Berg, 1994), suggesting that similar mechanisms may regulate α7 expression in these two populations of neurons.

To investigate whether α7 gene expression in regulated by electrical activity, De Koninck and Cooper (1995) cultured SCG neurons in the presence of high extracellular K^+ concentrations to mimic electrical activity. They found that high K^+ stimulated α7 gene expression: increases in α7 mRNA and surface α-BTX-binding were

found (De Koninck and Cooper, 1995). This increase most likely occurs via increased Ca^{2+} influx through L-type Ca^{2+} channels (De Koninck and Cooper, 1995). The high K^+ effect is specific for $\alpha 7$ as the levels of the other four transcripts were unaffected by this treatment. Neither activators nor inhibitors of PKA, PKC or tyrosine kinases affected nAChR expression in control cultures or prevented the high K^+ induced increase in $\alpha 7$ mRNA levels (De Koninck and Cooper, 1995). The effects of depolarization could be blocked by a specific Ca^{2+}/calmodulin-dependent protein kinase (CaM kinase) inhibitor, providing the first demonstration of a link between neuronal activity and neurotransmitter gene expression operating through a CaM kinase pathway (De Koninck and Cooper, 1995).

C) 5-HT_3 Receptors

The preceding section discusses factors and mechanisms that regulate neuronal nAChR expression on autonomic neurons during development. An important issue is whether the factors that influence nAChR expression, such as presynaptic and target innervation, are specific for nAChR expression or are also important for the expression of other neurotransmitter-gated ion channels on autonomic neurons. To address this issue, I have investigated the expression of the serotonin 5-HT_3 receptor on developing peripheral neurons.

The neurotransmitter serotonin (5-hydroxytryptamine, 5-HT) activates a broad family of receptors that can be divided into four major classes based on their pharmacology and their modes of action: 5-HT_1, 5-HT_2, 5-HT_3 and 5-HT_4 (Lambert et al., 1995). Of the 16 distinct 5-HT receptors cloned so far, all are G-protein-linked receptors except for the 5-HT_3R which is a neurotransmitter-gated ion channel (Lambert et al., 1995; Peroutka, 1995).

The 5-HT_3R is a unique member of the ligand-gated ion channel family in that only one gene codes for this receptor's subunits. The 5-HT_3R cDNA was first cloned from a mouse neuroblastoma cell line by Julius's laboratory in 1991 (Maricq et al., 1991). This cDNA encodes a 487 amino acid polypeptide whose primary structure contains all of the conserved characteristics of neurotransmitter-gated ion channels (Maricq et al., 1991). Several groups have cloned a splice variant of this channel that contains a six (mouse and human) or five (rat) amino acid deletion in the long intracellular loop between M3 and M4 (Isenberg et al., 1993; Hope et al., 1993; Miquel et al., 1995; Miyake et al., 1995). In spite of extensive cloning efforts by several research groups, no additional 5-HT_3R subunits have been identified over the last 7 years.

Like neuronal α7 nAChR subunits, 5-HT_3R subunits form a homomeric receptor composed of five identical subunits (Apud, 1993; Lambert et al., 1995). When expressed in *X.* oocytes or in HEK 293 cells, each of the two splice variants mediates 5-HT-evoked currents that are indistinguishable from one another (Lambert et al., 1995). The splice variants differ little from one another pharmacologically except in their sensitivity to the agonist 2-methyl 5-HT (Downie et al., 1994; Sepùlveda and Lummis, 1994). While both variants are co-expressed in the several neuronal tissues (Hope et al., 1993; Miquel et al., 1995), their functional differences, if any, are unknown. As the spliced domain contains a serine residue, it is speculated that this residue could be phosphorylated and may serve to discretely modulate receptor function (Hope et al., 1993).

Expression and physiological function of 5-HT_3Rs

Peripheral 5-HT_3Rs

Serotonin 5-HT_3Rs are expressed by most autonomic, enteric, and sensory neurons (Jackson and Yakel, 1995). Serotonin 5-HT_3Rs on primary afferent sensory fibers are

involved in nociception while those on enteric neurons modulate intestinal contractions and fluid and electrolyte secretions (Jackson and Yakel, 1995; Johnson and Heinemann, 1995; Lambert et al., 1995). Peripheral 5-HT_3Rs are also implicated in a variety of reflexes including reflex bradycardia, reflex swallowing and the baroreceptor reflex in hypotension (Gaddum and Picarelli, 1957; Yoshioka et al., 1994; Lambert et al., 1995).

Central 5-HT_3Rs

In contrast to the PNS, 5-HT_3R expression in the CNS is much more restricted. Hot spots of 5-HT_3R expression are found in certain regions including the entorhinal cortex, amygdala, hippocampus, nucleus accumbens, caudate nucleus, and the dorsal vagal complex in the medulla (Jackson and Yakel, 1995). The clearest roles of central 5-HT_3Rs are in reflex emesis and anxiety (Jackson and Yakel, 1995).

The majority of 5-HT_3Rs are believed to be located at the nerve terminals (Lambert et al., 1995). The best example of this is in the dorsal vagal complex that composed of the nucleus tractus solitarius (NTS), the area prostrema, and the dorsal motor nucleus of the vagus nerve. These nuclei, which received primary visceral afferents from the glossopharyngeal and vagal cranial nerves, have high levels of 5-HT_3R radioligand-binding (Ohuoha et al., 1994). However, removal of the vagal nodose ganglion in the periphery significantly diminished 5-HT_3R radioligand-binding in the NTS (Pratt and Bowery, 1989). In addition, *in situ* hybridization experiments show that 5-HT_3R mRNA expression is absent in the dorsal vagal complex, indicating that protein expression most likely occurs in the periphery (Tecott et al., 1993). Taken together, these data suggest that 5-HT_3Rs are synthesized in nodose neuron cell bodies and transported axonally along the vagus nerve to these central locations (Peters et al., 1993).

Cellular 5-HT_3R functions

The function of terminally located receptors is most likely to modulate neurotransmitter release (Kawa, 1994; Nichols and Mollard, 1996). This modulatory role was first shown in 1957 by Gaddum and Picarelli in their classical paper in which they show that peripheral 5-HT_3R activation stimulates neurotransmitter release (Gaddum and Picarelli, 1957). Many subsequent studies have shown that central 5-HT_3Rs modulate the release of many different neurotransmitter including acetylcholine, dopamine, GABA, noradenaline and cholescystokinin (reviewed in Ohuoha et al., 1994). The mechanism of this modulation is thought to be due to increased Ca^{2+} influx into the terminals which in turn facilitates neurotransmitter release (Nichols and Mollard, 1996). However, 5-HT_3Rs are relatively impermeable for Ca^{2+} ions (Jackson and Yakel, 1995). Rather, the opening of 5-HT_3Rs induces a strong membrane depolarization, largely caused by the inward flow of Na^+ ions, which in turn stimulates the opening of voltage-sensitive Ca^{2+} channels, allowing Ca^{2+} influx into the terminal (reviewed in Nichols and Mollard, 1996). It should be noted that not all central 5-HT_3Rs are presynaptic: the existence of postsynaptic 5-HT_3Rs that mediate fast synaptic transmission has been documented on neurons in the amygdala and the developing visual cortex, as well as on hippocampal interneurons (Sugita et al., 1992; Roerig et al., 1997).

Clinical applications

The major clinical applications of 5-HT_3R antagonists have been to control nausea and emesis, a common and severe side effect of cancer chemotherapy and radiation therapy (Tyers, 1992). The most effective drug is ondansetron (pharmaceutical name Zofran), a potent and selective blocker of 5-HT_3Rs (Tyers, 1992). It is not clear if the site of this antiemetic action is central or peripheral; a good candidate region is the dorsal vagal complex because it is an important modulator of gastrointestinal function and

emesis, and receives vagal afferents of gastrointestinal origin that have abundant 5-HT_3Rs (Ohuoha et al., 1994).

Expression of 5-HT_3Rs during embryonic development

Recent studies have shown that 5-HT_3R gene expression occurs early during embryonic development in the brain and in the periphery. In the mouse CNS, 5-HT_3R transcripts are detected as early as E12.5 in regions of active proliferation that give rise to the cerebral cortex, amygdala, and hypocampus, consistent with receptor expression in the adult (Johnson and Heinemann, 1995; Tecott et al., 1995). In the periphery, there is robust expression in several cranial sensory ganglia derived from the ectodermal placodes. In one such ganglion, the sensory nodose ganglion, 5-HT_3R transcripts are first detected at E10.5 and persist during development, such that by birth nodose neurons contain abundant 5-HT_3R transcripts (Johnson and Heinemann, 1995; Tecott et al., 1995). 5-HT_3R mRNA is also detected, although at much lower levels, in several neural crest-derived ganglia, including sympathetic ganglia, dorsal root ganglia and the myenteric plexus in enteric nervous system (Johnson and Heinemann, 1995; Tecott et al., 1995).

Little is known about the factors and mechanisms that govern the expression of 5-HT_3R during development and in mature neurons. NGF stimulates 5-HT_3R mRNA and protein expression in PC12 cells (Gordon and Roland, 1990; Furukawa et al., 1992; Isenberg et al., 1993). However, it is not known whether NGF directly stimulates 5-HT_3R expression or if the increase is simply a consequence of NGF induced PC12 differentiation. Nevertheless, this suggests that neurotrophins such as NGF may regulate 5-HT_3R expression in neurons.

Because nodose neurons express high levels of 5-HT_3Rs during embryogenesis and at birth while sympathetic neurons express much lower levels, I hypothesize that different mechanisms regulate 5-HT_3R gene expression in these two neuronal populations. In

Chapter 2 of this thesis, I present my investigation of the factors that regulate the expression of 5-HT_3Rs in neonatal nodose and sympathetic neurons.

D) Gene Transfer into Neurons

Gene transfer is one of the most important techniques in molecular and cellular biology and provides an excellent approach for studying the regulation of ion channels in neurons. DNA transfection into established cell lines has been widely used to characterize novel gene products, to understand the physiological function of normal and mutated proteins, and to produce large amounts of recombinant proteins. Recent extremely powerful gene transfer techniques include the development of transgenic and "knockout" mice and viral vectors.

Achieving efficient gene transfer in neurons has proven to be a major obstacle for neurobiologists. Traditionally, gene transfer into transformed cell lines was accomplished by a variety of chemical and physical methods such as Ca^{2+}phosphate-DNA precipitation and electroporation. However, a variety of cell types are very resistant to transfection by conventional methods for reasons that are unclear. These recalcitrant cells types are for the most part post-mitotic cells and include primary neurons, glia, cardiac and liver cells. The recent generation of recombinant viral vectors has to a large extent solved this problem, allowing for high efficiency gene transfer into many non-dividing cell types and tissues. Some of the major gene transfer techniques and their potential usefulness for transfecting primary neurons are described below.

Chemical and Physical Transfection Methods

Calcium phosphate-DNA precipitation

Ca^{2+}-phosphate-mediated gene transfer, developed by Graham and van der Eb (1973), is the most widely used gene transfer method (Okayama and Chen, 1991). The basic protocol involves mixing $CaCl_2$, DNA, and a carefully buffered solution containing phosphate that together form a fine visible precipitate. The Ca^{2+}-phosphate-DNA precipitate is taken up by target cells by nonspecific endocytosis and the endocytosed DNA is then transported to various cellular compartments including degradative lysosomes (Okayama and Chen, 1991). Some DNA is transported to the nucleus where it is transcribed into RNA (Okayama and Chen, 1991). This technique generally yields transient transfection efficiencies of 10% or higher in cell lines (Okayama and Chen, 1991). Stable transformation, which involves the non-specific recombination of the transfected DNA into the host cell's genome, occurs at much lower efficiencies that range from $1/10^3$ to $1/10^6$ transfected cells (Watson et al., 1992). For reasons that are not clear, the Ca^{2+}-phosphate-DNA precipitation method produces poor transfection efficiency for many types of neurons (Castro et al., 1996), including sympathetic neurons as I show in Chapter 3.

DEAE-Dextran

DEAE-dextran transfection is one of the oldest gene transfer methods. It involves the incubation of naked DNA with DEAE-dextran, a molecule composed of the positively charged group DEAE (diethyl-aminoethyl) and dextran, an inert carbohydrate polymer (Watson et al., 1992). The DNA-DEAE-dextran complex, formed by electrostatic interactions, is taken up by tissue culture cells by endocytosis in much the same way as

the Ca^{2+}phosphate-DNA precipitate is (Lake and Owen, 1991). This method is inefficient for many cell types, including neurons, and is less reliable than Ca^{2+}phosphate-mediated transfection (Watson et al., 1992; Castro et al., 1996).

Liposomes

Over the past several years liposome-mediated transfection has become increasingly popular because of its high efficiency and ease of use (Felgner, 1991). Positively charged lipids such as DOTMA and DOTAP form vesicles or liposomes that can interact spontaneously with polyanions such as DNA or RNA (Felgner, 1991). The resulting cationic liposomes adhere and fuse with the anionic lipid membranes of cultured cells. The liposomes appear to bypass the degradative lysosomes, giving a more efficient delivery of DNA to the nucleus than the Ca^{2+}phosphate method. Liposomes are effective in a wide variety of actively dividing cell lines and can be used to introduce DNA, RNA and double stranded RNA. In Chapter 3, I describe my experiments on liposome-mediated gene transfer for cultured sympathetic neurons.

DNA injection

Direct injection of DNA into the nucleus or RNA into the cytoplasm yields good levels of ectopic gene expression. For example, both neuronal and muscle nAChRs are very efficiently expressed by injecting subunit cDNA or RNA into *X.* oocytes. However, the number transfected cells is limited to the number of injected cells. Because of this limitation, I chose not to use DNA injection to transfect sympathetic neurons.

Electroporation

Electroporation involves the application of a high voltage pulse to DNA and cells in suspension between two electrodes in a special cuvette (Spencer, 1991). The electrical pulse creates tiny transient pores in the cell's membrane that allow DNA to enter into the cytoplasm, bypassing the degradative lysosomes (Spencer, 1991). Electroporation has been successfully used on many different cell lines and is as efficient as Ca^{2+} phosphate-mediated transfection (Spencer, 1991). In particular, electroporation is routinely used to introduce DNA into embryonic stem cells for generating "knockout" mice. The major limitation of electroporation is that good transfection efficiency is obtained only in actively dividing cells (Spencer, 1991).

Viral Transfection Methods

Viral vectors are becoming the vehicles of choice for manipulating gene expression in the nervous system. The last several years has seen an explosion in the development of new and improved viral vectors, and the list is still growing. In fact, in perusing a current issue of any of the top virology journals, one is sure to find several articles on the use of viral vectors for gene transfer. Viral vectors differ widely in their host and cellular tropisms, capacity to incorporate DNA, host cell toxicity and ease of use. Most viral vectors are constructed by first inserting the gene of interest into a region of the viral genome where specific viral genes have been deleted. The resultant recombinant virus is then propagated with the aid of a helper virus or a complementing packaging cell line.

There are now many different types of viral vectors that differ in their suitability as gene transfer agents into neurons. The earliest viral vectors, based on the monkey tumor virus SV40, are very effective for producing high levels of foreign proteins, but

unfortunately can only infect monkey cells, thereby limiting their use (Watson et al., 1992). Baculoviruses, which are useful for producing large amounts of recombinant proteins, on the other hand, infect only insect cells (Bailey and Possee, 1991). Other viral vectors, such the Semliki forest virus (SFV), are too pathogenic for long-term cellular expression. SFV is an alpha RNA virus that can be harnessed to produce substantial amounts of foreign protein shortly after infection; unfortunately SFV kills its host cell within 24-48 hr (Liljestrom and Garoff, 1991). Nevertheless, SFV has proven to be very useful in studying intracellular trafficking of neosynthesized proteins (de Hoop et al., 1994). Lastly, another alpha RNA virus, the Sindbis virus, shows interesting potential as a gene transfer agent into quiescent cells (Dubensky et al., 1996). This Australian mosquito born bird virus has a large capacity for foreign DNA and a broad host range (Altman-Hamamdzic et al., 1997). Several recent reports show that new recombinant Sindbis vectors can efficiently transduce neurons and muscles (Dubensky et al., 1996; Corsini et al., 1996; Parks et al., 1997).

Vaccinia Virus Vectors

Vaccinia virus is the cowpox virus that was used to immunize people against smallpox. Vaccinia viral vectors have been used effectively as gene transfer agents for some time (Mackett, 1991). The vaccinia virus has, however, a rather large DNA genome of 180 kb that renders it cumbersome to manipulate (Watson et al., 1992). Instead, vaccinia viral vectors are more commonly used in a versatile expression system developed to express large amounts of foreign proteins (Watson et al., 1992). New replication defective vaccinia viruses show great promise as safe immunization agents (Moss, 1996).

Retrovirus vectors

Retroviral vectors are efficient gene delivery systems for diving cells (Morgenstern and Land, 1991). Retroviruses are single strand RNA viruses that must transcribe their RNA genetic code into double stranded DNA in order to replicate (Bannerji, 1995). This task is accomplished with reverse transcriptase, an RNA-dependent DNA polymerase, that these viruses produce (Bannerji, 1995). After infection, viral RNA is copied into DNA that is then stably and more or less randomly integrated into the host's genome. The integrated provirus then directs the constitutive synthesis of viral proteins and new virions without any detrimental effects to the host cell. The most commonly used retroviral vector is the Moloney murine leukemia virus (MoMLV) (Bannerji 1995).

The advantages of retroviral vectors are that they provide very high efficiency gene transfer (nearing 100% in tissue culture experiments!) and stable gene expression because of their integration into the host cell's genome (Bannerji, 1995; Philips, 1997). In addition, retroviruses can infect a wide range of cells in many different species. However, retroviral integration into the host's genome can disrupt important genes, making it less suitable for use in gene therapy (Bannerji, 1995). The greatest disadvantage is that most retroviruses can only integrate and express their transgene in actively dividing cells such as transformed cell lines, bone marrow cells and fibroblasts (Philips, 1997). For this reason, retroviral vectors are not suitable for gene transfer into post-mitotic cells such as neurons.

Adeno-Assosiated Virus

Adeno-associated virus (AAV)-mediated gene transfer has been receiving much attention lately because of its efficiency and potential safety for use in gene therapy (Philips, 1997). AAVs are non-pathogenic non-replicative parvoviruses, originally

isolated as contaminants of adenoviral stocks (Philips, 1997). AAVs are dependent on helper viruses, such as adenovirus or herpes simplex virus, to provide the necessary proteins for replication and packaging, and as such are classified as "dependoviruses" (Kaplitt and During, 1995). In the absence of helper virus, AAV is integrated into its host's genome where it can persist indefinitely as a provirus, an important feature for long-term expression that is essential for effective gene therapy (Philips, 1997). This latency can be rescued by super-infection with helper virus, allowing the AAV genome to be excised, replicated, and packaged into virus particles that are released from the host cell; this is how AAVs are produced in the laboratory (Philips, 1997). Interestingly, AAV is one of the smallest viruses and has a diameter of 20-24 nm (Bartlett and Samulski, 1995).

AAV has a linear single stranded DNA genome of either plus or minus polarity; each strand is packaged into separate virions (Bartlett and Samulski, 1995). The AAV DNA is 4.7 kb long and contains two inverted terminal repeats (ITR) that form hairpin structures (Bartlett and Samulski, 1995). These two ITRs are the only sequences necessary for chromosomal integration (Bartlett and Samulski, 1995). Therefore, most of the intervening DNA sequences can be replaced with foreign DNA of up to 4.5 kb in length (Philips, 1997). Such recombinant AAVs (rAAVs) can be easily rescued, replicated, and packaged in tissue culture cell lines in the presence of helper virus and certain exogenously expressed AAV structural proteins (provided by plasmid transfection) (Bartlett and Samulski, 1995). The major limitation of producing rAAVs is that the helper virus must be completely eliminated from the viral stocks; since the helper virus and rAAVs differ in size, they can be easily separated (Philips, 1997).

Recombinant AAVs do not express viral proteins which greatly diminishes potential toxic and immune effects (Philips, 1997). Important rAAV features include a broad host range, their ability to transduce quiescent cells, including neurons as well as long-term persistence and transgene expression (Bartlett and Samulski, 1995; Xiao et al., 1997).

Herpes simplex virus vectors

Herpes simplex virus type 1 (HSV) is a naturally neurotropic virus that has attracted much attention as a gene delivery vehicle into the CNS. HSV has a broad host range and can infect most quiescent cell types. In addition, HSV vectors can persist in their host cell's nucleus in a latent state for indefinite periods of time, an attractive feature for achieving long-term gene transfer in gene therapy (Federoff, 1995). HSV vectors have been used successfully to express a variety of foreign genes in neurons. For example, an HSV vector expressing NGF was able to prevent axotomy induced declines in tyrosine hydroxylase levels in SCG ganglia (Federoff et al., 1992) while a trkA expressing HSV vector was able to confer NGF responsiveness to sensory neurons (Xu et al., 1994). The major drawbacks of HSV vectors are their cytotoxicity and poor infection efficiency of neurons *in vivo* (Johnson et al., 1992a,b; Lieb and Oliva, 1993).

HSV has a linear double stranded DNA genome of 152 kb that codes for some 75 genes (Glorioso et al., 1995). The HSV genome is enclosed in an icosahedral protein capsid which in turn is surrounded by an additional protein layer called the tegument (Glorioso et al., 1995). Finally, a glycoprotein viral envelope forms the outer shell of this virus. HSV enters the cell by attaching and fusing its viral envelope to the cell membrane and then ejecting the viral capsid into the cytoplasm (Glorioso et al., 1995). The capsid is then translocated to the nucleus where viral DNA enters the nucleus via nuclear pores (Glorioso et al., 1995).

HSV exists either in a lytic or latent state. The lytic cycle leads to viral replication and cell death; in neurons, the lytic cycle is often interrupted and latency is established (Glorioso et al., 1995). During latency, which can persist for long periods of time, there is little viral gene expression, except for the latency-associated transcripts whose functions are unclear (Johnson et al., 1992b). This shut off of viral transcription appears to decrease

transgene expression but can be overcome by inserting the transgene into regions associated with the latency-associated transcripts (Ho and Mocarski, 1989).

Two types of HSV vectors have been developed for gene transfer into neuron: recombinant whole virus vectors and plasmid-based amplicons (Kwong and Frenkel, 1995). Whole virus vectors contain a single copy of the gene of interest inserted into non-essential regions of the HSV genome (Roizman and Jenkins, 1985). These vectors are generated through homologous recombination between a plasmid containing the gene of interest flanked by viral sequences and a replication defective viral backbone, provided by a replication defective HSV virus (Roizman and Jenkins, 1985). These whole virus vectors are often very cytotoxic because they express low levels of viral proteins (Johnson et al., 1992a,b; Lieb and Oliva, 1993).

Of the two HSV vectors types, amplicon vectors have been favored because of the facility of their construction (Kwong and Frenkel, 1995). Amplicon vectors were so named to describe the fact that their genome is made of amplified copies of the DNA of interest arranged in a head to tail manner. Amplicon vectors were developed based on the DNA structure of replication defective HSVs originally isolated as contaminants of wild-type HSV laboratory stocks: these defective HSVs contain multiple repeats of the HSV origin of replication and packaging sequences.

To generate an HSV amplicon vector, the gene of interest along with a strong promoter is first cloned into a "seed" plasmid that contains an HSV origin of replication, and an HSV cleavage and packaging sequence (reviewed in Kwong and Frenkel, 1995). This "seed" plasmid is transfected into a mammalian cell line that is co-infected with a helper HSV which supplies the necessary viral replication and packaging machinery. The resultant amplicon vectors contain properly packaged genomes composed of concatenated units of the original plasmid of up to 150 kb in the length, the size of wild-type HSV DNA. These amplicon vectors can readily infect cells and express the gene of interest but are intrinsically unable to replicate. Unfortunately, amplicon viral stocks are also

contaminated by significant amounts of helper virus. Because wild-type helper virus is pathogenic, the presence of helper virus in amplicon vector stocks is a serious problem. Much effort is being placed on engineering complementing packaging cell lines and helper viruses that are replication incompetent or impaired.

Adenovirus vectors

Recombinant adenovirus (Ad) vectors are one of the most promising gene transfer agents for primary neurons. The advantages of using Ad vectors are: (1) the ease of manipulating the Ad genome using recombinant DNA techniques; (2) the ability of Ad vectors to express high levels of ectopic protein; and (3) the capacity of Ads to infect many dividing and quiescent cell types in humans, primates, canines and rodents (Hitt et al., 1995). In addition, recombinant Ad vectors are replication-defective and helper virus free (Hitt et al., 1995). Many recent studies, including one by our laboratory described in Chapter 3 of this thesis, demonstrate that Ad vectors can be used to efficiently transfect neurons both in culture and *in vivo* (Le Gal La Salle et al., 1993; Neve, 1993; Moriyoshi et al., 1996; Slack et al., 1996; Holtmatt et al., 1997; Baumgartner and Shine, 1997; Lisovoski et al., 1997)

Over 40 different human Ad serotypes have been identified. The serotypes 2 and 5 are the best studied Ads and are therefore most often used in making recombinant Ad vectors (Douglas and Curiel, 1997). In addition, Ad2 and Ad5 are non-oncogenic in rodents, an added bonus for work in rodent models (Douglas and Curiel, 1997). Infection of humans by wild-type Ad2 or Ad5 generally causes only mild upper-respiratory tract disease, pharyngitis or conjunctivitis that is self-limiting and short-lived (Ginsberg, 1988; Douglas and Curiel, 1997).

Adenoviruses are medium-sized viruses of approximately 70 nm in diameter (Graham and Prevek, 1991). The Ad genome is a linear double stranded 36 kb DNA

molecule that encodes some 2700 distinct viral proteins (Philips, 1997). This DNA molecule is contained within an icosahedral capsid studded with a protruding fiber protein at each of its 12 vertices (Douglas and Curiel, 1997). The fiber protein contains a tail, that serves to attach the fiber to the capsid, and a rod-like shaft with a globular structure known as the knob (Douglas and Curiel, 1997). At the base of the fiber is a penton base protein that contains 5 conserved repeats of the Arg-Gly-Asp (R-G-D) amino acid sequence (Douglas and Curiel, 1997).

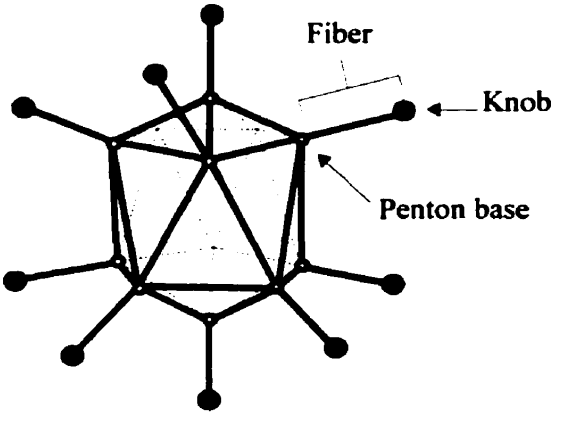

Adenovirus

Adenovirus adsorption and internalization into cells occurs through a two step process (reviewed in Hong et al., 1997). First, the knob of the fiber protein binds to its cellular receptor, recently identified as the α2 domain of heavy chain of the human major histocompatibility (MHC) class I molecule (Hong et al., 1997). Second, the R-G-D sequences of the penton base proteins interact with cellular $\alpha_v\beta_3$ and $\alpha_v\beta_5$ integrins stimulating the endocytosis of the bound virus. After acidification in the lysosome, the virion is transported to the nucleus. The viral DNA is then translocated into the nucleus and virus replication is initiated.

The Ad replication cycle can be divided into an early and a late phase. The early phase involves all events prior to DNA replication and includes the transcription and translation of early genes as well as the activation of the host's DNA and protein synthesis machinery (Graham and Prevek, 1991; Shenk, 1995). The late phase involves viral DNA replication, expression of the late genes which encode most of the structural proteins, and the assembly and release of progeny virions. The early genes are organized into four noncontiguous regions within the Ad genome and are termed E1-E4. The E1 (E1A and E1B), E2 and E4 genes encode proteins that are essential for viral replication while E3 genes encode proteins that are not essential, at least *in vitro* (Graham and Prevek, 1991). In particular, the E1A gene products are the first viral proteins to be expressed after infection and govern the expression of all other viral genes (Hitt et al., 1995; Shenk, 1995). Therefore, Ads that contain deletions in E1 are unable to replicate in all cell types except in E1-complementing HEK 293 cells (Hitt et al., 1995). Therefore, E1 provides a convenient site for the insertion of foreign genes into the Ad genome for the generation of recombinant replication-defective Ads.

Recombinant Ad vectors are most often generated using a plasmid-based approach because of its simplicity and ease of use (Hitt et al., 1995). This method involves the cloning the gene of interest into a shuttle plasmid that contains a small part of the Ad genome in which E1A and E1B have been deleted and replaced with a versatile polycloning sequence. This shuttle plasmid is then co-transfected along with a large circular plasmid that contains the entire Ad genome (except for the E1 genes) into HEK 293 cells. This large plasmid contains a bacterial origin of replication and the ampicilin resistance gene inserted into its deleted E1 region; this plasmid is too large to be packaged into viral capsid and is therefore non-infectious (Hitt et al., 1995).

Through rare homologous recombination events, a full length Ad genome containing the gene of interest, but lacking essential genes for replication, can be recovered as a viral plaque (Hitt et al., 1995). Recombinant adenoviruses have the ability

to infect most mammalian cells but are unable to replicate because they lack specific genes necessary for replication; such Ad vectors can only replicate in HEK 293 cells which express the necessary E1A and E1B proteins for viral replication.

Recombinant Ad vectors have a relatively large cloning capacity. Ad vectors can package up to 105% of their wild-type genome (an additional 1.8 kb), and therefore the maximum size of insert is limited to the size of the deletion plus 1.8 kb (Bett et al., 1994). Deletions in E1 allow a maximum insert of 4.7-4.9 kb (Bett et al., 1994). Additional cloning capacity can be provided by deletions in the E3 region which is not essential for replication; Ads with E1 and E3 deletions can accommodate inserts of up to 8.3 kb (Bett et al., 1994).

Statement of objectives and overview

The overall objective of my thesis research is to learn more about the various factors and mechanisms that promote the expression and the maintenance of neurotransmitter-gated ion channels on neurons. To do this, I have focused on studying the gene expression of two different neurotransmitter-gated ion channels on developing rat peripheral neurons: the 5-HT_3R and the neuronal nAChR. Because developing peripheral neurons express both 5-HT_3Rs and neuronal nAChRs, one of my interests is to compare the mechanisms that influence the gene expression of these two receptors in order to gain a better understanding of neurotransmitter-gated ion channel expression.

The 5-HT_3R represents a relatively simple system: only one gene codes for 5-HT_3R subunits that co-assemble to form homomeric receptors. Little known about 5-HT_3R expression on peripheral neurons during early postnatal development or about the factors

that regulate its expression. I have focused on neurons from two peripheral ganglia, the sensory nodose ganglion and the sympathetic superior cervical ganglion (SCG) during the period of early postnatal development. Nodose neurons express high levels of 5-HT_3Rs during embryogenesis and at birth while SCG neurons express much lower levels, suggesting that different mechanisms regulate 5-HT_3R gene expression in these two neuronal populations. The objective of the first part of this thesis is to investigate the factors that influence 5-HT_3R expression on neonatal rat sympathetic and sensory neurons.

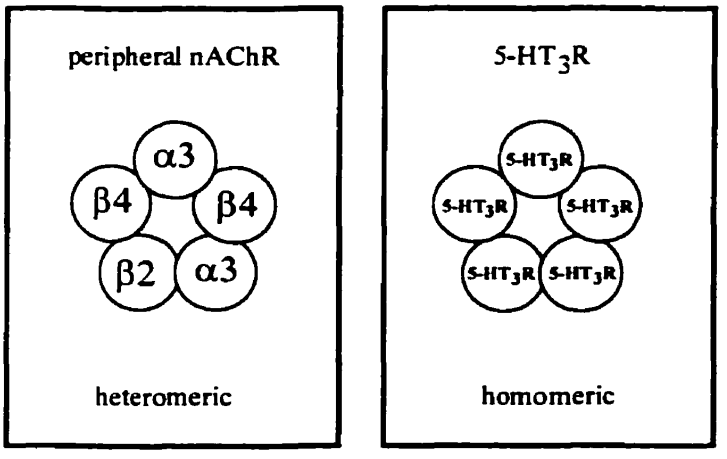

In comparison, the expression of neuronal nAChRs on neonatal rat sympathetic neurons is more complex: these neurons express 5 different nAChR subunit genes whose proteins that can potentially combine to give numerous different receptor subtypes. From my laboratory's data on the developmental expression of nAChR subunits in neonatal rat sympathetic neurons *in vivo* and in culture, I hypothesize that most functional nAChRs on SCG neurons are likely to contain α3, β2 and β4 in the same receptor complex, and that α3 subunit expression may be rate-limiting for the assembly and insertion of new functional nAChR in the cell membrane.

The goal of the second part of this dissertation is to alter the expression of nAChR subunits in order to understand the contribution of specific subunits to functional nAChRs expressed on sympathetic neurons. Specifically, my objective is to manipulate α3 mRNA and protein levels in order to alter the functional properties of nAChRs that are assembled and inserted into the surface membranes of cultured sympathetic neurons.

In Chapter 2, I investigate the factors that govern 5-HT_3R expression in neonatal rat sympathetic and vagal sensory neurons *in vivo* and in culture. I show that 5-HT_3R gene expression is differentially regulated in these two populations, and I provide the first demonstration that 5-HT_3R expression is regulated, in part, by neurotrophins.

In Chapter 3, I test the efficacy of several gene transfer techniques on sympathetic neurons. I demonstrate that recombinant adenovirus vectors are very effective gene delivery vehicles for sympathetic neurons, and do not adversely affect neuronal survival or physiology. In addition, I determine the conditions for optimal gene transfer using adenovirus vectors. Lastly, I describe the successful construction of a recombinant adenovirus expressing the marker protein green fluorescent protein (GFP).

Lastly, in Chapter 4, I investigate the contribution of α3 subunits to ACh-evoked currents on cultured sympathetic neurons using recombinant adenovirus vectors that express sense and antisense α3 mRNA. I demonstrate that α3 subunits are an important component of functional nAChRs expressed on sympathetic neurons.

Chapter 2

Developing Neonatal Rat Sympathetic and Sensory Neurons Differ in their Regulation of 5-HT_3 Receptor Expression

Abstract

Serotonin 5-HT_3 receptors (5-HT_3Rs) are ligand-gated ion channels expressed by many peripheral neurons and are involved in several physiological processes. To learn more about the developmental regulation of 5-HT_3R expression, we investigated rat sympathetic and vagal sensory neurons. We found that sympathetic and sensory neurons differ in their regulation of 5-HT_3R expression during early postnatal life, and as these neurons develop in culture. In SCG neurons, 5-HT_3R transcript levels are low at postnatal day 1 (P1) and increase 7.5 fold by P21; this increase occurs even after elimination of the preganglionic innervation. In comparison, 5-HT_3R mRNA levels in P1 nodose neurons are over 14 fold greater than in P1 SCG, and change little by P21. We show that 5-HT_3R transcript levels in nodose neurons depend on intact target innervation and drop by 60% after axotomy. When P1 SCG neurons develop in culture, we observed a significant increase in 5-HT_3R expression: after 7 days in culture, transcript levels increase 9 fold versus a 3 fold increase for neurons developing for 7 days *in vivo*. In contrast, 5-HT_3R mRNA levels in cultured nodose neurons drop by 70% within 24 hr; however, this drop is transient. After 2 days, transcript levels begin to increase and after 7 days, they are above initial values. We show that this delayed increase in 5-HT_3R expression depends on neurotrophins. In both nodose and sympathetic neurons, we found that the changes in 5-HT_3R gene expression correlate directly with the appearance of 5-HT-evoked current densities.

Introduction

The serotonin 5-HT_3 receptor (5-HT_3R), a neurotransmitter-gated ion channel (Yakel and Jackson, 1988; Derkach et al., 1989; Maricq et al., 1991) present on many

mammalian peripheral neurons, participates in several diverse physiological functions (Fozard, 1984; Jackson and Yakel, 1995). Activation of 5-HT_3Rs located on peripheral vagal sensory nerve endings initiates reflexes affecting respiration, circulation, emesis and swallowing (Douglas, 1975; Sanders-Bush and Mayer, 1996). 5-HT_3Rs on spinal and vagal sensory neurons are involved in nociceptive signaling and nausea (Fozard, 1984). In the CNS, 5-HT_3Rs are implicated in anxiety, depression and drug dependence (Apud, 1993; Greenshaw, 1993). In addition, 5-HT_3Rs are expressed by sympathetic neurons; however, the role for these receptors in sympathetic function has not been fully determined (Wallis and North, 1978; Yang et al., 1992).

Many vagal afferent neurons expressing 5-HT_3Rs are located in the nodose ganglion. These sensory neurons have typical unipolar polarities; their axons bifurcate into a peripheral branch which innervates much of the viscera, including heart, lungs, trachea and gut, and a central branch which terminates mainly in the nucleus tractus solitarius (Andresen and Kunze, 1994). The physiological responses to serotonin elicited from these vagal afferents depend, to a large extent, on the functional densities of 5-HT_3Rs at these nerve endings. However, the factors and mechanisms that ensure the appropriate expression of 5-HT_3Rs on these nerve terminals are largely unknown.

Recent studies have shown that during embryonic development 5-HT_3R gene expression in nodose ganglia is observed as early as embryonic day 10 (E10) in rodents (Tecott et al., 1995; Johnson and Heinemann, 1995), and that by birth, these ganglia contain abundant 5-HT_3R mRNA (Tecott et al., 1995). In contrast, 5-HT_3R expression in embryonic sympathetic neurons is low and at birth, few sympathetic neurons have detectable levels of 5-HT_3R mRNA (Johnson and Heinemann, 1995). These results suggest that embryonic sensory and sympathetic neurons use different mechanisms to regulate 5-HT_3R gene expression. Our interest is to learn more about factors and mechanisms that influence 5-HT_3R expression as peripheral neurons differentiate.

In this study, we have asked: a) whether the expression of 5-HT_3Rs in vagal sensory neurons from the nodose ganglion changes during the first few postnatal weeks, a time when many autonomic reflexes become active; b) whether 5-HT_3R expression depends on intact target innervation; c) whether neurotrophins influence 5-HT_3R expression by nodose neurons; and d) whether the regulation of 5-HT_3R expression in neonatal nodose neurons is similar to that which occurs in sympathetic neurons.

Our results demonstrate that 5-HT_3R transcript levels in neonatal nodose neurons are relatively abundant, change little over the first 3 postnatal weeks, and depend on target innervation. In comparison, we find that in SCG neurons 5-HT_3R transcript levels increase steadily, and are 7.5 fold greater at postnatal day 21 (P21) than at P1; this increase occurs even after elimination of the preganglionic innervation. Our results with SCG and nodose neurons in culture indicate that the regulation of 5-HT_3R expression by sympathetic neurons differs from that by nodose neurons during neonatal development. An abstract of our initial results has appeared previously (Rosenberg, Séguéla and Cooper, 1994).

Materials and Methods

Tissue samples and RNA extraction

Superior cervical ganglia (SCG), nodose ganglia, and trigeminal ganglia were dissected from postnatal day 1 (P1), P7, P14, and P21 (Sprague-Dawley CD strain, Charles River, Canada) rats. Total RNA was prepared from these tissues using the guanidium isothiocyanate-phenol-chloroform extraction method of Chomczynski and Sacchi (1987). The ganglia were placed into ice cold L-15 media without sodium bicarbonate during the dissection, and then placed into GTC solution (+β-

mercaptoethanol) and homogenized for 10 sec using a TEK polytron. Total RNA was prepared from this lysate using standard phenol-chloroform extraction and ethanol precipitation.

SCG preganglionic denervation and nodose axotomy

The surgical procedures used to cut the preganglionic nerve to the SCG in P1 rats were similar to those described previously (McFarlane and Cooper, 1992; Voyvodic 1987). Briefly, P1 rats were anaesthetized by cooling on ice, and the right sympathetic trunk was exposed and crushed midway between the ganglion and the first rib. The trunk was then cut rostral to the crush and the caudal stump was pushed away ventrally to prevent regeneration. The animals were returned to their mother, and 2 weeks after the surgery the denervated SCG ganglia were dissected and total cellular RNA was prepared from the ganglia as described above. Total cellular RNA was also prepared from the contralateral control SCG ganglia whose preganglionic inputs were left intact. Similar surgical procedures were performed for nodose axotomy in P0 and P8 rats. A partial right nodose axotomy was performed by crushing and cutting the vagus nerve midway between the nodose ganglion and the first rib; the caudal stump was pushed away to prevent regeneration. After 24 hr, the P1 and P9 axotomized and control nodose ganglia were dissected and total RNA was prepared as described above.

Neuronal cultures and RNA extraction

SCG and nodose ganglia were dissected from P1 animals and dissociated mechanically and enzymatically as previously described (Mandelzys and Cooper, 1992; McFarlane and Cooper 1992). Briefly, the ganglia were dissected under sterile conditions from animals killed by cervical dislocation. The ganglia were incubated for 15 min at

37°C in Hank's balanced salt solution (without Ca^{++} or Mg^{++}) containing collagenase (1 mg/ml, type I, Sigma) and Dispase (2.4 mg/ml, grade II, Boehringer-Mannheim). The ganglia were then transferred to a similar solution containing only dispase, and the ganglia were gently triturated every 15 min using a fire-polished pasteur pipette for a total of 3-4 hours. Following dissociation, the cells were centrifuged through a 35% Percoll density gradient (Pharmacia) to separate neurons from non-neuronal cells. The neuronal fraction was washed twice with L-15 medium supplemented with 10% horse serum and plated at a density of 5000-8000 cells per cm^2 onto laminin-coated (30 μg/ml, overnight at 4°C; gift of Dr. S. Carbonetto, McGill University) aclar coverslips (Allied Chemicals) in modified petri dishes. The petri dishes (35 mm, Corning) were modified by boring a 1.5 cm diameter hole in the bottom and then gluing aclar cover slips from underneath with silicone rubber (3140 MIL-A-46146 RVT coating, Dow Corning); this created a 2 mm deep well with a volume of approximately 200 μl. The neurons were grown in 1.5 ml of L-15 medium supplemented with 5% rat serum, vitamins, cofactors, penicillin, streptomycin, and sodium bicarbonate as previously described (Hawrot and Patterson, 1979). For SCG neurons, the media was supplemented with nerve growth factor (2.5S NGF, 25 ng/ml). Nodose neurons were grown in L-15 growth media described above either without added neurotrophins; with NGF, brain-derived neurotrophic factor (BDNF, 25 ng/ml; gift of Amgen) and neurotrophin-3 (NT-3, 25 ng/ml; gift of Amgen); or with NGF, BDNF, NT-3 and elevated potassium (final $[K^+]$ = 40 mM). After 2 days in culture, cytosine arabinofuranoside (Ara-C, 10 μM, Sigma) was added to the cultures for 2-3 days to kill the few remaining non-neuronal cells. The cultures were maintained at 37°C in a humidified incubator with an atmosphere of 5% CO_2 - 95% air. The media was replaced every 3 days with fresh media. In some experiments, we treated nodose neurons with 1 μg/ml cycloheximide (1 in 5000 dilution of a 5 mg/ml ethanol solution; Sigma) for the first 10 or 24 hr after dissection; this concentration of cycloheximide has previously been shown to block protein synthesis in cultured neonatal SCG neurons (Martin et al., 1988).

Cycloheximide was added to the plating media and all solutions used during the dissociation procedure. Sister cultures were treated with vehicle alone and showed no difference from untreated controls.

Total cellular RNA was prepared from cultures of P1 SCG and nodose neurons at either day 0 (D0; immediately after dissociation), D1, D2, D4, D7, or D14 using either the RNeasy total RNA kit (Qiagen) or the guanidium isothiocyanate-phenol-chloroform extraction method as previously described (De Koninck and Cooper, 1995). Typically four petri dishes were pooled together for each RNA sample. The yield of total RNA obtained with either RNA preparation method was similar and ranged from 2-3 μg. Total RNA was also prepared from the non-neuronal cells in a similar way. Less than 10% of total cellular RNA from the ganglia was present in non-neuronal cell fractions; previously, we determined that this value changes little over the first two weeks of development for SCG (Mandelzys et al., 1994).

RNase protection assays

RNase protection assays were performed as described by Krieg and Melton (1987) with minor modifications (Mandelzys et al., 1994). Briefly, ^{32}P-UTP-labeled antisense RNA probes to rat 5-HT$_3$R and GAPDH were transcribed *in vitro* using T7 RNA polymerase from linearized plasmids containing portions of the cDNA clones. The 5-HT$_3$R antisense probe was synthesized from a partial rat 5-HT$_3$R cDNA clone (in Bluescript SK, Stratagene; gift of Dr. P. Séguéla, Montreal Neurological Institute) obtained by RT-PCR amplification using oligonucleotide primers for the mouse 5-HT$_3$R cDNA sequence (Maricq et al., 1991). This partial rat 5-HT$_3$R cDNA was sequenced and found to be identical to the published rat 5-HT$_3$R cDNA sequence (Miyake et al., 1995). The 5-HT$_3$R antisense probe protects 563 bases of the rat 5HT$_3$R transcript between positions 268 and 831 of the rat cDNA sequence (Miyake et al., 1995). Both nodose and

SCG neurons express two alternatively spliced 5-HT_3R transcripts that encode receptor proteins that differ by 5 amino acids located between hydrophobic domains M3 and M4 at position 1153 (Miyake et al., 1995; Miquel et al., 1995), however, the physiological role for each variant remains unclear (Downie et al., 1994). The probe we used detects both splice isoforms. The GAPDH antisense probe, synthesized from the mouse GAPDH (mouse pTRI-GAPDH, Ambion), protects 316 bases of the rat GAPDH mRNA transcript. The thermal stabilities of all the probes, based on their melting temperatures, were found to differ by less than 1°C.

The labeled riboprobes were gel purified before use. For each reaction 1 μg total RNA was combined with radiolabeled 5-HT_3R probe (200 000 cpms) and GAPDH probe (30 000 cpms), and allowed to hybridize at 60°C overnight. The unhybridized single-stranded RNAs were digested with RNase T1 (Sigma) and the protected RNA:RNA hybrids were denatured and separated on 5% polyacrylamide 8 M urea gels. The gels were dried, exposed to a phosphor imaging screen (Fujix BAS 2000 and Molecular Dynamics) to quantify the hybridization signals, and then exposed to X-ray film (Kodak XAR) with intensifying screens for 2-3 days at -80°C. The 5-HT_3R hybridization signals were normalized to those for GAPDH to take into account minor differences in the amount of RNA used per reaction. Each RNA sample was tested in duplicate or triplicate reactions. The relative amount of 5-HT_3R mRNA expression for each condition is the average of the values determined from 3 or more independently prepared RNA samples. The mRNA levels for both 5-HT_3R and GAPDH in P1 SCG and P1 nodose ganglia were similar to that of freshly dissociated D0 SCG and D0 nodose neurons respectively, as the contribution of non-neuronal cells to the total ganglionic RNA is small (Mandelzys et al., 1994).

In situ hybridization

The *in situ* hybridization experiments were performed on tissue sections and on neuronal cell cultures according to the methods of Barthel and Raymond (1993) and Litman et al. (1993). Briefly, antisense digoxigenin (DIG)-labeled 5-HT_3R probe was synthesized by *in vitro* transcription using T7 RNA polymerase and DIG-11-UTP (Boehringer Mannheim) and the plasmid containing the portion of the rat 5-HT_3R cDNA described above. Because we were unable to quantify accurately the concentration of DIG-labeled probes using spectrophotometry, we measured the amount of DIG-labeled antisense 5-HT_3R probe by RNase protection assays using ^{32}P-labeled sense 5-HT_3R probe; this also allowed us to verify that the *in vitro* transcription produced full length DIG-labeled probes. To do this, we first synthesized unlabeled antisense 5-HT_3R cRNA which we quantified by spectrophotometry, and then hybridized different amounts of unlabeled antisense 5-HT_3R cRNA with 200 000 cpms of ^{32}P-labeled sense 5-HT_3R to generate a standard curve. We then compared the hybridization signals obtained with the DIG-labeled antisense 5-HT_3R probe to the standard curve to determine the concentration of DIG-labeled antisense 5-HT_3R probe.

The *in situ* RNA hybridization experiments were performed on fresh frozen cryostat sections of P5 and P21 SCG and nodose ganglia. The SCG and nodose ganglia were dissected together with the carotid artery, embeded in O.C.T. Compound (Tissue Tek) and frozen in isopentane cooled on dry ice. The frozen tissue samples were cut at 16 μm thickness using a -20°C cryostat and placed onto Probe On Plus slides (Fischer Scientific). Next, the sections were fixed for 5 min with 3% paraformaldehyde in 0.1 M Na phosphate buffer (0.1 M NaH_2PO_4:0.1 M Na_2HPO_4, pH 7.4), rinsed with phosphate buffered saline (PBS), rinsed with DEPC water, dehydrated with alcohol, air dried, and stored at -80°C. The sections were warmed to room temperature and pre-hybridized for 3 hr at 43°C in a solution containing salmon sperm DNA (250 μg/ml, Pharmacia), yeast

tRNA (500 μg/ml, Sigma), ribonucleoside vanadyl complex (20 mM, New England Biolabs), 4X SSC (0.3 M NaCl, 0.03 M Na citrate in DEPC water), 50% formamide, 3X Denhart's solution, 1% sarcosyl, and 20 mM Na phosphate buffer, pH 6.8. The pre-hybridization solution was then replaced with the hybridization solution which contained the same ingredients plus dextran sulfate (10%), DTT (60 mM), and differing amounts of riboprobe (0.25-12.5 ng/μl). The sections were incubated at 43°C overnight, washed 3X for 15 min in 2X SSC at 43°C, and treated with RNase T1 (1000 units/ml) and RNase A (2 μg/ml; Pharmacia) in RNase buffer (0.3 M NaCl, 0.1 M Tris pH 7.5, 5 mM NaEDTA, pH 8.0) for 30 min at 37°C to digest unhybridized RNAs. The sections were rinsed with 1X SSC, 0.5X SSC, and 0.1X SSC for 15 min each at 43°C. The sections were then rinsed with Tris buffered saline (TBS), incubated for 1 hr at room temperature in TBS containing 1% Blocking Reagent for Nucleic Acids (Boehringer Mannheim), and then incubated for 1 hr with same buffer supplemented with 3.4 μl/ml of anti-DIG-alkaline phosphatase conjugate, Fab fragment (Boerhinger Mannheim). The sections were rinsed 3X with TBS for 10 min each, and the bound probe was detected using standard alkaline phosphatase histochemistry. The reactions were typically developed for 18-24 hr in the dark. We performed controls with RNase T1 pretreatment or with DIG-labeled sense 5-HT_3R probe on tissue sections; these controls indicated that non-specific signals were low. To verify the specificity of the 5-HT_3R probe, we pretreated the tissue sections with 400 fold excess unlabeled antisense 5-HT_3R probe which competitively blocked the hybridization of the DIG-labeled antisense 5-HT_3R probe. Adjacent sections were stained with Masson's trichrome stain (Sigma) to identify the cellular components of the two ganglia.

In situ hybridizations were also performed on P1 SCG and nodose neurons grown in culture for 7 days. The nodose neurons were grown in the presence of NGF, BDNF and NT-3 as described above. The cell cultures were fixed for 10 min with 4% paraformaldehyde in 0.1 M Na phosphate buffer pH 7.4, rinsed with PBS, and stored in

70% ethanol at -20°C. The cultured neurons were permeablized with ice cold 100% ethanol, rehydrated with PBS, and then pre-hybridized and hybridized as described above. We performed similar controls as described above with 400 fold excess unlabeled 5-HT_3R antisense probe, with RNase T1 pretreatment or with DIG-labeled sense 5-HT_3R probe.

Electrophysiology recordings and data analysis

5-HT-evoked current densities were measured with whole-cell patch-clamp techniques (Hamil et al., 1981). The currents were recorded at room temperature (22-24°C) using a List EPC-7 amplifier, filtered at 1.5 kHz with an eight-pole Bessel filter (Frequency Devices Inc.), then sampled at 5 kHz, displayed and stored on-line with a 386-based PC computer (AT class with EISA bus running at 33 MHz and a 64 K cache and A/D card; Omega). The program PATCHKIT (Alembic Software, Montreal) was used for data acquisition and analysis. Pipette resistances ranged from 2-6 MΩ and were balanced to zero with the pipette immersed in the perfusion solution. Neurons were voltage clamped at -60 mV, and 5-HT (100 μM or 1 mM) was applied using a rapid agonist application method as previously described (Mandelzys et al., 1995). Tetrodotoxin (TTX) was added to all solutions to eliminate unclamped Na^+ currents. In some nodose neurons, 5-HT application evoked a burst of TTX-insensitive Na^+ currents which were superimposed on 5-HT-evoked currents; however, because of the rapid time course of the Na^+ currents, they did not interfere with our ability to measure the amplitude of the 5-HT-evoked currents. The 5-HT-evoked current densities were calculated by dividing the peak current by the whole-cell capacitance; the whole-cell capacitance was obtained by integrating the capacity current evoked by a 5 mV hyperpolarizing pulse from a holding potential of -60 mV. The control perfusion solution consisted of 140 mM NaCl, 5.4 mM KCl, 0.33 mM NaH_2PO_4, 0.44 mM KH_2PO_4, 0.28 mM $CaCl_2$, 0.18 mM

$MgCl_2$, 10 mM HEPES, 5.6 mM glucose, 2 mM glutamine, 5 μg/ml phenol red, and 0.5 μM TTX (Sigma); pH was adjusted to 7.4. For drug application, we used an identical solution in which we added 5-HT (0.1-1 mM). The pipette solution contained 65 mM KF, 55 mM KAc, 5 mM NaCl, 1 mM $MgCl_2$, 10 mM EGTA, and 10 mM HEPES; pH was adjusted to 7.4. During the recording, the cultures were perfused at 1 ml/min with control perfusion solution.

Statistical analysis. The results are expressed as the mean ± standard error of the mean (SEM) and Student's *t* tests were used to assess statistical significance.

Results

We present our results on 5-HT_3R gene expression in neonatal SCG and nodose neurons in two parts: 1) during early postnatal development *in vivo*, and 2) as these neurons develop in culture.

5-HT_3R Gene Expression In Neonatal SCG And Nodose Neurons *In Vivo*

5-HT_3R mRNA levels increase in SCG during early postnatal development

We examined 5-HT_3R gene expression in rat SCG during the first 3 weeks of postnatal development using RNase protection assays (Fig. 2.1A). For each reaction, we assayed GAPDH mRNA levels as internal controls and quantified the hybridization signals with a phosphor imaging system. Figure 2.1B shows the changes in 5-HT_3R mRNA levels relative to those at P1. These results demonstrate that 5-HT_3R gene expression increases steadily over the first 3 postnatal weeks, such that by P21, the levels are 7.5 fold greater than at P1.

Figure 2.1. Developmental increase in 5-HT_3R mRNA expression in SCG. ***A,*** RNase protection assay for 5-HT3R and GAPDH mRNA expression in total RNA isolated from P1, P7, P14, and P21 rat SCG. 1 mg of total RNA was used for each reaction and the protected riboprobe sizes are 563 bases for 5-HT_3R and 316 bases for GAPDH. GAPDH mRNA expression was assessed to ensure that equal amounts of total RNA were used in each reaction. ***B,*** Quantification of 5-HT_3R mRNA expression in SCG: 5-HT_3R expression increases 7.5 fold during the first 3 weeks of postnatal life. ***C,*** This figure shows that when P1 SCG ganglia are denervated for 2 weeks, there is no significant change in 5-HT_3R mRNA expression, suggesting that innervation does not contribute to the observed developmental increase in 5-HT_3R expression. Each point represents the mean of 6-8 experiments and the error bars represent the SEM.

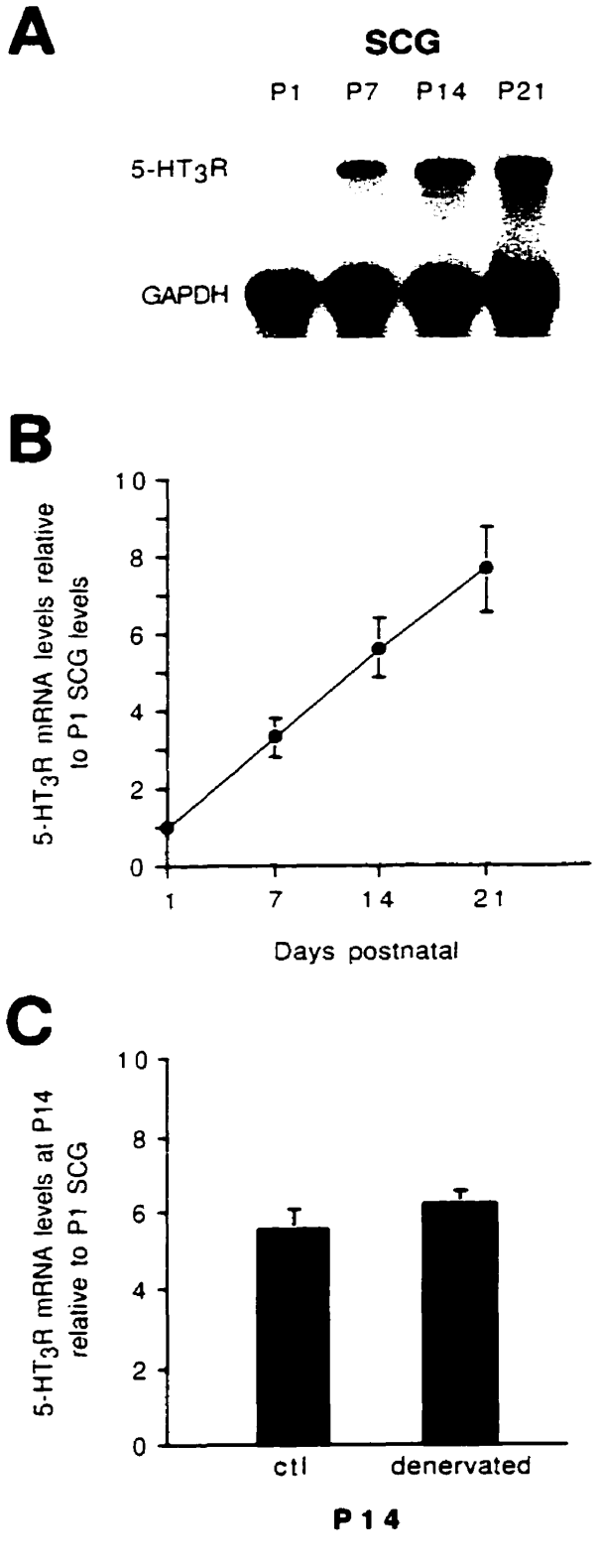
A
SCG
P1
P7
P14
P21
5-HT3R
GAPDH
B
5-HT3R mRNA levels relative to P1 SCG levels
10
8
6
4
2
0
1
7
14
21
Days postnatal
C
5-HT3R mRNA levels at P14 relative to P1 SCG
10
8
6
4
2
0
ctl
denervated
P14

To verify that 5-HT_3R transcripts are present only in neurons of the SCG ganglia, we dissociated P1 SCG, separated neurons from non-neuronal cells using a density gradient, and measured 5-HT_3R mRNA levels in both cell fractions. Our results indicated that these transcripts were detectable only in the neuronal fractions.

Influence of preganglionic innervation. During the first 3 postnatal weeks, preganglionic nerve terminals form 90% of their adult number of synapses on SCG neurons (Smolen and Raisman, 1980). To determine whether the increase in 5-HT_3R gene expression in SCG neurons during postnatal development is a consequence of increasing innervation, we cut the preganglionic nerve at P1, and measured 5-HT_3R mRNA levels in the denervated neurons 2 weeks later. We found that the 5-HT_3R mRNA levels in denervated neurons were not significantly different ($p>0.2$) from innervated contralateral or unoperated P14 SCG neurons (Fig. 2.1C). These results indicate that the developmental increase in 5-HT_3R gene expression in SCG neurons during the postnatal period does not require preganglionic innervation.

5-HT_3R transcripts are differentially expressed in SCG and nodose ganglia

To determine what proportion of neurons in the ganglia express 5-HT_3R transcripts, we carried out *in situ* hybridization experiments using DIG-labeled riboprobes. As one of the objectives of our study was to compare 5-HT_3R expression in sympathetic neurons with that in sensory neurons, we used tissue sections that included both the SCG and nodose ganglion (Fig. 2.2). Our results from P5 and P21 ganglia indicate that most SCG neurons express 5-HT_3R mRNA, and that the levels in these neurons increase with development, as we show quantitatively with RNase protection assays (see Fig. 2.1). Figure 2.2 also shows that nodose neurons contain abundant 5-HT_3R transcripts, consistent with previous studies reporting 5-HT_3R mRNA expression in embryonic nodose neurons (Tecott et al., 1995; Johnson and Heinemann, 1995). The medial neurons

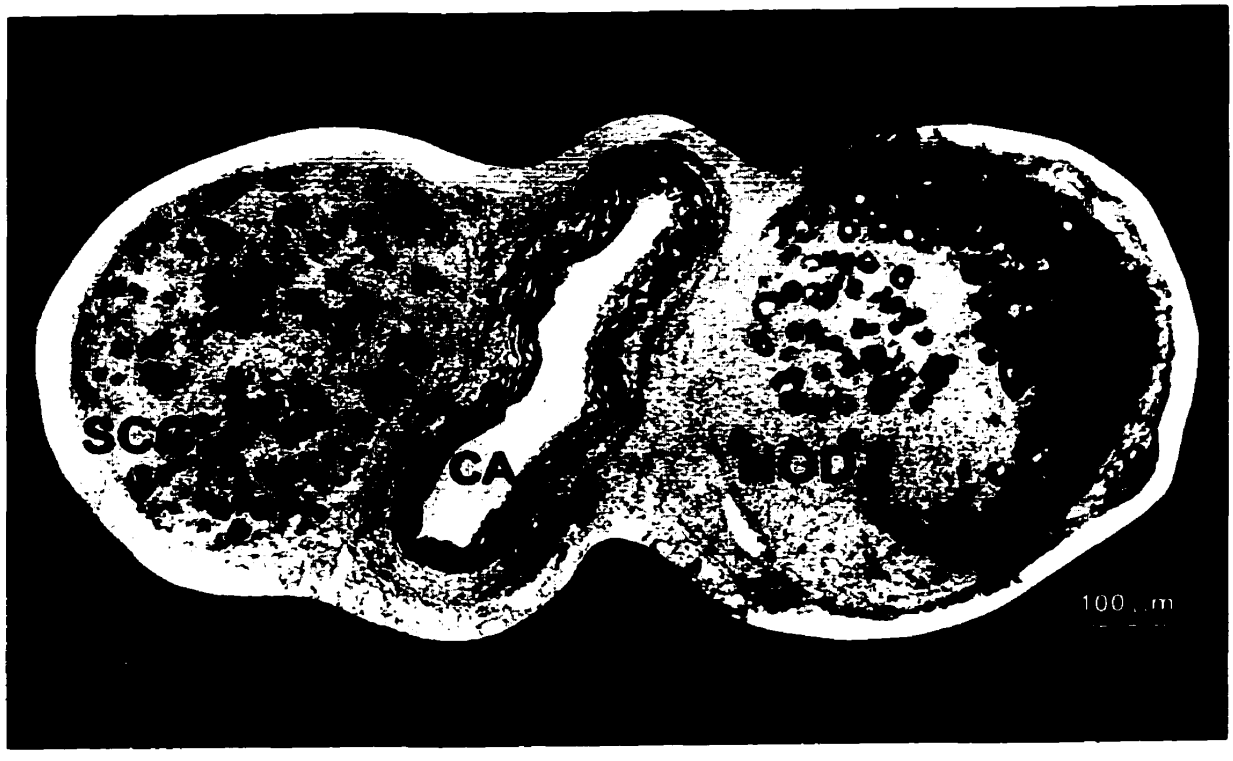

Figure 2.2. Differential 5-HT_3R mRNA expression in SCG and nodose neurons. *In situ* hybridization using DIG-labeled antisense 5-HT_3R probe on a section through P21 rat SCG, carotid artery (CA), nodose (NOD), and associated connective tissue. This figure is a montage of photomicrographs taken with a 20X objective and DIC optics on a Zeiss Axiovert 35 microscope. This figure shows that 5-HT_3R mRNA is expressed at high levels in most nodose neurons, at lower levels in most SCG neurons, and is not detectable in non-neuronal cells.

in nodose ganglia appear to have lower amounts of 5-HT_3R mRNA than the lateral neurons. In cat and rabbit, nodose neurons that project to specific targets are topographically organized within the ganglion (Mei, 1970; Portalier and Vigier, 1979; Donoghue et al., 1982). However comparable experiments have not been done in rat. Our results with *in situ* hybridizations also confirm that 5-HT_3R transcripts are present only in the neurons and not in the non-neuronal cells of either ganglia.

5-HT_3R mRNA levels in nodose neurons change little during early postnatal development

We quantified 5-HT_3R mRNA levels in nodose neurons during postnatal development using RNase protection assays (Fig. 2.3A and B). In contrast to the developmental increase observed in SCG, 5-HT_3R mRNA levels in nodose neurons change little over the first 3 postnatal weeks. To compare the expression between nodose and SCG, we normalized 5-HT_3R mRNA hybridization signals to those of GAPDH. At P1, we find that 5-HT_3R mRNA levels in nodose are over 14 fold greater (Fig. 2.3C and D); however, at P21, the 5-HT_3R mRNA levels in nodose are only 3 fold higher than in SCG (Fig. 2.3D) because, as we have shown above, the levels in SCG increase significantly during the first few weeks.

Our results indicate that regulation of 5-HT_3R gene expression in nodose neurons differs temporally from that in SCG neurons. To determine whether other sensory neurons regulate 5-HT_3R expression in a similar manner to nodose neurons, we measured 5-HT_3R mRNA levels in trigeminal ganglia. Our results indicate that, unlike nodose neurons, 5-HT_3R mRNA levels in trigeminal ganglia are low in P1 animals and increase steadily over the first 3 postnatal weeks , and are 4-5 fold greater at P21 (Fig. 2.3D). These results suggest that 5-HT_3R gene expression is not identical in all sensory neurons.

Figure 2.3. 5-HT_3R mRNA is highly expressed during early postnatal development in nodose ganglia. ***A***, RNase protection assay for 5-HT_3R mRNA expression performed as in Figure 1 on 1 μg of total RNA isolated from P1, P7, P14, and P21 rat nodose ganglia. ***B***, Quantification of 5-HT_3R mRNA expression in nodose: 5-HT_3R expression changes little during the first 3 weeks of postnatal development. ***C***, RNase protection assay depicting a comparison of 5-HT_3R mRNA expression in 1 μg of total RNA prepared from P1 and P21 nodose, SCG and trigeminal ganglia. ***D***, Quantification of 5-HT_3R mRNA expression in nodose, SCG and trigeminal ganglia at P1 and P21. Each point represents the mean of 6-8 experiments and the error bars represent the SEM. In P1 SCG, P1 nodose and P21 trigeminal, the error bars are too small to resolve. This figure shows that at P1 5-HT_3R expression is 14 fold higher in nodose than in SCG or trigeminal. However, in SCG and trigeminal, 5-HT_3R mRNA expression increases significantly during the first 3 postnatal weeks such that by P21, the levels in nodose are only 3 fold larger than in SCG and 4 fold larger than in trigeminal.

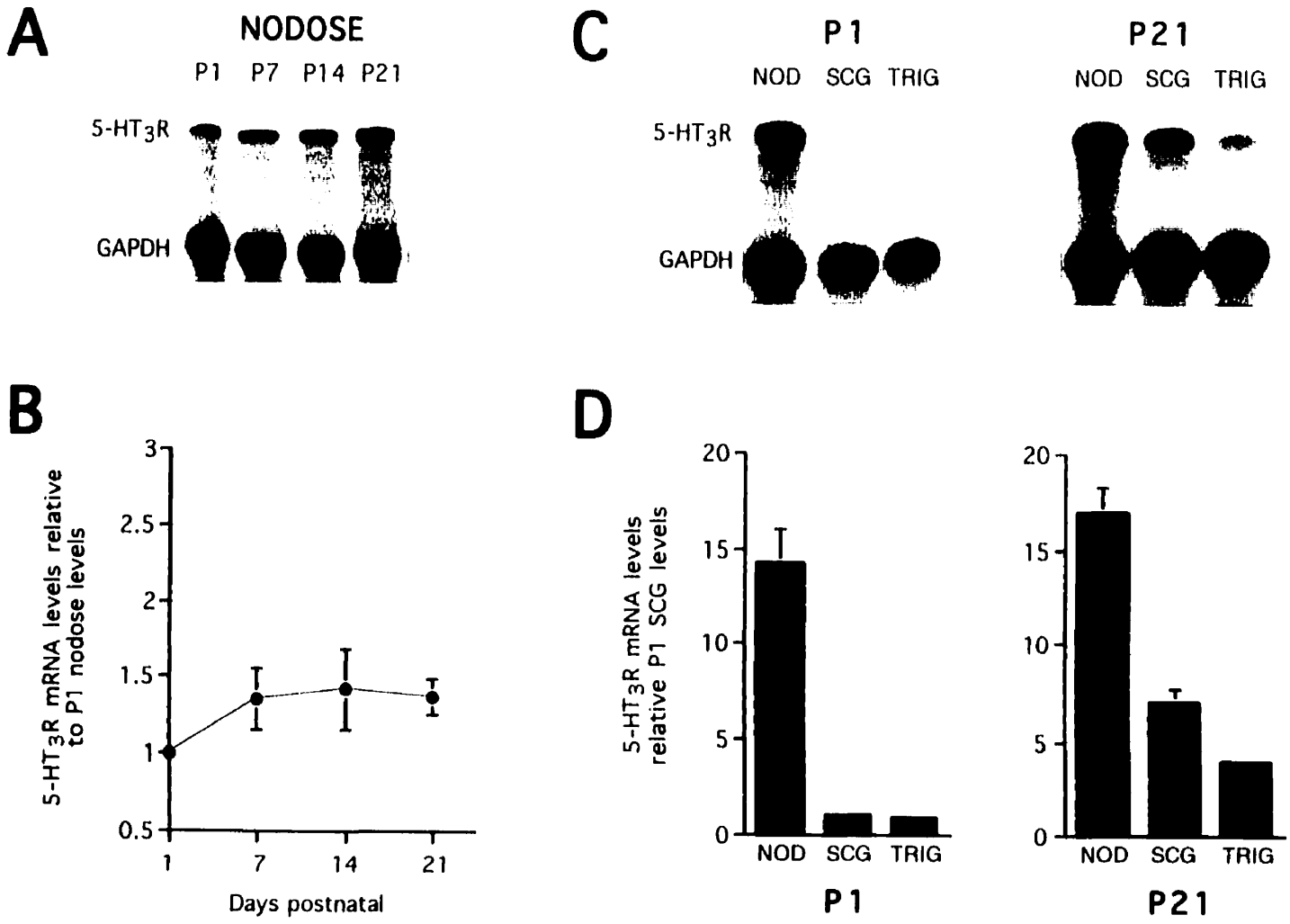
A
NODOSE
P1 P7 P14 P21
5-HT3R
GAPDH
C
P1
NOD SCG TRIG
P21
NOD SCG TRIG
5-HT3R
GAPDH
B
5-HT3R mRNA levels relative to P1 nodose levels
3
2.5
2
1.5
1
0.5
1 7 14 21
Days postnatal
D
5-HT3R mRNA levels relative P1 SCG levels
20
15
10
5
0
NOD SCG TRIG
P1
P21

Effects of axotomy

One factor known to regulate gene expression in peripheral sensory neurons is target innervation (Hökfelt et al., 1994a,b; Herdegen and Zimmerman, 1994). To determine whether target innervation influences 5-HT_3R transcripts levels in nodose neurons, we cut the vagus nerve distal to the ganglion, and then quantified 5-HT_3R mRNA levels in the axotomized neurons 24 hr later (Fig. 2.4). Cutting the vagus nerve in P0 animals resulted in a 60% decrease in 5-HT_3R mRNA levels relative to contralateral control neurons. This experiment was done also on P8 animals, and as we found a similar decrease after axotomy, we combined the results from both groups in Fig. 2.4B. These findings indicate that 5-HT_3R mRNA expression in postnatal nodose neurons depends on intact target innervation.

5-HT_3R Gene Expression In Neonatal SCG And Nodose Neurons In Culture

Most nodose and SCG neurons developing in culture express 5-HT_3R mRNA

To learn more about the regulation of 5-HT_3R gene expression in peripheral neurons, we investigated sympathetic and nodose neurons developing in culture. Figure 2.5 shows examples of *in situ* hybridization experiments using DIG-labeled 5-HT_3R probes on P1 nodose and SCG neurons that had developed in culture for 1 week in the virtual absence of ganglionic non-neuronal cells. Figure 2.5 shows that most SCG and nodose neurons in these cultures express 5-HT_3R transcripts. To demonstrate that the hybridization signals represent specific 5-HT_3R transcripts, we preincubated nodose cultures with 400 fold excess unlabeled antisense 5-HT_3R cRNA which competitively blocked hybridization of the DIG-labeled antisense 5-HT_3R riboprobe (Fig. 2.5C). In addition, pretreatment of the cultures with RNases prevented antisense riboprobe hybridization; similarly, DIG-labeled sense riboprobes did not hybridize.

Figure 2.4. 5-HT_3R gene expression in nodose neurons depends on intact target innervation. ***A***, RNase protection assay performed as in Figure 1 on 1 μg of total RNA prepared from P1 nodose ganglia that were axotomized 24 hr earlier and from control contralateral P1 nodose ganglia. ***B***, Mean (± SEM) 5-HT_3R mRNA levels for axotomized P1 and P9 nodose ganglia are significantly different from control contralateral ganglia ($p<0.001$, $n=12$).

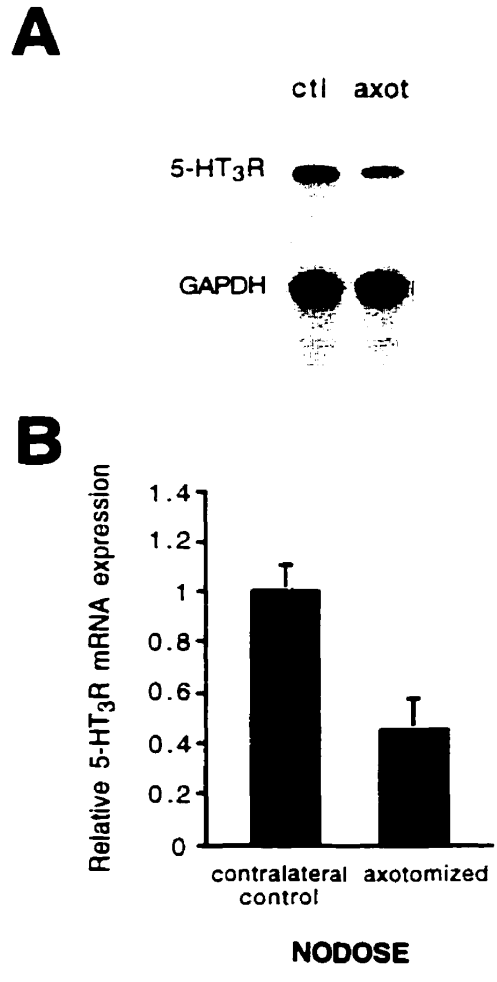
A
ctl
axot
5-HT3R
GAPDH
B
Relative 5-HT3R mRNA expression
1.4
1.2
1
0.8
0.6
0.4
0.2
0
contralateral control
axotomized
NODOSE

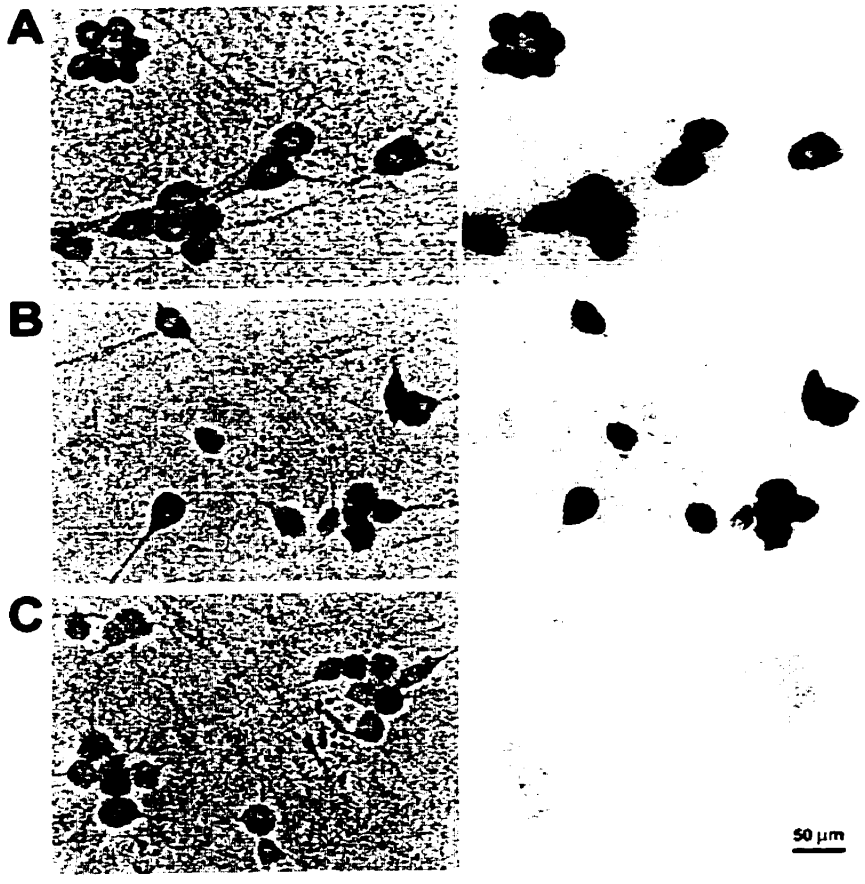

Figure 2.5. Most SCG and nodose neurons in culture express 5-HT_3R transcripts. *In situ* hybridization using DIG-labeled riboprobe for 5-HT_3R mRNA expression in P1 SCG and nodose neurons grown in culture for 7 days: *A*, SCG; *B*, nodose; and *C*, control, nodose neurons prehybridized with 400 fold excess unlabeled antisense 5-HT_3R probe. Phase contrast (left) and DIC (right) photomicrographs were taken with a 40X objective on a Zeiss Axiovert 35 microscope. 5-HT_3R mRNA is expressed by most D7 SCG and D7 nodose neurons.

5-HT_3R gene expression increases in neonatal SCG neurons developing in culture

Figure 2.6 shows that 5-HT_3R mRNA levels increase in P1 SCG neurons developing in culture. The specific increase in 5-HT_3R mRNA levels in cultured neurons is greater than that *in vivo*: after 7 days in culture, transcript levels have increased 9 fold, whereas after a similar time *in vivo* there is only a 3 fold increase (see Fig. 2.1B). This difference may reflect either that a factor(s) in these cultures stimulates 5-HT_3R gene expression, or that an extrinsic factor(s) *in vivo* modulates its expression.

5-HT_3R gene expression decreases rapidly and transiently in cultured nodose neurons

As neonatal rat nodose neurons express mRNA for *trk*A, *trk*B, *trk*C and p75 receptors, we grew P1 nodose neurons in culture under conditions similar to those of SCG neurons, except that we supplemented the growth media with BDNF and NT-3 in addition to NGF (all at 25 ng/ml). Within 24 hr after plating, 5-HT_3R mRNA levels in cultured nodose neurons drop to 30% of initial values (Fig. 2.7A). In early experiments, we supplemented the media with only NGF or BDNF and observed similar decreases. This rapid decrease in 5-HT_3R mRNA levels is similar to that observed in axotomized neurons *in vivo*, and presumably occurs because the axons of these neurons are cut when the neurons are placed in culture.

Lack of effect of elevated K^+ on the initial decrease. In a previous study, we observed a significant decrease in mRNA levels for the α_7 neuronal nicotinic acetylcholine receptor (nAChR) subunit in cultured SCG neurons (De Koninck and Cooper, 1995), similar to the decrease we observed in 5-HT_3R mRNA levels in cultured nodose neurons. We showed that the decrease in α_7 mRNA in SCG neurons could be

Figure 2.6. Developmental expression of 5-HT_3R transcripts by neonatal SCG neurons in culture. ***A***, RNase protection assay performed as in Figure 1 on 1 μg of total RNA extracted from freshly dissociated SCG (day 0) neurons and SCG neurons grown in culture for 2, 4, and 7 days. ***B***, Quantification of 5-HT_3R mRNA in cultured SCG neurons relative to D0. Each point represents the mean of 6-8 experiments and the error bars represent the SEM.

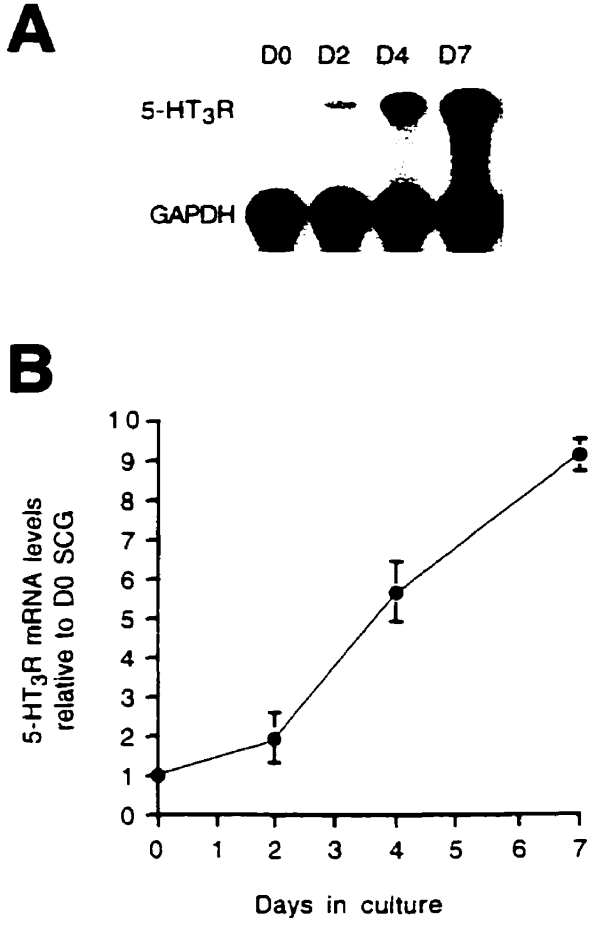
A
D0 D2 D4 D7
5-HT3R
GAPDH
B
5-HT3R mRNA levels relative to D0 SCG
0 1 2 3 4 5 6 7 8 9 10
0 1 2 3 4 5 6 7
Days in culture

Figure 2.7. 5-HT_3R mRNA levels decrease transiently in neonatal nodose neurons in culture. ***A***, RNase protection assay and quantification performed as in Figure 1 on 1 μg of total RNA extracted from freshly dissociated nodose (day 0) neurons and nodose neurons grown in culture in the presence of NGF, BDNF, and NT-3 for 2, 4, 7, and 14 days. ***B***, Quantification of 5-HT_3R mRNA in cultured nodose neurons relative to P1: freshly dissociated (D0), with neurotrophins (+NT) for 48 hr, without neurotrophins (-NT) for 48 hr, with 40 mM K^+ (K^+) for 48 hr, with cycloheximide for 24 hr (D1 24 hr CycloHex). ***C***, Quantification of 5-HT_3R mRNA in cultured nodose neurons relative to D2 measured at D7. Nodose neurons were grown for 2 days without neurotrophins (-NT), then grown for 5 additional days with or without neurotrophins. 5-HT_3R mRNA levels in nodose neurons after 5 days in neurotrophins were significantly greater ($p<0.001$) than neurons grown in the absence of neurotrophins. Each data point represents the mean of 3 separate cultures and each RNA sample was assayed twice; the error bars represent the SEM.

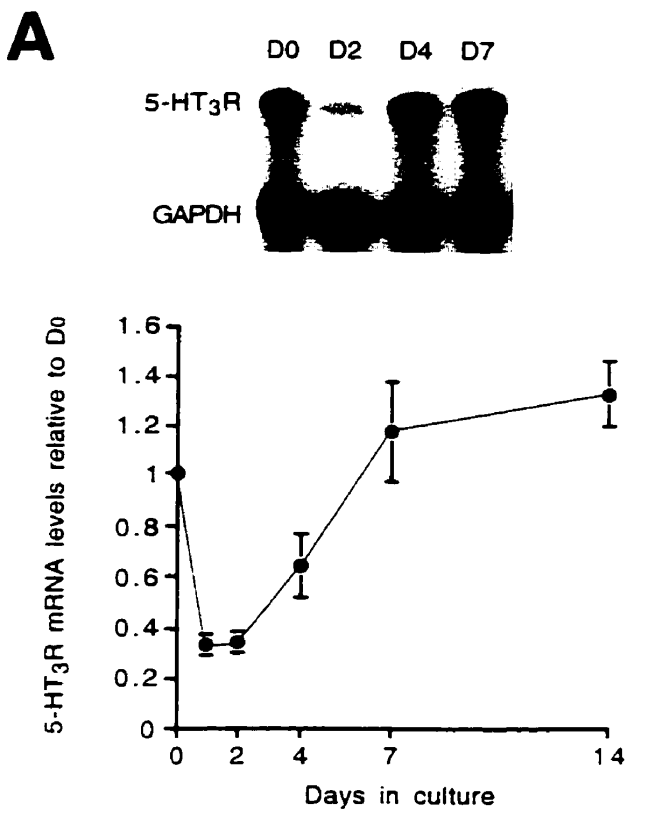
A
D0 D2 D4 D7
5-HT3R
GAPDH
5-HT3R mRNA levels relative to D0
1.6
1.4
1.2
1
0.8
0.6
0.4
0.2
0
0 2 4 7 14
Days in culture
B
5-HT3R mRNA levels relative to P1
1.2
1
0.8
0.6
0.4
0.2
0
D0 +NT -NT K+ D1 24 hr cyclohex
D2

C

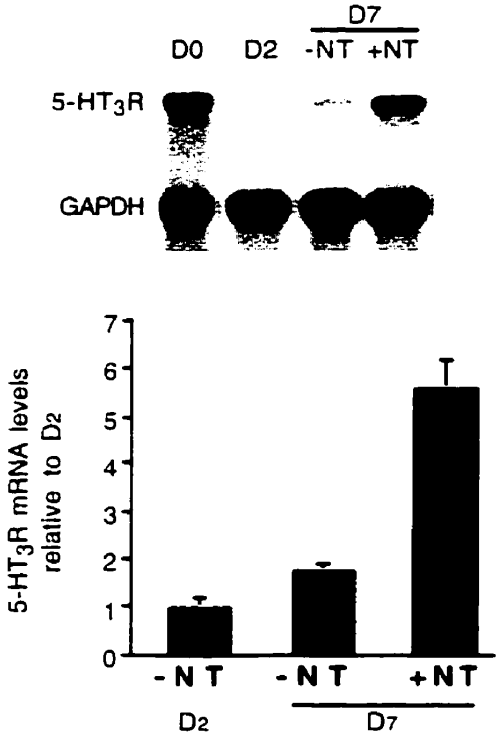
D7
D0
D2
-NT
+NT
5-HT3R
GAPDH
5-HT3R mRNA levels relative to D2
7
6
5
4
3
2
1
0
-NT
-NT
+NT
D2
D7

prevented by culturing the neurons in elevated (40 mM) K^+; the resultant depolarization increased intracellular Ca^{2+} levels and increased α_7 mRNA levels by activating a Ca^{2+}/calmodulin-dependent kinase (CaM kinase) pathway (De Koninck and Cooper, 1995). To test whether similar mechanisms regulate 5-HT_3R gene expression, we cultured nodose neurons in elevated K^+; however, this did not prevent the rapid drop in 5-HT_3R mRNA levels (Fig. 2.7B), indicating that increases in intracellular Ca^{2+} are unlikely to regulate 5-HT_3R mRNA levels in cultured nodose neurons.

The decrease 5-HT_3R mRNA levels requires protein synthesis. We added cycloheximide, a protein synthesis inhibitor, to cultures of P1 nodose neurons for the first 24 hr after plating: this treatment largely prevented the drop in 5-HT_3R mRNA levels, indicating that this decrease in nodose neurons is an active process that depends on *de novo* protein synthesis (Fig. 2.7B). In addition, treating neurons with cycloheximide for only the first 10 hr partially prevented the drop in 5-HT_3R mRNA levels: the levels were 45% of initial levels after 24 hr, and 58% of initial levels after 48 hr in culture.

Interestingly, SCG neurons grown in culture show no such decrease in mRNA levels; this observation further demonstrates that 5-HT_3R gene expression is differentially regulated in these two types of neurons.

Neurotrophins increase 5-HT_3R gene expression in cultured nodose neurons

We observed that the decrease in 5-HT_3R mRNA levels in cultured nodose neurons is transient: after 2 days in culture, transcript levels begin to increase, and after 7 days in culture, 5-HT_3R mRNA levels are above their initial levels (Fig. 2.7A). Since the neurotrophins NGF, BDNF and NT-3 were present in these cultures, we asked whether these neurotrophins stimulated the delayed increase in 5-HT_3R gene expression. As nodose neurons do not require exogenously supplied neurotrophins to grow in culture

(Mandelzys and Cooper, 1992; De Koninck et al., 1993), we grew P1 nodose neurons for 2 days without neurotrophins, allowing the drop in 5-HT_3R mRNA to occur, and then we divided the cultures into three groups. We used one group to measure 5-HT_3R mRNA levels at D2. We added 25 ng/ml of NGF, BDNF and NT-3 to the second group and allowed the neurons to grow for an additional 5 days. We grew the third group for an additional 5 days in the absence of neurotrophins. The number of neurons in all three groups did not differ by more than 10%. In the group receiving neurotrophins, the 5-HT_3R mRNA levels at D7 were 4.5 fold greater than those at D2 (Fig. 2.7C), whereas in the group that did not receive neurotrophins, the levels were only 1.3 fold greater than those at D2. These results suggest that neurotrophins stimulate 5-HT_3R expression in these neurons.

Correlation of 5-HT_3R mRNA levels with 5-HT-evoked current densities

To determine whether changes in 5-HT_3R gene expression affect the appearance of functional 5-HT_3Rs on these neurons, we measured 5-HT-evoked currents on P1 nodose and SCG neurons developing in culture (Fig. 2.8A). We examined nodose neurons at two different times: early, after 1-3 days in culture when 5-HT_3R mRNA levels in these neurons are low; and after 6-14 days in culture when 5-HT_3R mRNA levels are 4-5 fold larger. Figure 2.8B shows the mean 5-HT-evoked current densities for nodose neurons in cultured for 1-3 days (n=36) and for 6-14 days (n=25), and indicates that 5-HT-evoked current densities increase with time in culture. After 1-3 days in culture, 83% of neurons (30/36) had 5-HT-evoked current densities below detectable levels (<1 pA/pF) whereas the mean 5-HT-evoked current density of the remaining 17% was 12.7 pA/pF ± 2.6 (SEM). In comparison, after 6-14 days in culture, only 20% of neurons (5/25) had current densities less than 1 pA/pF; the mean 5-HT-evoked current density of the remaining 80% was 36.5 pA/pF ± 6.9 (SEM). These results demonstrate that changes in 5-HT_3R gene expression correlate directly with the appearance of functional 5-HT_3Rs on nodose

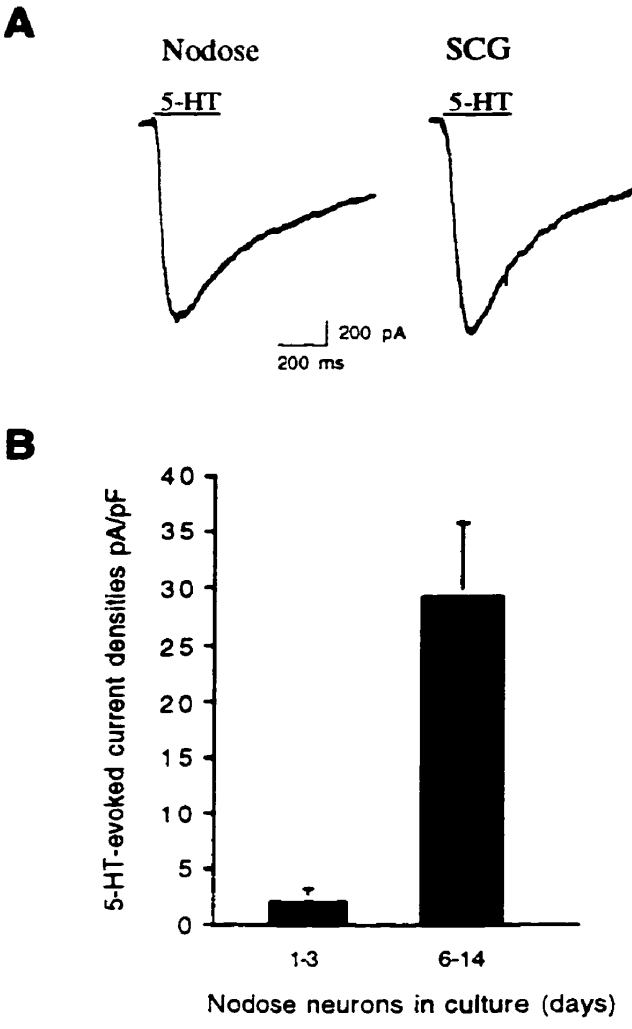

Figure 2.8. Nodose and SCG neurons express 5-HT-evoked currents. 5-HT-evoked currents were recorded from P1 nodose and SCG neurons grown in culture. *A*, Examples of 5-HT-evoked currents from D6 nodose and D7 SCG neurons. *B*, mean 5-HT current densities (pA/pF) in nodose neurons grown for 1-3 days (n=36) and 6-14 days (n=25); the error bars represent the SEM.

neurons. We found a similar correlation for SCG neurons: most SCG neurons in culture for 1-3 days had small 5-HT-evoked current densities, and these 5-HT-evoked currents densities increased over the first week in culture.

Discussion

In this study, we have investigated factors and mechanisms that influence 5-HT_3R expression as sympathetic and nodose neurons differentiate during early postnatal life, a time when many autonomic reflexes become active. By comparing sympathetic and nodose neurons, we have identified cell-type specific mechanisms that regulate 5-HT_3R gene expression during neonatal development and as the neurons differentiate in culture. These mechanisms are likely to play a role in determining the appropriate spatial and temporal expression of 5-HT_3Rs in sensory and sympathetic neurons during early postnatal life.

Our results demonstrate that neonatal nodose and SCG neurons differ in 5-HT_3R mRNA expression. This differential expression may be due to the embryological origins of these two neuronal populations: SCG neurons originate from the neural crest while nodose neurons are derived from the placodes (Le Douarin, 1984). Nodose neurons *in vivo* express high levels of 5-HT_3R mRNA: at P1, the levels are 14 fold greater than in SCG neurons, and change little over the first 3 postnatal weeks. Presumably, these high levels ensure that nodose neurons express appropriate densities of functional 5-HT_3Rs at birth. The 5-HT_3R mRNA levels in sympathetic neurons increase 7.5 fold during the first 3 weeks of postnatal development. This increase may be related to increasing sympathetic target innervation during this neonatal period (Black, 1978). Less is known about the postnatal development of target innervation by rat nodose neurons. The lack of change in 5-HT_3R mRNA levels in nodose neurons during the first 3 postnatal weeks suggests

either: 1) that similar factors regulate 5-HT_3R expression in SCG and nodose neurons and that target innervation by vagal afferent neurons is essentially complete by birth; or 2) that both types of neurons are increasing their target innervation during neonatal development, yet the factors that regulate 5-HT_3R gene expression in nodose and SCG neurons are different.

The increase in 5-HT_3R mRNA levels in SCG neurons *in vivo* is much greater than the increase in neuronal nAChR subunit transcripts expressed by these neurons. We showed previously that the expression of the α_3 and α_7 nAChR subunits increases 4 and 3 fold, respectively, over a similar postnatal period, whereas the expression of the other nAChR subunits, β_2, β_4 and α_5, does not change significantly (Mandelzys et al., 1994). This indicates that in SCG neurons the regulation of 5-HT_3R gene expression differs from that of nAChR subunits. In addition, we show that the developmental increase in 5-HT_3R mRNA levels, like that for nAChR transcripts (Mandelzys et al., 1994), is not dependent on preganglionic innervation; this suggests that neither electrical activity nor factors derived from the preganglionic nerve terminals stimulate 5-HT_3R expression in these neurons.

Surprisingly, we observed a significantly greater increase in 5-HT_3R gene expression when neonatal SCG neurons develop in culture compared to when they develop *in vivo*: after 1 week in culture, 5-HT_3R mRNA levels increase 9 fold versus a 3 fold increase over the same time period *in vivo*. The greater stimulation of 5-HT_3R expression in cultured SCG neurons presumably results from either the removal of an inhibitory influence present *in vivo*, the addition of stimulatory factors to the cultures, or a combination of both. The greater increase in 5-HT_3R expression in cultured SCG neurons cannot be explained by changes in *trk*A or p75 receptor expression (unpublished results).

When neonatal nodose neurons develop in culture in the presence of neurotrophins, 5-HT_3R mRNA levels drop by 70% in 24 hr, begin to increase after 48 hr, and are above initials levels after 1 week. This relatively rapid biphasic change in 5-HT_3R mRNA levels

was unexpected as we did not observe a similar change in SCG neurons or with nodose neurons developing *in vivo*. We show that this increase in 5-HT_3R expression after 48 hr in culture is mediated by neurotrophins. The increase in 5-HT_3R expression cannot be explained by changes in neurotrophin receptor expression by nodose neurons over this time in culture. Since neurotrophins are released from non-neuronal cells in degenerating peripheral nerve stumps after axotomy (Heumann et al., 1987; Raivich et al., 1991), as well as from target tissues, this mechanism could ensure that, after a brief delay (24 hr), regenerating nodose axons will continue to express 5-HT_3R. Conceivably, neurotrophins also play a role in regulating 5-HT_3R expression in SCG neurons.

The initial rapid drop 5-HT_3R mRNA levels is likely due to the effects of axotomy since the axons of these neurons are cut when they are placed in culture. We show that cutting the peripheral branch of nodose axons in neonatal animals results in a rapid 60% decrease in 5-HT_3R mRNA levels in 24 hr. The decrease we observed in cultured neurons is greater than that in axotomized neurons *in vivo*, presumably because in cultured nodose neurons both the central and peripheral axons were cut. This indicates that the high 5-HT_3R transcript levels in developing nodose neurons are actively maintained by mechanisms that depend on intact innervation, possibly involving target-derived factors, similar to what has been shown for nAChRs in chick ciliary neurons (Jacob and Berg, 1987; Levey et al. 1995; Levey and Jacob, 1996). Similar decreases in mRNA and protein levels have been reported for a number of neuropeptides and their receptors following axotomy of sensory neurons, and the decrease of many of these proteins can be prevented by target-derived factors (Hökfelt et al, 1994a,b; Herdegen and Zimmerman, 1994). However, we show that the rapid drop in 5-HT_3R mRNA levels in cultured nodose neurons is not prevented by neurotrophins, suggesting that cutting the axons may initiate events that actively decrease 5-HT_3R mRNA levels in nodose neurons.

Our results on culturing nodose neurons in elevated K^+ indicate that chronic depolarization and the resulting increase in intracellular Ca^{2+} do not prevent the drop in

5-HT_3R mRNA levels. These experiments suggest that the rapid drop in 5-HT_3R mRNA levels in cultured nodose neurons, and presumably after axotomy *in vivo,* is not a result of Ca^{2+}-dependent second messenger pathways. When we treat nodose cultures with cycloheximide, a protein synthesis inhibitor, the initial decrease in 5-HT_3R mRNA levels is largely prevented, suggesting that this decrease is an active process that requires *de novo* protein synthesis.

Our results indicate that the biphasic change in 5-HT_3R mRNA levels in cultured nodose neurons represents the net effect of two separate processes that regulate gene expression: one triggered by axotomy that decreases 5-HT_3R mRNA levels, and the other mediated by neurotrophins that increases the levels. Since the drop occurs during the first 24 hr, even in the presence of neurotrophins, the events initiated by axotomy in nodose neurons must outweigh the stimulatory effects of neurotrophins, but are short lived. We did not observe any decrease in 5-HT_3R mRNA levels in cultured SCG neurons. One possible explanation is that the stimulatory effects of neurotrophins on sympathetic neurons override the effects of axotomy. A second possibility is that sympathetic neurons differ from sensory neurons in their response to axotomy.

To address whether changes in 5-HT_3R gene expression affect the appearance of functional 5-HT_3Rs, we measured 5-HT-evoked currents on nodose and SCG neurons in culture. Our electrophysiological results indicate that changes in 5-HT_3R mRNA levels correlate well with the appearance of functional 5-HT_3R on these neurons. For nodose neurons, after 1-3 days in culture, when 5-HT_3R mRNA levels are low, we found that few neurons had detectable 5-HT-evoked currents, whereas 6-14 days later over 80% had detectable 5-HT-evoked currents. Similar results were observed for SCG neurons in culture. Our results demonstrate that changes in 5-HT_3R gene expression directly reflect changes in the appearance of functional receptors.

Chapter 3

Adenoviral Vectors are Efficient Gene Transfer Agents for Sympathetic Neurons

Introduction

Cooper and colleagues have previously shown that rat sympathetic neurons express five different nAChR subunits: α3, α5, α7, β2 and β4 (Mandelzys et al., 1994). Their data indicate that most nAChRs on sympathetic neurons are likely to contain α3, β2 and β4 in the same receptor complex (Mandelzys et al., 1995). However, the subunit composition of nAChRs on these neurons has not been definitively established. Therefore, to investigate the contribution of specific subunits to the appearance of ACh-evoked currents, my objective is to alter nAChR subunit expression in sympathetic neurons and determine how these changes influence the physiology of functional receptors. Specifically, my goal is to manipulate nAChR subunit expression by overexpressing either sense or antisense cDNA constructs coding for the different nAChR subunits. However, achieving efficient gene transfer into neurons is difficult. Until recently, there were few reports of successful gene transfer into neurons and none on ectopically expressing ion channels in neurons. Therefore, to carry out my studies on nAChRs, first I modified existing gene transfer procedures and adapted them for rat sympathetic neurons. In this chapter, I present the results of these experiments.

The development of efficient gene delivery systems for the nervous system is an essential tool for basic neurobiological research. The ability to express foreign proteins or to overexpress endogenous proteins in primary neurons provides an important means to investigate the role of numerous proteins in neuronal function. Furthermore, the development of efficient gene transfer procedures is a prerequisite for gene therapy of neurodegenerative diseases and CNS malignancies. Efficient gene transfer into neurons *in vivo* or in culture is difficult because neurons are generally resistant to transfection by the methods that work well for established cell lines (Castro et al., 1996). However, with the

recent development of replication defective viral vectors, such as HSV and Ad vectors, it is now possible to manipulate gene expression in the nervous system.

In this study, my objective is to develop efficient procedures to introduce foreign genes into mammalian neurons in culture in a manner that is not toxic to the cell.

Materials and Methods

Neuronal cultures

Primary cultures of postnatal day 1 (P1) rat sympathetic SCG neurons and sensory trigeminal neurons were prepared according to the procedures described in Chapter 2. Briefly, SCG and trigeminal neurons were plated at densities of 4000-8000 cells/cm^2 in modified 35 mm petri dishes. These modified dishes were created by boring either a 0.5 cm or a 1.5 cm hole in the center of the dish, and then gluing aclar (Allied Chemicals) cover slips from underneath with silicone rubber (3140 MIL-A-46146 RVT coating, Dow Corning); this created a 2 mm deep well with a volume of ≈30 µl for the 0.5 cm diameter wells and ≈200 µl for the 1.5 cm diameter wells. Neuronal cultures in 0.5 cm wells were preferentially used for experiments involving X-gal histochemistry or GFP fluorescence (see below) while cultures in 1.5 cm wells were used for experiments involving RNA measurements. For both SCG and trigeminal neuron cultures, the growth media (see Chapter 2) was supplemented with nerve growth factor (2.5S NGF, 25 ng/ml). The SCG and trigeminal neuron cultures were treated with cytosine arabinofuranoside (Ara-C, 10 µM), an anti-mitotic agent, for the first 2-3 days in culture. Ara-C killed the faster growing satellite and Schwann cells, leaving only a few slowly dividing fibroblast-like cells.

HEK 293 cell cultures

Low passage HEK 293 cells were obtained from Dr. Phil Branton (McGill University) and maintained in α-MEM media supplemented with 10% fetal bovine serum, α-MEM non-essential amino acids, α-MEM essential vitamins, 2.5 μg/ml Fungizone, 2 mM L-glutamine, 100 U penicillin and 0.1 g/ml streptomyocin (all ingredients were purchased from Gibco BRL). When 80-90% confluent, the cells were harvested using citric saline (135 mM KCl, 15 mM Na citrate) and then replated at 1/3 to 1/5 of their original density. Cells were refed with fresh media every 3 days. The cells were grown at 37°C in a 5% CO_2 humidified incubator.

Plasmids

For Ca^{2+}phosphate- and liposomes-mediated transfection experiments, the β-galactosidase (β-gal) expressing plasmid pCH110 (Pharmacia) was used as a marker for transfection efficiency. In certain experiments with liposomes, we used the full length rat α3 nAChR cDNA cloned into the mammalian expression vector pcDNA1neo (Invitrogen) (gift of Dr. Philippe Séguéla, Montreal Neurological Institute). For the construction of recombinant Ades, the plasmid pJM17 was generously given to us by Dr. Phil Branton while the plasmid pCA13 was purchased from Microbix (Toronto, Ontario). The plasmid pGREENLANTERN (Gibco BRL) was obtained from Dr. John Marshall, Brown University. All plasmid stocks were amplified in the *Escherichia coli* (*E. coli*) strains DH5αF' or MC1061/P3 and purified by standard $CsCl_2$ banding protocols (Sambrook et al., 1989) or with Plasmid Maxi Kits (Qiagen).

Ca^{2+}phosphate and liposome transfection procedures

Ca^{2+}phosphate-mediated transfection was performed using a modified version of the protocol described by Graham and Van der Eb (1973)(Sambrook et al., 1989). Briefly, 5-

20μg of sterile plasmid DNA in 1 ml of 0.25 M $CaCl_2$ was slowly mixed with 1 ml of sterile 2XHBSS (42 mM HEPES, 0.275 M NaCl, 10 mM KCl, 1.4 mM Na_2HPO4, 11 mM glucose, pH 7.1) and allowed to stand at room temperature for 0.5-1 hr during which time a fine Ca^{2+}phosphate-DNA precipitate formed. Next, 10-30 μl of this precipitate solution was applied to the center well of culture dishes containing SCG neurons. After 4-16 hr, the neurons were then fed with fresh media.

Liposome-mediated transfection was performed on cultured P1 SCG and trigeminal neurons using either Lipofectamine (Gibco BRL), DOTAP or DOTAP:DOTMA (1:1) (both gifts of Dr. John Silvius, McGill University). Transfection efficiencies were tested for different DNA:lipid ratios (μg:μg) for Lipofectamine: 1:10, 1:4, 1:2 and 1:1, and for DOTAP and DOTAP:DOTMA: 1:20, 1:10, and 1:5. I also tested increasing amounts of DNA:lipid, ranging from 25 ng to 100 ng DNA with the corresponding amounts of lipid. I used sterile polystyrene tubes to mix the DNA and lipids in serum-free L15 growth media, supplemented with NGF. In some conditions, normal serum was added to the L15 media to determine whether it would improve transfection efficiency. The liposome mixture was added to the neurons for 3 hr and then the neurons were refed with normal growth media. In a time course experiment, liposomes were added for 3, 6, 12 and 24 hr. Except for the time course experiment, all of these experiments were repeated 2 or more times.

Typically, the neurons were transfected 3 days after plating and allowed to grow for an additional 2-5 days prior to fixing and staining for β-gal expression (see below) or harvesting RNA.

X-gal histochemistry assay

X-gal histochemistry assays were performed according to Bondi et al. (1982). Briefly, neuronal cultures were fixed for 10 min in 2% paraformaldehyde, 0.2%

gluteraldehyde in 0.1 M Na phosphate buffer pH 7.3, washed 3X with PBS (15 mM Na phosphate buffer pH 7.3, 150 mM NaCl) and then incubated in an X-gal stain composed of 1 mg/ml X-gal (Promega), 3 mM $K_3Fe(CN)_6$, 3 mM $K_4Fe(CN)_6$, 1.3 mM $MgCl_2$, and 0.1 M Na phosphate buffer pH 7.3. The cells were incubated in the X-gal stain at room temperature in the dark for up to 24 hr. The reaction was stopped by rinsing the cells with PBS supplemented with 1 mM EDTA.

RNA preparation and RNase protection assays

RNA was prepared from cultures of trigeminal neurons as described in Chapter 2. Some RNA samples were treated with DNase I (0.5 U/μl; Pharmacia) to remove traces of DNA. RNase protection assays were performed as described in Chapter 2. Antisense ^{32}P-UTP-labeled RNA probes to rat α3 nAChR and rat potassium channel Kv3.4 were transcribed *in vitro* using SP6 and T3 RNA polymerase respectively. The α3 probe was synthesized from a linearized plasmid containing the rat nAChR cDNA clone. The full length α3 riboprobe was 299 bases while the protected probe length was 238 bases. We assessed the expression of Kv3.4 in these RNA samples to verify whether equal amounts of RNA were used for each reaction; Kv3.4 is expressed at moderate levels in rat trigeminal neurons (A. Fraser and E. Cooper, unpublished results). The full length Kv3.4 riboprobe was 424 bases in length while the protected probe length was 393. The thermal stabilities of all the probes, based on their melting temperatures, were found to differ by less than 1°C. Each hybridization reaction was performed with 1μg of total cellular RNA and 100 000 cpms of both riboprobes. The acrylamide gels were dried and exposed to X-ray film (Kodak XAR).

Virus rescue: building recombinant adenoviruses

A recombinant replication defective Ad expressing GFP was built using a plasmid-based technique developed by Dr. Frank Graham (McMaster University, Hamilton, Ontario) (Graham and Prevec, 1991; Hitt et al., 1995). The plasmid-based approach involved the *in vivo* recombination of a shuttle plasmid containing the gene of interest flanked by Ad5 sequences and a large plasmid that contained essentially the entire Ad5 genome except for E1 sequences (Fig. 3.1). Two additional replication defective Ad vectors expressing sense and antisense α3 nAChR subunit mRNA were also developed using this method and are described in the following chapter.

Subcloning GFP into the shuttle vector. Briefly, the GFP cDNA was excised from the vector pGREENLANTERN and subcloned into the polycloning site of the shuttle plasmid pCA13. This shuttle plasmid contains a bacterial origin of replication, the gene for ampicilin resistance and the first 6.6 kb of the leftward Ad genome except for a 3.1 kb deletion in the E1 region (Hitt et al., 1995; see Chapter 1). Into the deleted E1 region, the human cytomegalovirus immediate-early gene (HCMV) promoter, a versatile polycloning site, and the SV40 polyadenylation signal have been inserted in a parallel orientation with respect to the E1 transcription unit; this orientation results in significantly higher gene expression than the antiparallel orientation, even in the presence of a strong promoter (Hitt et al., 1995). To ensure that GFP was correctly cloned into pCA13, this construct, denoted as pCA13GFP, was transiently transfected into HEK 293 cells by the Ca^{2+}-phosphate-DNA precipitation method, and the expression of GPF was verified 2 days later by fluorescence microscopy (see below).

Co-transfection and virus rescue. Next, the shuttle plasmid, pCA13GFP, and a large plasmid called pJM17 containing essentially the entire Ad5genome except for certain E1 sequences, were co-transfected into low passage HEK 293 cells (Fig. 3.1).

Figure 3.1. Schematic outline of the plasmid-based method for generating replication defective recombinant adenoviruses. ***A***, The gene of interest is first subcloned into the shuttle plasmid pCA13. ***B***, Next, this shuttle plasmid containing the gene of interest is co-transfected into HEK 293 cells along with pJM17, a large circular plasmid that contains most of the Ad5 genome except for deletions in E1 genes. *In vivo* recombination between a 2 kb sequence common to both plasmids generates a replication defective E1-deleted viral DNA molecule. Because HEK 293 cells express the missing E1 genes, recombinant viral DNA molecules are packaged into virions; such recombinant adenoviruses are unable to replicate in all cell types except in HEK 293 cells. pJM17 DNA molecules are too large to be packaged into virions and are therefore non-infectious.

A Subcloning gene of interest into shuttle vector

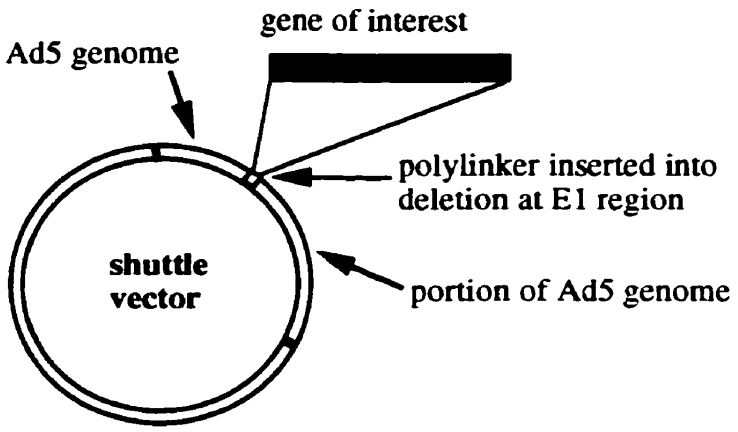

B Cotransfection into 293 cells that express E1 region genes

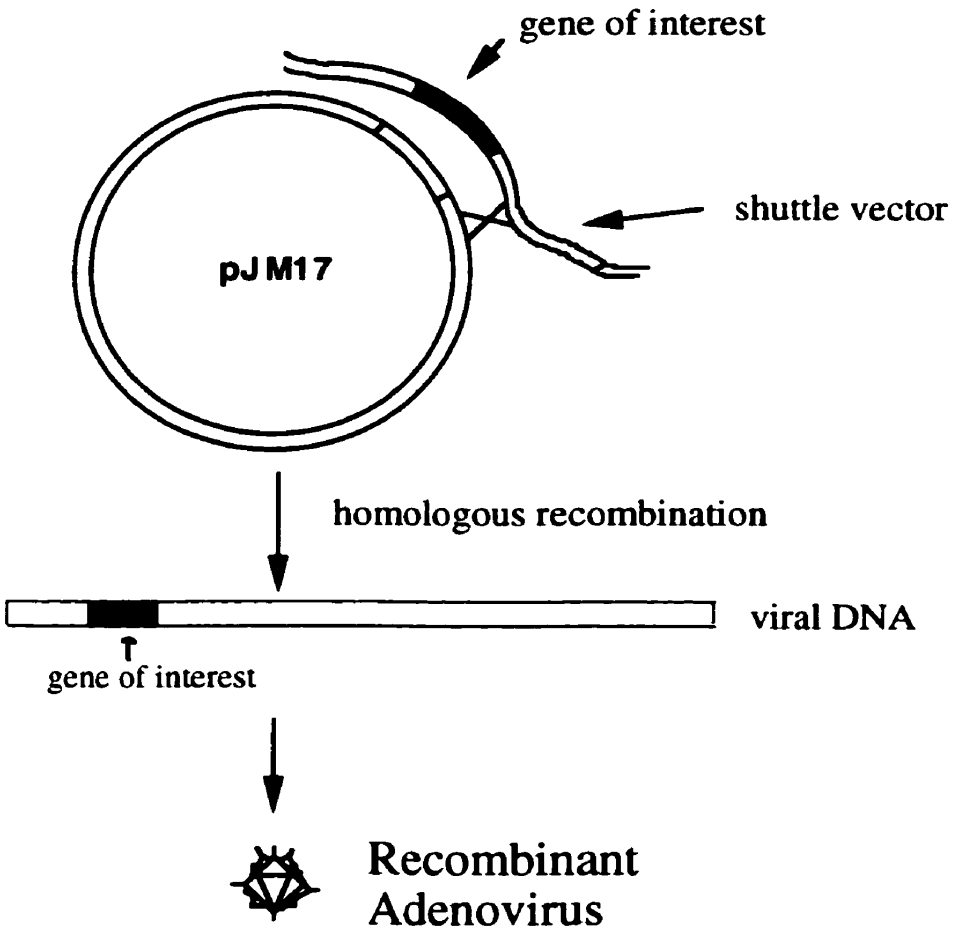

Typically, each 60 mm tissue culture dish containing 70% confluent HEK 293 cells was transfected by Ca^{2+}phosphate-DNA precipitation with 5μg of shuttle plasmid and 10 μg of pJM17 in a final volume of 0.5 ml. After 4-6 hr, the media was replaced with 5 ml of an agarose-α-MEM overlay made of a 1:1 mixture of sterile 1% agarose in H_2O and 2X α-MEM media. The 2X α-MEM media was prepared from powder, sterilized by filtration through a 0.22μm filter, and supplemented with 10% fetal bovine serum, 4 mM L-glutamine, 200 U penicillin, 0.2 g/ml streptomyocin, 5 μg/ml Fungizone, 2X α-MEM non-essential amino acids, and 2X α-MEM essential vitamins. The cells were then placed into a humidified incubator at 37°C with 5% CO_2, and after 1 week refed with an additional 5 ml of agarose-media.

Virus rescue occurs through homologous recombination events between the homologous Ad sequences found in pCA13 and pJM17. Because of the insertion of the bacterial origin of replication and ampicilin resistance sequences from the plasmid pBR322 into its E1 region, pJM17 is too large to be packaged into virions, and is therefore non-infectious (Hitt et al., 1995). Successful recombinations result in viral DNA molecules that are capable of replicating in HEK 293 cells because these cells express the missing Ad E1 genes. In general, if successful recombination occurs, plaques become visible 6-14 days after transfection.

Analysis of viral plaques. Potential GFP containing plaques were isolated and regrown on HEK 293 cells. After 3-5 days, most cells exhibited cytopathic effect and were rounded and floating. The cells were separated from the culture media by low speed centrifugation. High concentrations of virus are found within the infected cells while lower concentration are found in the media (Ginsberg, 1985; Hitt et al., 1995). Glycerol was added to a final concentration 10% to the media fraction which was then frozen at -80°C until needed for the next step of virus purification. Viral DNA was prepared from the infected cells by first lysing the cells for 2 hr at 37°C in lysis buffer (0.4% SDS, 50

μg/ml proteinase K (Fischer Scientific), 10 mM Tris HCl pH 7.4, and 10 mM EDTA pH 8.0). The cellular debris was removed by centrifugation, and the supernatant was extracted with phenol (Tris saturated), and then with chloroform:isoamyl alcohol (24:1), and finally precipitated with absolute ethanol. The presence of the correct insert was determined by analysis of polymerase chain reaction (PCR) products obtained by the amplification of viral DNA with primers for regions flanking the polycloning site of pCA13 [pCA13Forward (GACCTCCATAGAAGACACCG) and pCA13Reverse (ACC-ACAACTAGAATGCAGTG); synthesized by Sheldon Biotechnology Center, McGill University] using Ready to Go PCR beads (Pharmacia). The PCR protocol included a denaturation step at 95°C for 5 min, followed by 25 cycles of amplification (95°C for 45 sec, 53°C for 40 sec, 72°C for 40 sec), and a final elongation step at 72°C for 5 min.

Purification and preparation of high titer viral stocks. Candidate recombinant AdGFP viruses were purified by 3 rounds of plaque purification as described by Hitt et al. (1995). Briefly, HEK 293 cells were infected with serial dilutions of Ad, and overlaid with agarose-α-MEM media. After 6 and 8 days, isolated plaques were picked and regrown on HEK 293 cells. Viral DNA was prepared and analyzed for the presence of insert. The procedure was repeated an additional 2 times to obtain pure recombinant AdGFP.

A high titer stock of AdGFP was prepared by infecting ten 150 mm tissue culture dishes containing 80% confluent HEK 293 cells. After 2-3 days, when most of the cells were rounded and floating, the infected cells were collected by low speed centrifugation and then lysed by 6 freeze-thaw cycles (-70°C to 37°C). The cellular debris was removed by centrifugation, glycerol was added to a final concentration of 10%, and the crude lysate stock was aliquoted and frozen at -80°C.

The recombinant AdGFP stock was titered by plaque assay on HEK 293 cells (Hitt et al., 1995). Briefly, HEK 293 cells were infected with serial dilutions of AdGFP and

then overlaid with agarose-α-MEM media. After 6 and 8 days, the number of plaques were counted. Two separate serial dilutions were done in parallel and the titration was repeated twice. The titer of viral stocks, expressed as the number of plaque forming units (pfu) per ml, ranged from $5X10^9$ to $1.5X10^{10}$ pfu/ml.

Infecting neurons with adenovirus

To examine Ad infection of SCG neurons, we used the AdGFP that we built and a recombinant Ad that expressed β-gal, called AdHCMVsp1LacZ, generously given to us by Dr. Frank Graham. Stocks of AdHCMVsp1LacZ were prepared and titered as described above. P1 SCG neurons in culture for 1-14 days were infected with different concentrations of either AdGFP or AdHCMVsp1LacZ. Cultures of SCG neurons were infected by replacing the growth media with regular growth media supplemented with virus. While we normally used 1.5 ml of growth media for each petri containing neuronal cultures, for Ad infections we typically used only 30 μl placed into the inner 0.5 cm diameter culture well in order to minimize the amount of virus used. The cells were placed at 37°C in a 5% CO_2 incubator and the infection was allowed to proceed for 1-20 hr. The cells were then refed with 1.5 ml of regular growth media and allowed to grow for an additional 2-10 days at 37°C in a 5% CO_2 incubator. The number of days after infection refers to the number of days from the beginning of the virus application.

Amount of Ad applied to target cells. The standard virology term used to describe the amount of virus applied to cells is multiplicity of infection, or more simply MOI. The MOI represents the number of plaque forming units that are applied per target cell (pfu/cell). In our early experiments, we tested the efficiency of SCG infection with the β-gal expressing Ad at a variety of MOI. For a given MOI, such as 100 pfu/cell, we consistently found that the number of infected neurons as well as the intensity of the blue

X-gal cleavage product was significantly higher in cultures with high neuronal densities in comparison to those with low neuronal densities. One explanation is that because the center wells of our culture dishes have a relatively fixed volume, therefore for a given MOI, high density cultures receive higher net concentrations (pfu/μl) of virus than low density cultures. Indeed, we found that for our cultures we obtained more reproducible infection rates when we expressed the amount of virus applied as concentrations (pfu/volume) compared to MOI (pfu/cell). Therefore, in our studies, we expressed the amount of virus as a concentration.

Infecting neurons with replication defective Herpes Simplex Virus 1 vectors

Cultured SCG neurons were infected with the replication defective HSV 1 vector RH105 (Ho and Mokarski, 1988), using the procedures described for Ad vectors, except that HSV was applied onto the neurons for only 1 hr. This virus contains the LacZ gene inserted into the thymidine kinase gene of the HSV genome (Ho and Mokarski, 1988; Wei et al., 1995).

Microscopy

We assessed X-gal staining in neuronal cultures using bright field and phase contrast microscopy on a Zeiss Axiovert 35 microscope using either 20X or 40X objectives. We visualized GFP expression in neuronal cultures infected with AdGFP using a 40X objective on a Zeiss Axiovert 35 microscope and FITC optics.

Electrophysiology

To verify that Ad infection does not modify the electrophysiological properties of infected neurons, we measured voltage-gated outward potassium (K) currents and ACh-

evoked currents on Ad-infected and control SCG neurons using voltage clamp whole-cell patch recording techniques.

K currents. To measure outward K currents, we used procedures established by McFarlane and Cooper (1992, 1993). Briefly, the total outward current is composed of three voltage-gated currents that differ in their kinetic and voltage-dependent properties: a non-inactivating current (IK); a fast transient A-type current (IA); and a small slow transient A-type current (IAs). By holding the membrane at different potentials, we were able to selectively activate one or two currents and thus characterize the individual currents by subtraction techniques. The whole-cell membrane capacitance (pF) was estimated by integrating the capacity current evoked by a 5 mV hyperpolarizing voltage step from a holding potential of -60 mV.

For recording K currents, 2-3 day old cultures of SCG neurons were infected with AdHCMVsp1LacZ for 16-20 hr and then grown for an additional 6 days (total of 7 days from start of infection) before we performed the electrophysiological recordings. Immediately after recording from 5-8 neurons in a given cultures dish, the neurons were fixed and stained with X-gal to assess β-gal activity as described above. Only cells that were β-gal positive were considered to be infected neurons.

The whole-cell patch clamp recordings were performed essentially as described in Chapter 2. All the solutions were identical to those described in Chapter 2 except for the perfusion solution which consisted of 140 mM choline Cl, 2 mM NaCl, 5.4 mM KCl, 0.4 mM $CaCl_2$, 0.18 mM $MgCl_2$, 10 mM HEPES, 5.6 mM glucose, 2 mM glutamine, 1.5 mM $CoCl_2$, 5 μg/ml phenol red, and 0.5 μM TTX (Sigma); pH was adjusted to 7.4 (McFarlane and Cooper, 1992). These experiments were performed before we built AdGFP.

ACh-evoked currents. To measure ACh-evoked currents, we used procedures described in Chapter 2. Briefly, P1 SCG neurons in culture for 2-3 days were infected

with AdGFP and then grown for an additional 4-6 days (total of 5-7 days from start of infection) prior to electrophysiological recording. The perfusion solution consisted of 140 mM NaCl, 5.4 mM KCl, 2.8 mM $CaCl_2$, 0.18 mM $MgCl_2$, 10 mM HEPES, 5.6 mM glucose, pH 7.4. For drug application, we used the above perfusion solution to which we added 100 μM ACh (Sigma). The ACh solution was applied onto the neurons by two methods (Mandelzys et al., 1995; De Koninck and Cooper, 1995). In one method, the ACh solution was applied from a large, double barreled glass tubing attached to an electrochemical switching device. Each barrel had an opening of 200 μm; one barrel was filled with control perfusion solution, the other with ACh-perfusion solution (the flow rates of each barrel were 8-12 μl/sec). The central axis of one barrel, filled with normal perfusion solution was positioned 30-50 μm above the cell body. By triggering the switching device the 2nd barrel rapidly swung into position and perfused the cell body and proximal processes. We estimated that the entire cell body was perfused with agonist in less than 2 msec. In the second method, the ACh solution was applied by pressure ejection from an electrode with a tip diameter of 10-20 μm. The pipette tip was positioned 20-30 μm away from the cell body; on application of light pressure (≈10-30 KPa from nitrogen in pressurized tank), the drug solution perfused the entire cell body and proximal processes). Both methods gave comparable results on peak ACh-evoked current densities. The whole-cell membrane capacitances were estimated as described above. The ACh-evoked current densities (pA/pF) were calculated by dividing the peak amplitude of the evoked inward currents by the whole-cell membrane capacitances.

Statistical analysis. The results are expressed as the mean ± standard error of the mean (SEM) and Student's *t* tests were used to assess statistical significance.

Results

Non-viral transfection procedures

As a first approach to develop efficient gene transfer techniques for primary cultures of sympathetic neurons, we attempted Ca^{2+}phosphate- and liposome-mediated transfection. To qualitatively evaluate the efficiency of transfection, we used the mammalian expression vector pCH110 that contained the LacZ gene under the control of the HCMV promoter. For the majority of our transfection experiments, we used P1 SCG neurons in culture for 2-4 days. The neurons at this stage of *in vitro* development are well attached to the laminin substrate and are actively growing in size and extending neuritic processes.

Ca^{2+}phosphate-DNA precipitation does not efficiently transfect SCG neurons

To ensure that our Ca^{2+}phosphate transfection procedures were being appropriately performed, we first carried out control transfections with the β-gal expressing plasmid pCH110 in HEK 293 cells; on average ≈ 10% of these cells were transfected, as judged by X-gal staining. Next, we transfected cultured SCG neurons using the same procedures. When we stained the cultures for βgal expression 3 days later, we found very few neurons expressed β-gal in cultures of 700-1000 neurons. Typically, between 0-2 neurons were β-gal positive (Fig. 3.2A); however, we often observed 5 or more β-gal positive non-neuronal cells per culture dish (Fig. 3.2B, C).

Liposome are inefficient gene transfer agents for SCG neurons

In view of our low success with the Ca^{2+}phosphate-DNA precipitation method to tranfect neurons, we investigated liposome-mediated transfection because this technique

Figure 3.2. SCG neurons are inefficiently transfected by Ca^{2+}phosphate-DNA precipitation. ***A***, Phase contrast photomicrograph of cultured P1 SCG neurons transfected with the plasmid pCH110 that expresses the marker protein β-gal using the Ca^{2+}phosphate transfection method. The neurons were stained for β-gal expression with X-gal 3 days after transfection. The arrow shows one SCG neuron that expressed β-gal. ***B***, and ***C***, Photomicrographs showing non-neuronal cells that express β-gal (shown by arrows). Scale bar, 200 μM.

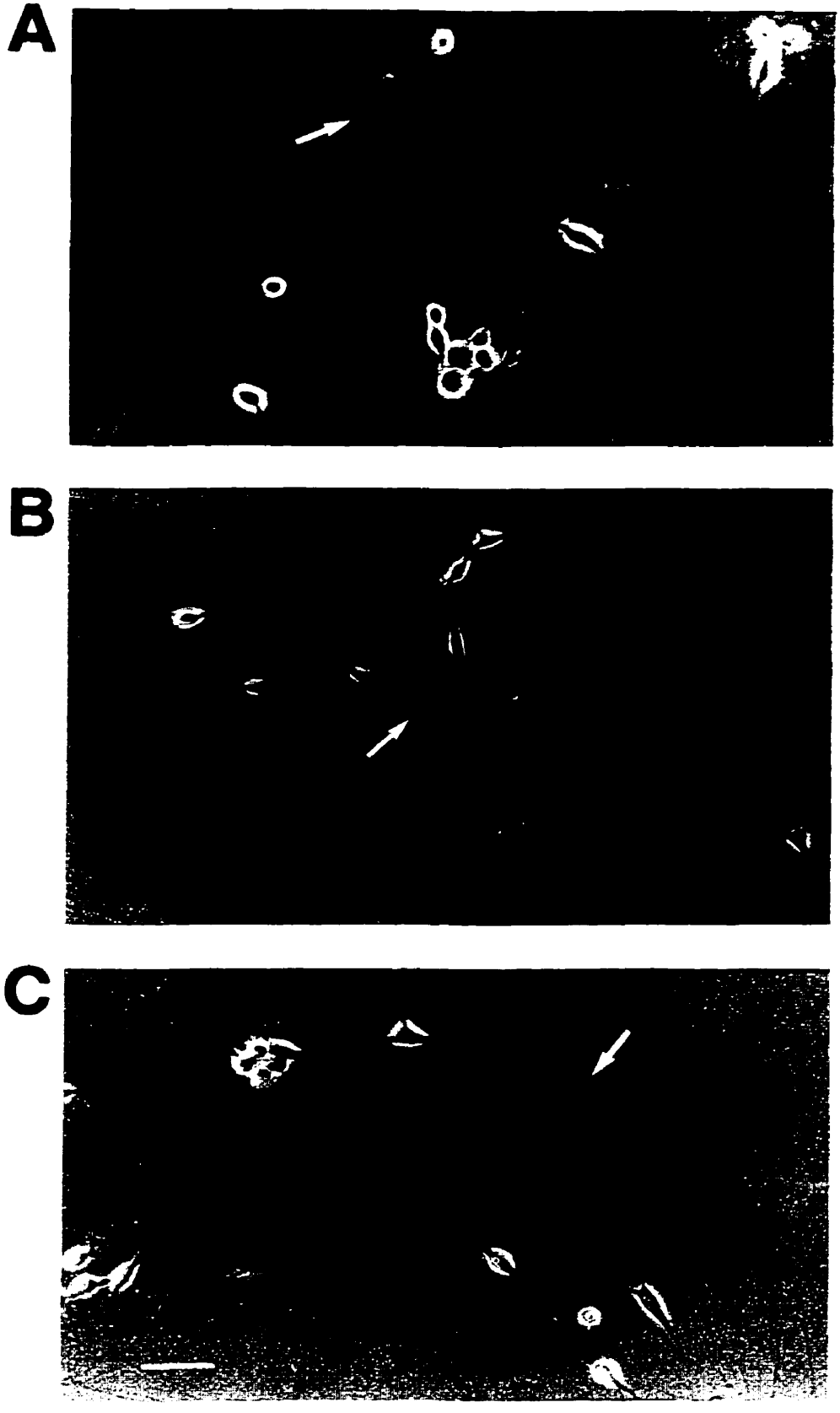
A
B
C

generally gives higher transfection efficiencies than Ca^{2+}phosphate-DNA precipitation in transformed cell lines (Felgner, 1991). We made liposomes with the β-gal expressing plasmid pCH110 and different cationic lipids: Lipofectamine, DOTAP, or a mixture of DOTAP and DOTMA. We tested several different ratios of DNA to lipid as well as different amounts of DNA and lipid. In cultures of 700-1000 neurons, we found that, at best, only 1-5 neurons expressed the LacZ gene; however, we observed that numerous non-neuronal cells were β-gal positive (Fig. 3.3). There were no differences between Lipofectamine- and DOTAP-mediated transfection efficiencies.

To determine if longer incubation with liposomes increased transfection efficiency, we applied the liposomes onto the neurons for 3, 6, 12 and 24 hr and assayed for β-gal activity 3 days later. We observed no improvement in the transfection efficiency, however, longer incubation times appeared to be toxic to the cells. Overall, liposome-mediated gene transfer yielded slightly higher transfection efficiencies for SCG cultures than Ca^{2+}phosphate-DNA precipitation, as judged by the number of β-gal positive non-neuronal cells.

Measuring liposome gene transfer efficiency using RNase protection assays

While X-gal staining is a qualitative measure of β-gal protein expression, we wondered whether the level of transgene might be better detected by measuring the mRNA levels of the transgene. For this experiment we used neonatal rat trigeminal neurons transfected with the α3 nAChR cDNA. We chose this system for two reasons: (1) our goal was to overexpress nAChR transcripts in neurons, and (2) in preliminary experiments, we had previously determined that neonatal trigeminal neurons express extremely low levels of endogenous α3 mRNA. Using DOTAP, we transfected cultured trigeminal neurons with full length α3 nAChR cDNA subcloned into the mammalian expression vector pcDNA1neo. We harvested total cellular RNA 3-5 days later and

Figure 3.3. Liposomes are inefficient gene transfer agents for cultured SCG neurons. Graph depicting the number of β-gal positive neurons and non-neuronal cells per culture dish in a series of experiments in which cultures of SCG neurons were transfected with various concentrations of DOTAP and the β-gal expressing plasmid pCH110; each culture dish contained ≈700-1000 neurons. The filled symbols represent β-gal positive neurons while the hollow symbols represent β-gal positive non-neuronal cells; the triangles, circle and square represent the plasmid DNA:DOTAP ratio of 1:20, 1:10 and 1:5 (μg:μg) respectively.

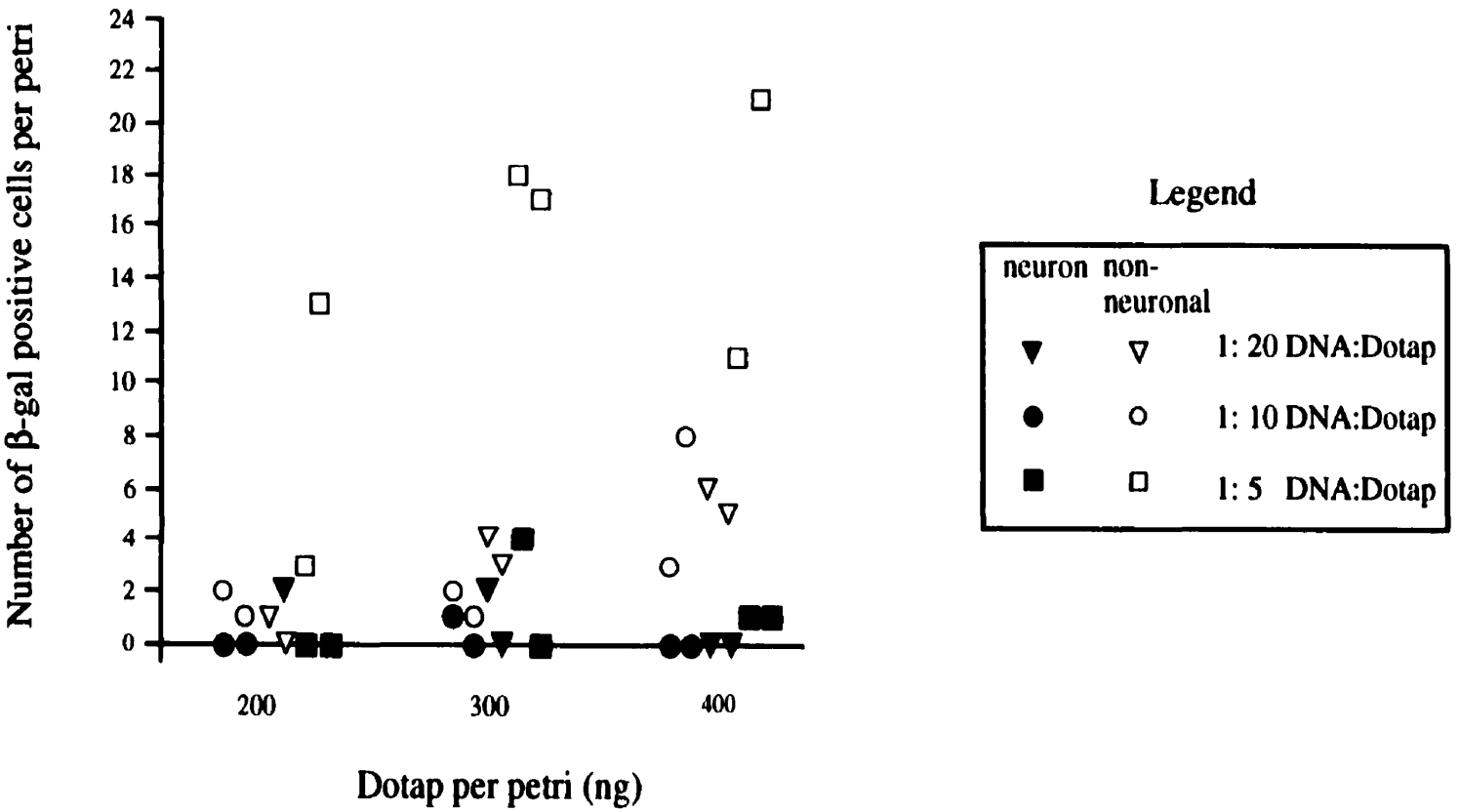
Number of β-gal positive cells per petri
24
22
20
18
16
14
12
10
8
6
4
2
0
200
300
400
Dotap per petri (ng)
Legend
neuron
non-neuronal
1: 20 DNA:Dotap
1: 10 DNA:Dotap
1: 5 DNA:Dotap

measured α3 mRNA levels with RNase protection assays, a sensitive method of detecting mRNA expression. We did not detect α3 mRNA in transfected trigeminal neurons (Fig. 3.4). In our initial experiments, we detected hybridization signals that corresponded to the size of the full length α3 riboprobe (Fig. 3.4). However, when we treated our RNA samples with DNase, these hybridization signals disappeared (Fig. 3.4). These results suggest that some transfected α3 cDNA molecules remained in the culture dish, perhaps attached to the cells, and were harvested along with the RNA.

Overall, our results show that Ca^{2+}phosphate and liposome-mediated DNA transfection produce very low levels of gene transfer for cultured sympathetic and trigeminal neurons. Because these transfection efficiencies were not sufficient for our planned experiments on nAChR subunit expression, we turned to alternative gene transfer techniques.

Viral-mediated gene transfer

Replication defective HSV vectors

At the outset of this project, we tested the effectiveness of an HSV vector to transfect sympathetic neurons because HSV vectors are naturally neurotropic and have been used by others to transfect a variety of neurons (see Chapter 1). In collaboration with Dr. Robert Dunn, (Montreal General Hospital), we tested the transfection efficiency of RH105, a replication defective whole virus HSV-1 vector that expressed β-gal. We found that this vector was very cytotoxic to cultured SCG neurons: it killed most neurons within 2-3 days, even at low concentrations of 1-5 MOI. Therefore, we did not pursue HSV as a gene transfer method for our system.

Figure 3.4. RNase protection assay for α3 mRNA expression in cultured trigeminal neurons transfected with the α3 cDNA using DOTAP. Hybridization bands corresponding to the predicted size for α3 mRNA were not detected in transfected trigeminal neurons. In RNA samples not treated with DNase, a band corresponding to the full length α3 riboprobe was visible while in RNA samples treated with DNase this band disappeared. The riboprobe for the K channel Kv3.4 was included in each reaction to verify whether equal amounts of RNA were used in each reaction. Additional controls included: (1) RNA from untransfected trigeminal neuron cultures (leftmost lane) that shows little endogenous α3 mRNA expression, and (2) DNase treated RNA from cultured SCG neurons (2nd lane from left) that shows abundant endogenous α3 mRNA expression that was not degraded by DNase treatment. A probe for GAPH appears in the probe lane (right most lane); this probe was used in an unrelated experiment that is not shown.

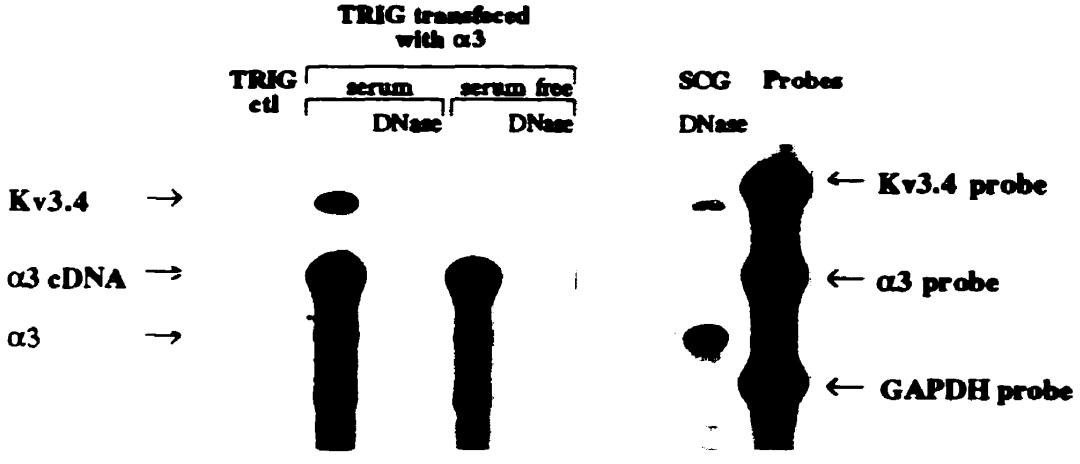
TRIG transfected with α3
TRIG ctl
serum
serum free
DNase
DNase
SCG
Probes
DNase
Kv3.4
α3 cDNA
α3
← Kv3.4 probe
← α3 probe
← GAPDH probe

Efficient gene transfer into SCG neurons with adenovirus vectors

Several groups reported that non-dividing cells, including neurons, can be efficiently transfected by adenovirus (Ad) vectors (Akli et al, 1993; Davidson et al., 1993; Le Gal La Salle et al., 1993). Therefore, we obtained a replication-defective β-gal expressing Ad, AdHCMVsp1LacZ, to determine whether Ad vectors could be used to transfect rat sympathetic neurons without causing harmful side effects.

In general, rodent cells are much less permissive to Ad infection than human cells (Hitt et al., 1995), most likely because they do not express the surface receptors for Ad. Efficient Ad infection of human cell lines, such as HEK 293 or Hela cells, is routinely achieved with incubation times of 0.5-1 hr (Graham and Prevec, 1991; Hitt et al., 1995). However, we found that 1 hr adsorption of AdHCVMsp1LacZ onto cultured SCG neurons gave very little infection, as measured by X-gal staining 2-4 days post-infection. By trial and error, we found that the highest infection efficiencies, ranging from 70-90%, were achieved by incubating the neurons with Ad for 16-20 hr (Fig. 3.5). Infection times longer than 24 hr appeared to have toxic effects on the neurons. However, we observed similar toxic effects in control "mock" infected neurons, suggesting that these effects result, in part, from our method of incubating our cultures in very small volumes of growth media (see Material and Methods); during prolonged incubation periods it is likely that essential growth factors are depleted from the media.

Determination of optimal virus concentrations

Next, we investigated the optimal amount of Ad to apply to cultured sympathetic neurons. In our studies we expressed the amount of virus applied to the cells as a concentration (pfu/volume)(see Material and Methods).

Figure 3.5. SCG neurons are efficiently transfected by recombinant adenovirus vectors. *A*, Phase contrast and ***B***, bright field photomicrographs of the same field of cultured SCG neurons infected 3 days prior with 50 pfu/nl of AdHCMVsp1LacZ: prominent X-gal staining is observed in most neurons and in the axons and dendrites of some high β-gal expressing neurons. Scale bar, 25 μm.

A

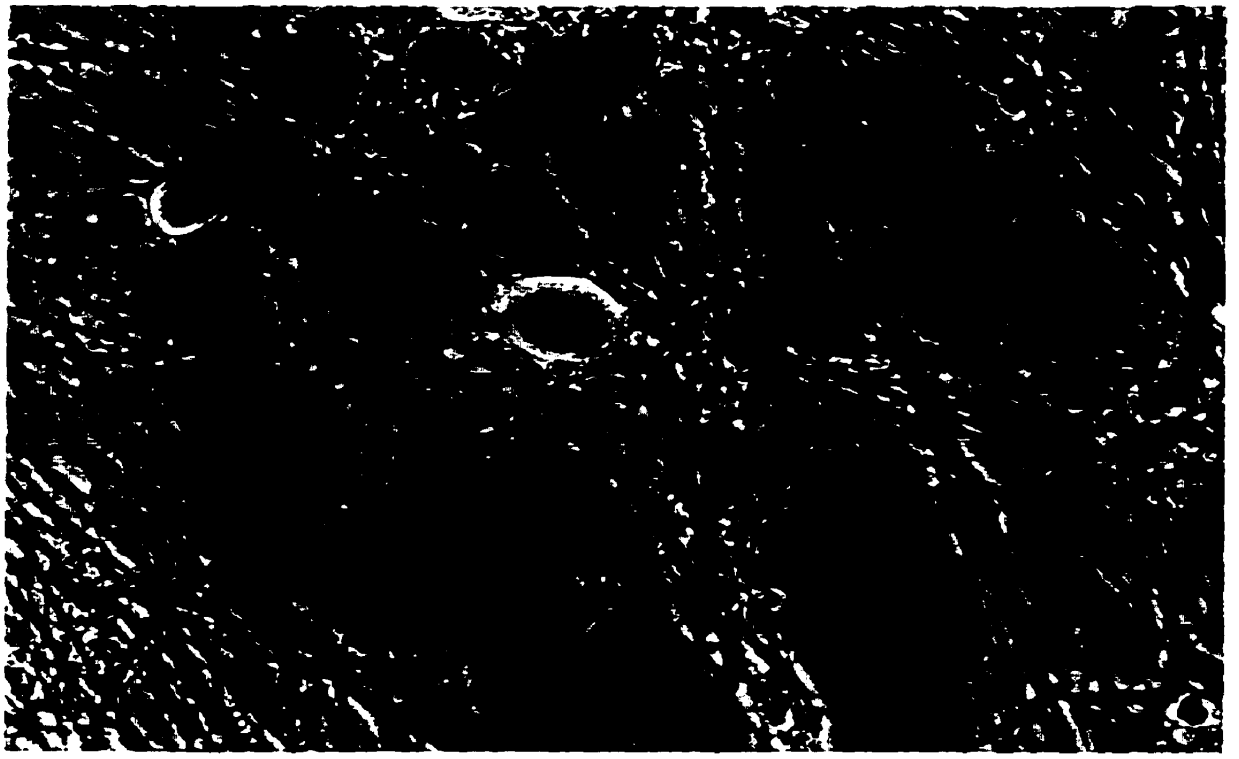

B

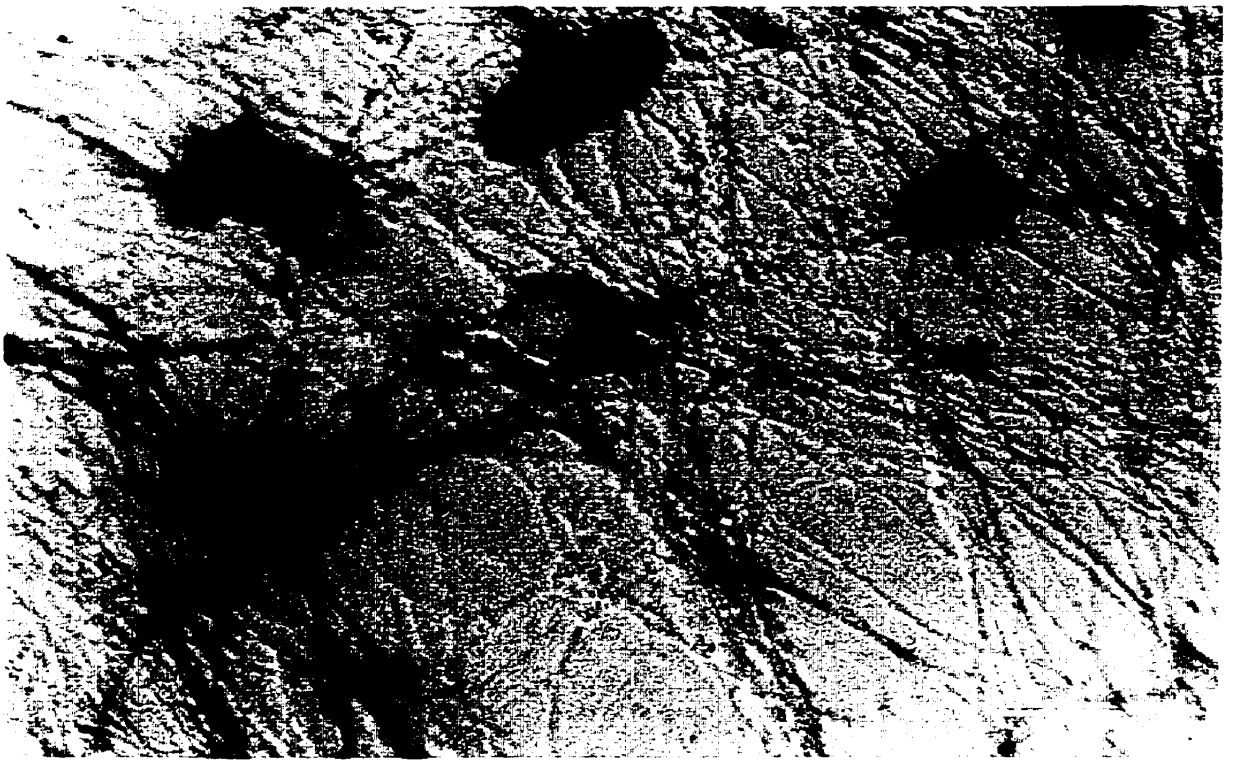

Empirically, we determined that a 60-80% infection rate could be routinely achieved using viral concentrations of 30-60 pfu/nl. At Ad concentrations of over 80-100 pfu/nl some degeneration of neurites, membrane ruffling and cell death was observed within 4-6 days whereas lower concentrations (0.1-15 pfu/nl) gave infection rate of ≈5-40%. Furthermore, at lower concentrations, we observed that the intensity of X-gal staining in infected neurons was noticeably lower than in neurons infected with higher Ad concentrations, suggesting that at higher Ad concentrations, individual neurons are infected with several viral particles.

It is worth noting that to infect SCG neurons, we used 100-1000 fold higher Ad concentrations than are needed to infect permissive cells such as HEK 293 cells. This large difference presumably arises from differences in the mechanisms by which Ad virus are taken up by permissive and non-permissive cells.

In addition, we observed that SCG neurons infected at the time of plating or after 1 day in culture were not very efficiently infected. Similarly, SCG in culture for more than two weeks were very poorly infected, showing little or no transgene expression 3-5 days post infection; the reasons for this refractoriness are not known.

Generation of a GFP-expressing adenovirus

To be able to identify living neurons expressing foreign genes and to monitor their fate over time, we built a recombinant Ad that expressed GFP. GFP, originally isolated from the jellyfish *Aequores victoria*, is a biofluorescent molecule that can be visualized in living cells (Chalfie et al., 1994). Figure 3.6 shows SCG neurons infected AdGFP: prominent fluorescence is observed in several neurons, while weaker or no fluorescence is observed in others. GFP fluorescence was observed in the cell body including the nucleus and the dendrites (Fig. 3.6 and 3.7). We also observed GFP expression in a few

Figure 3.6. AdGFP directs the expression GFP in infected SCG neurons. ***A***, and ***B***, Left panels show fluorescence photomicrographs of cultured SCG neurons infected 3 days prior with 30 pfu/nl of AdGFP. Right panels show phase contrast photomicrographs of the corresponding fields. Scale bar, 25μm.

A

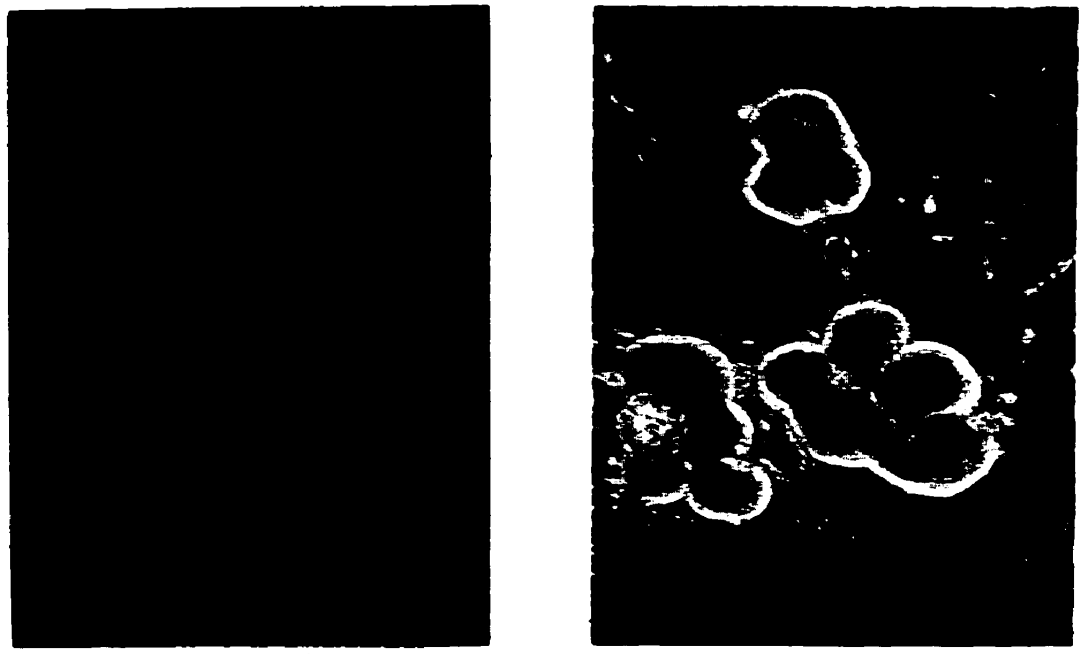

B

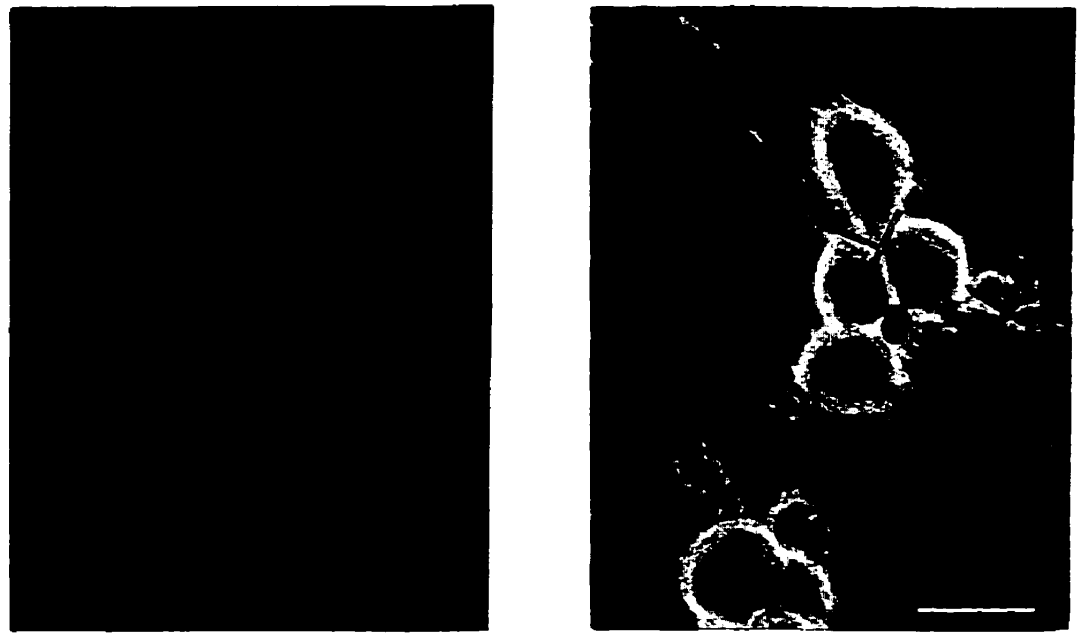

non-neuronal cells in our cultures. As expected, we found that the optimal infection conditions for AdGFP were identical to those for the β-gal expressing Ad.

Co-infection of SCG neurons with two different adenoviruses

Our results on infection with different virus concentrations suggested that neurons can take up several viral particles. Therefore, we tested whether neurons could be simultaneously infected by two different viruses. We found that when SCG neurons were infected with equal concentrations of AdHCMVLacZsp1 and AdGFP, we did indeed detect neurons that expressed both β-gal and GFP. Moreover, we observed that most neurons that expressed GFP also expressed β-gal. This was somewhat surprising since at the concentration that we used (15 pfu/nl of each virus), the rate of infection by each virus was ≈30-40% and if infection was random, we would have expected only ≈10-15% of the neurons to express both marker proteins.

To investigate this further, we infected SCG neurons with equal amounts of both viruses in a range of low concentrations to obtain low infection rates and then examined transgene expression 7 days later. We observed that if the X-gal reaction was allowed to proceed for more than 15 min, the X-gal cleavage products obscured the fluorescence of GFP; therefore, we stopped the reaction when the neurons were only pale blue (on average 7 min), and then counted the number of blue cells that also exhibited green fluorescence (Table 3.1).

Table 3.1 Co-infection of cultured SCG neurons with AdGFP and AdHCMVsp1LacZ

AdHCMVsp1LacZ and AdGFP (pfu/nl each)	Infection efficiency (percent of neurons expressing GFP)	Proportion of β-gal positive neurons that were also GFP positive	Percent of β-gal positive neurons expressing both GFP and β-gal
0.625	≈15%	18/24	75%
2.5	≈20%	37/47	78%
10	≈50%	46/58	79%

We found that on average 77% of the cells that displayed β-gal activity were also GFP positive. Our results indicate that when neurons are infected with Ad, they are likely to be infected by more than one virus particle.

Time course of transgene expression

To determine the time course of transgene expression in Ad-infected SCG neurons, we infected SCG neurons in culture for 2-3 days with various concentrations of either AdHCMVLacZspI or AdGFP for 16-20 hr, and then assayed for β-gal activity or GFP expression at one day intervals between 1-7 days after the start of infection. Transgene expression was detected as early as 1 day after the start of infection, with only a few neurons displaying transgene expression. The maximum number of β-gal and GFP positive cells appeared to be reached by 3 days post infection, however, the level of transgene expression continued to increase between 3 and 5 days and remained high for at least 7 days after infection. In several SCG neurons expressing high levels of either transgene, prominent X-gal staining and GFP fluorescence was observed in axons and dendrites (Fig. 3.7, see also Fig. 3.5 and 3.6). In particular, in some β-gal and GFP positive neurons, transgene expression was seen in axons that extend several hundred μm from the cell body (Fig. 3.7).

Adenovirus infection does not adversely affect neuronal growth or survival

Above, we show that recombinant Ad vectors can be used as efficient gene transfer vehicles for cultured SCG neurons. However, because recombinant Ad vectors express high levels of the transgene proteins and possibly low levels of viral proteins, it was

Figure 3.7. Transgene expression is detected in the axons and dendrites of SCG neurons infected with adenovirus vectors expressing either β-gal or GFP. ***A***, Bright field photomicrograph of X-gal stained SCG neurons infected with the β-gal expressing adenovirus. In high β-gal expressing neurons, prominent X-gal staining is visible in the dendrites (the thick processes that extend 10-40 μm away from the soma, shown by thick arrows), and the axons (thin process that extend up to several mm from the cell body, shown by thin arrows). This photomicrograph was taken with a 20X objective. Scale bar 50 μm. ***B***, Fluorescence photomicrograph of SCG neurons infected with AdGFP. GFP fluorescence is visible in the dendrites (thick arrows) and an axon (thin arrow) of the SCG neuron shown. This photomicrograph was taken with 40X objective. Scale bar, 25 μm.

A

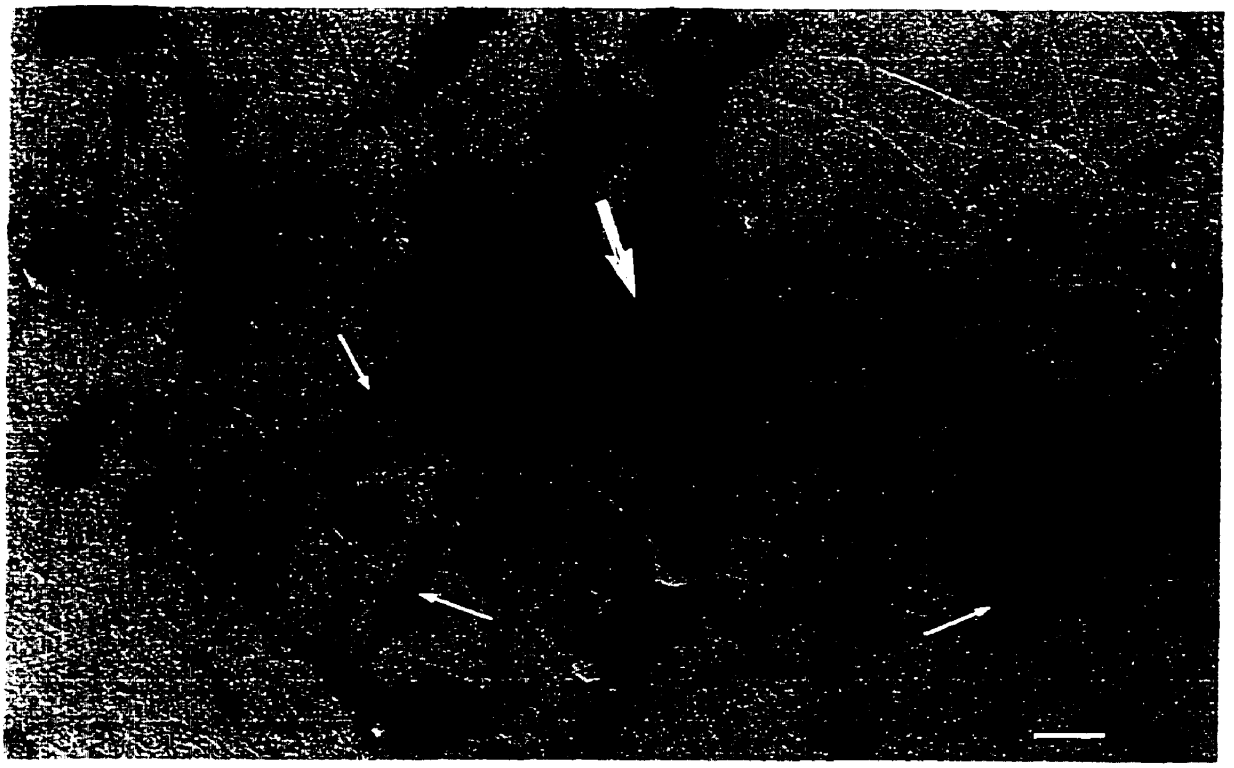

B

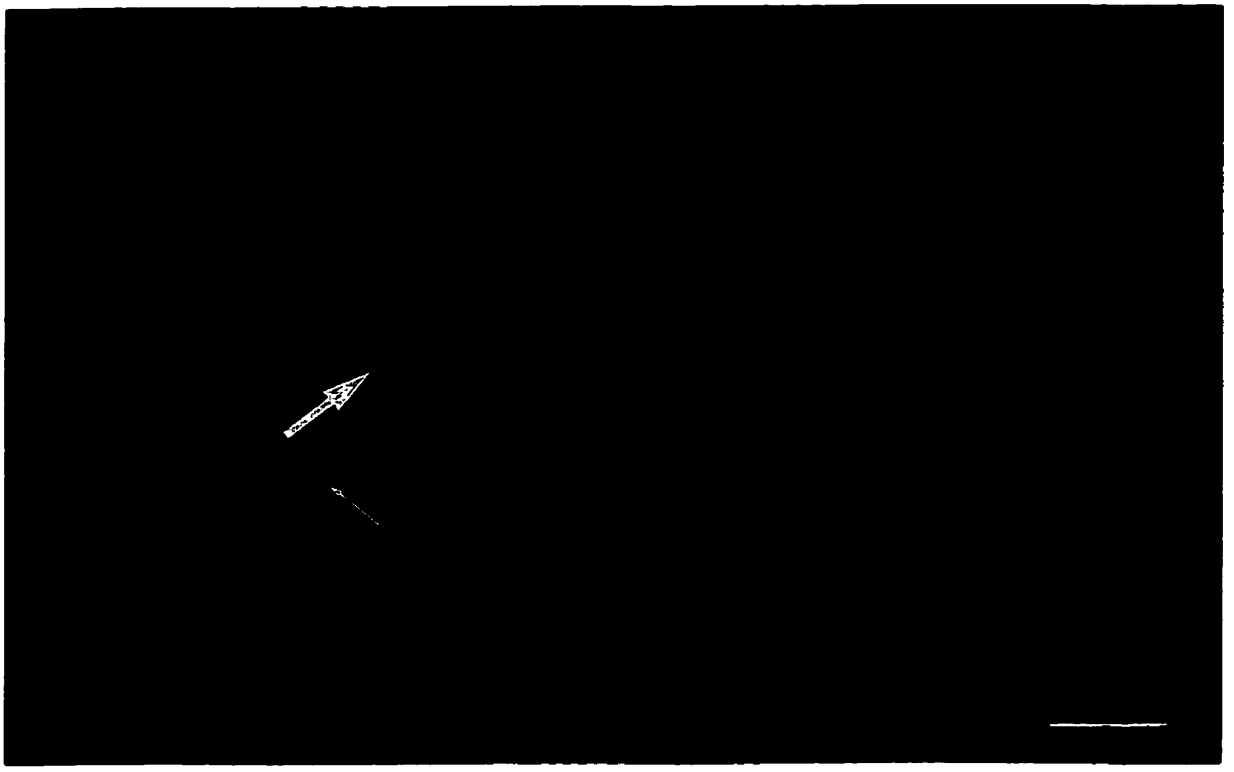

important to investigate whether Ad infection has any deleterious effects on normal neuronal physiology. First, we examined the impact of Ad infection on neuronal survival. We infected 3 day old cultures of SCG neurons with various concentrations of AdHCMVsp1LacZ (5, 15, 30, 60, and 100 pfu /nl), and then performed cell counts on 10 random fields 7 days later. We found that the cell counts for SCG cultures infected with 5-60 pfu/nl of Ad did not differ by more than 5-10% from control mock-infected sister cultures, while the number of surviving neurons in cultures infected with 100 pfu/nl were ≈30% lower than controls. Comparable data were obtained using mitochondrial function as an index of cell survival (Slack et al., 1996).

To determine whether Ad infection affected neuronal growth and morphology, we examined AdHCMVsp1LacZ- and AdGFP-infected neurons at various intervals for up to 10 days post-infection. For sympathetic neurons infected with up to 60 pfu/nl of Ad, we observed that the neurons continued to grow normally in size and extend processes, and are indistinguishable from their uninfected sister cultures for at least 1 week. SCG neurons infected with between 60-80 pfu/nl showed signs of neurite degeneration by 7 days after infection. For concentrations over 80 pfu/nl, we observed degeneration of neurites, changes in the appearance of the cell membrane and cell death within 4-6 days; these phenotypic changes occurred faster in conditions with higher viral concentrations.

Variability in transgene expression and apparent toxic effects. In a given infection experiment, we found, as expected, that the level of transgene expression was similar in sister cultures infected with the same concentration of virus. However, when we compared transgene levels for the same virus concentration in separate infection experiments, we observed some variability in transgene expression. In addition, we observed some variability in the apparent health of infected neurons: occasionally, SCG neurons infected with 60 pfu/nl or more of either Ad showed signs of neurite and cell membrane degeneration. This variability is not likely to be due to technical errors such as

pipetting because independent virus dilutions applied onto sister cultures gave similar transgene expression or toxic effects. Rather, this variability may reflect differences, such as age or other unidentified factors, that affect the ability of independently prepared SCG cultures to adsorb and internalize Ads.

Electrophysiological properties of SCG neurons infected with adenovirus

To determine if infection by recombinant Ad affects the neurons' electrophysiological properties, we examined the expression of endogenous K currents and ACh-evoked currents on Ad-infected cultured SCG neurons using whole-cell voltage clamp techniques. In experiments with cultured SCG neurons infected with 15-30 pfu/nl of AdHCMVLacZspl, we found that the current densities (pA/pF) for IK and IA measured at 5-7 days post-infection were similar to those on control uninfected sister cultures and to those previously reported for cultured SCG neurons (McFarlane and Cooper, 1993)(Fig. 3.8).

We measured ACh-evoked current densities on SCG neurons infected with 15-30 pfu/nl AdGFP. Because GFP fluorescence can be visualised in living cells, the advantage of using AdGFP is that one can easily determine which cells are infected prior to performing electrophysiological recordings. ACh-evoked currents on AdGFP infected neurons exhibited similar properties as ACh-evoked currents on control uninfected SCG neurons: they did not desensitise in the presence of agonist and showed strong inward rectification (Fig. 3.9A,B). The mean ACh-evoked current densities recorded from GFP-positive SCG neurons were 93.7 ± 10.5 pA/pF (mean ± SEM) (n=19) while those recorded from uninfected sister cultures were 89.0 ± 11.8 pA/pF (n=16) (Fig. 3.9C).

Figure 3.8. Endogenous outward voltage-gated K currents on SCG neurons are not altered by infection with recombinant Ad. Voltage-gated K currents were recorded from SCG neurons 7 days after infection with AdHCMVsp1LacZ (15-30 pfu/nl) and from uninfected age-matched controls. ***A***, Shows examples of current traces for: (1) IK, obtained by depolarising voltage steps from a holding potential of -10 mV (these steps activate only IK); and (2) IA, isolated by subtracting the currents evoked from holding potential of -40 mV (IK+IAs) from the total current (IK+IA+IAs). ***B***, Mean current densities for IK and IA on control and AdHCMVsp1LacZ-infected SCG neurons. SCG neurons were considered to be infected only if they displayed β-gal activity (see Materials and Methods); n=6 for β-gal positive neurons, n=5 for control neurons. Error bar represents the SEM.

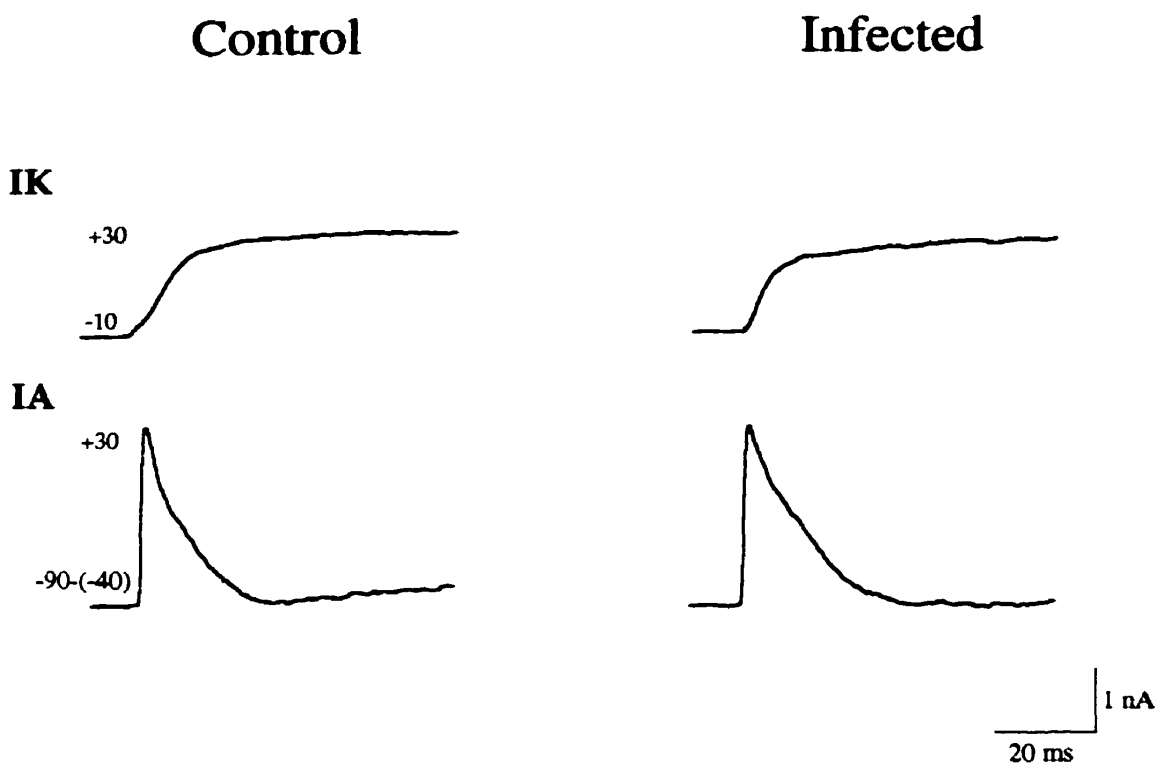
A
Control
Infected
IK
+30
-10
IA
+30
-90-(-40)
1 nA
20 ms

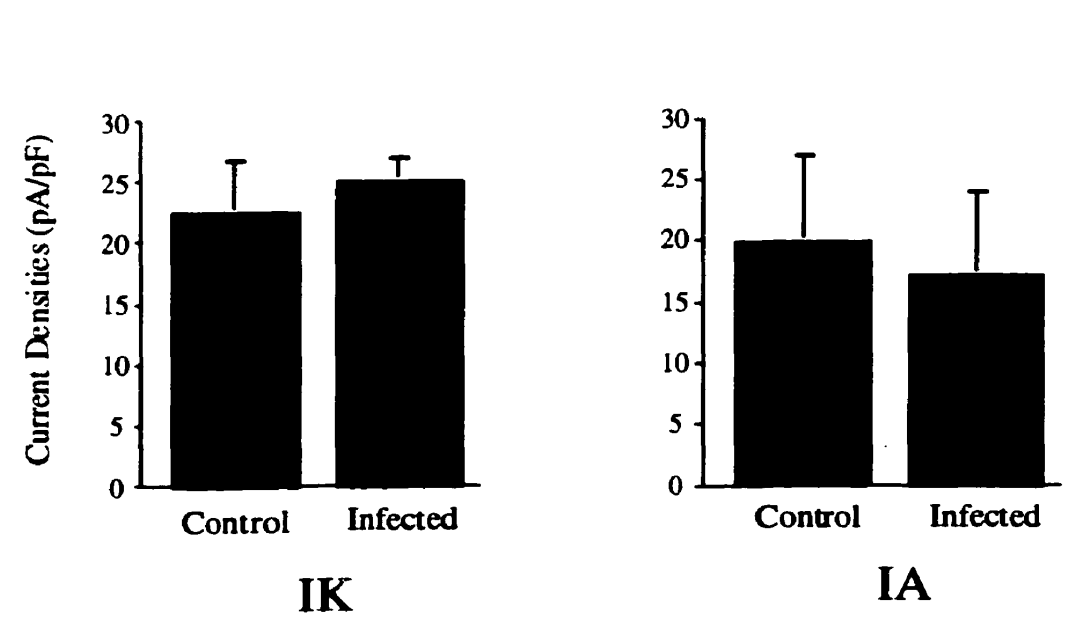
B
Current Densities (pA/pF)
30
25
20
15
10
5
0
Control
Infected
IK
IA

Figure 3.9. ACh-evoked currents on SCG neurons are not altered by infection with Ad vectors. ***A***. Examples of ACh-evoked currents from control and AdGFP-infected SCG neurons. ***B***, Current-voltage (*I/V*) relationship of ACh-evoked currents on a control and an AdGFP-infected SCG neuron. The whole-cell currents were recorded during a voltage ramp from –80 mV to +40 mV (333 mV/sec) and the whole cell *I-V* curves were obtained by subtracting the current in control solution from the current in the presence of ACh. The *I-V* plot shows strong inward rectification for both control and infected SCG neurons. ***C***, Mean ACh-evoked current densities (± SEM) on cultured SCG neurons infected with 15-30 pfu/nl AdGFP (n=19) and on control uninfected cultured SCG neurons (n=16). The mean ACh-evoked current densities on AdGFP infected SCG neurons were not significantly different from those on control uninfected neurons ($p>0.2$).

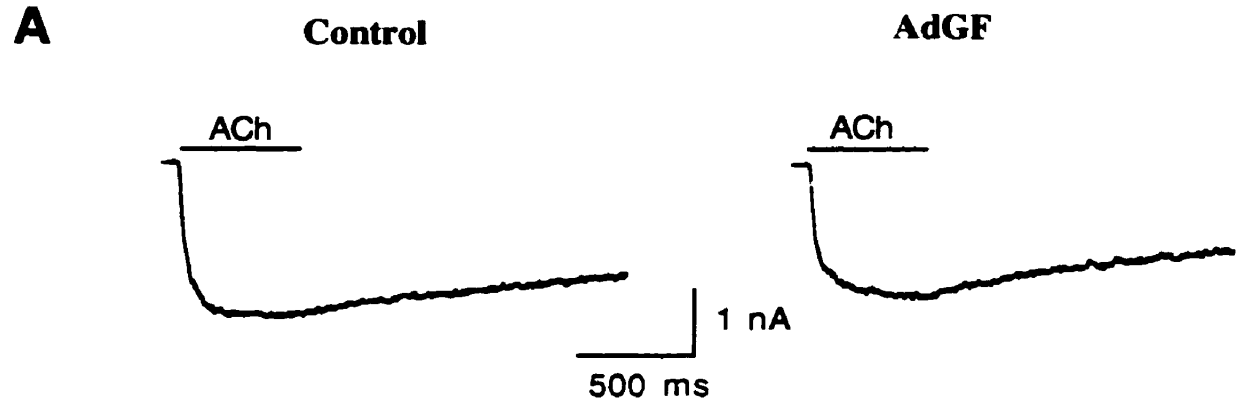
A
Control
AdGF
ACh
ACh
1 nA
500 ms

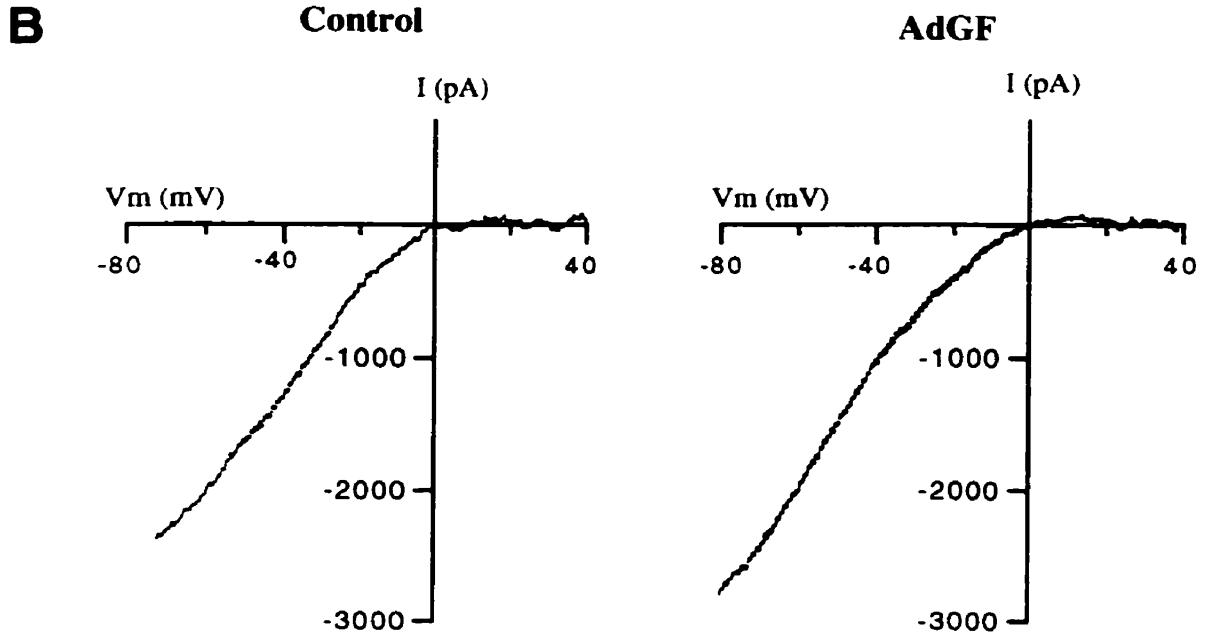
B
Control
AdGF
I (pA)
I (pA)
Vm (mV)
Vm (mV)
-80
-40
40
-80
-40
40
-1000
-2000
-3000
-1000
-2000
-3000

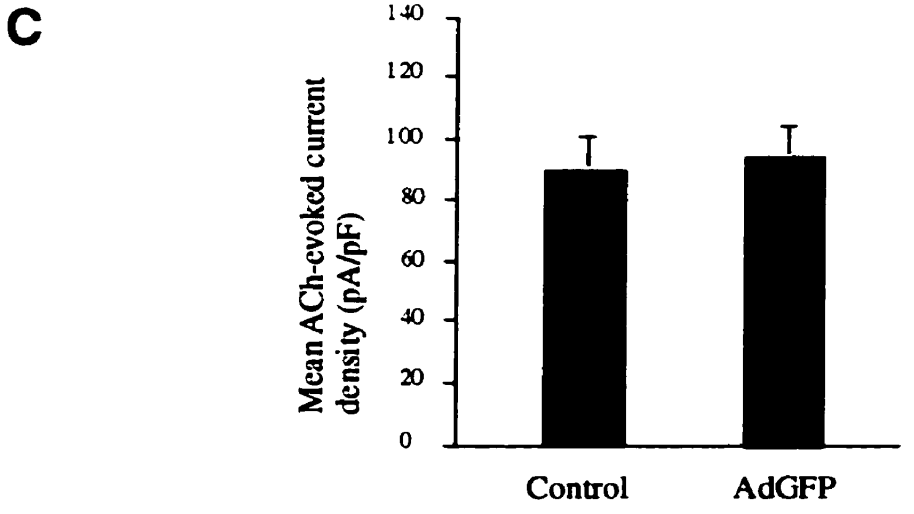
C
Mean ACh-evoked current density (pA/pF)
140
120
100
80
60
40
20
0
Control
AdGFP

These ACh-evoked current densities were similar to those previously recorded for SCG neurons in culture for 1-2 weeks (Mandelzys et al., 1995).

Discussion

The objectives of this study were to develop efficient transient transfection procedures for neonatal rat sympathetic neurons. To do this, we evaluated the efficacy of several different gene delivery methods for sympathetic neurons in culture. Of the techniques tested, our results clearly demonstrate that recombinant adenovirus vectors are the most efficient at transfecting cultured sympathetic neurons and do not adversely affect normal neuronal physiology.

First, we evaluated the efficacy of Ca^{2+}phosphate- and liposome-mediated transfection because these methods are simple and relatively inexpensive to perform. Our results showed that cultured sympathetic neurons are poorly transfected by these two methods, with efficiencies ranging from $\approx$ 0.1-1%. Because these two methods work best on actively dividing cell lines (Okayama and Chen, 1991; Felgner, 1991), the lack of transfection may be attributed to the fact that neonatal rat sympathetic neurons are post-mitotic. Interestingly, the few non-neuronal cells in our cultures were apparently more easily transfected, perhaps because they are still dividing. Because Ca^{2+}phosphate-DNA precipitates are internalized by non-specific endocytosis (Okayama and Chen, 1991), our results suggests the endocytosis and membrane turnover may be low in neurons. Alternatively, the inefficiency of both Ca^{2+}phosphate- and liposome-mediated transfection may lie in the poor transport of internalized foreign DNA to the nucleus for translation.

We examined the effectiveness of a β-gal expressing replication defective HSV vector to transfect SCG neurons. This HSV vector, RH105, contains the whole HSV

genome with the LacZ gene inserted into the thymidine kinase (TK) gene; this insertion into the TK gene renders the HSV vector replication incompetent in neurons which express very low levels of endogenous TK (Ho and Mocarski, 1988; Wei et al., 1995). We found that this HSV vector caused significant cell death within 2-3 days post-infection. This toxicity can be attributed to the expression of viral proteins and the shut down of host cell functions (Tomasec et al., 1996). The toxic effects of HSV whole vectors have been reported by others (Johnson et al., 1992a,b; Tomasec et al., 1996). New second-generation HSV vectors with additional mutations in viral genes are currently being generated (Fink and Glorioso, 1997) and show greater promise than the first generation HSV vectors. We did not test any amplicon based HSV vectors because when we initiated this study, HSV amplicons free of wild type helper virus contamination were not available to us.

We have successfully built a recombinant Ad that expresses the marker protein GFP. We show that recombinant Ad vectors can be produced in the laboratory using the straightforward plasmid-based approach developed by Dr. Frank Graham. Some of the general difficulties in generating replication-defective Ad vectors are discussed in Chapter 5.

In this study, we demonstrate that recombinant Ad vectors can be used to efficiently transfect cultured neonatal rat sympathetic neurons. Using a β-gal expressing Ad and a GFP expressing Ad, we successfully transfected up to 90% of cultured SCG neurons. We show that Ad vectors do not affect sympathetic neuron survival for at least 7 days post-infection. Moreover, infected sympathetic neurons continue to grow in size and extend processes. We show that high levels of GFP or β-gal expression produced by infection by AdGFP or AdHCMVsp1LacZ do not appear to be toxic to sympathetic neurons. Infection by recombinant Ads does not interfere with neuronal growth and morphology or with the expression of endogenous ACh-evoked currents and voltage-gated outward K currents on sympathetic neurons. Similar results reported by Smith et al. (1997) show that GFP

expressing Ads do not alter the electrophysiological properties of dorsal root ganglion (DRG) neurons. Interestingly, Smith et al. (1997) have also built an Ad that contains both 5-HT_3R and GFP and confers 5-HT sensitivity and GFP fluorescence to DRG neurons.

Our studies reveal several interesting aspects about the kinetics of Ad virus infection of neonatal rat sympathetic neurons. Firstly, in contrast to Ad permissive cells that are efficiently infected by 1 hr incubations with low amounts of Ad (Hitt et al., 1995), we found that incubations of 16-24 hr with significantly larger amounts of Ad were necessary to obtain maximal Ad infection of cultured sympathetic neurons. This indicates that the probability of an Ad being internalized into rat sympathetic neurons is much lower than for permissive cells. This difference is likely to be due to different modes of virus entry. In permissive cells, including many human cell types, Ad adsorption and internalization occur by receptor-mediated endocytosis involving two steps: (1) the attachment of the Ad fiber protein to the cellular receptor; and (2) the subsequent internalization of this complex by cellular integrins (Hong et al., 1997). Rodent cells are infected by Ad to a much lesser extent than permissive cells (Ginsberg, 1988; Hitt et al., 1995), most likely because they do not express the natural Ad receptor (Stevenson et al., 1997). Interesting studies on certain human cells that lack the Ad receptor show that Ad infection of these cells occurs with significantly lower efficiency and requires much higher amounts of Ad, similar to our results on rat sympathetic neurons (Huang et al., 1996). Ad entry in these human cells is thought to occur though the direct association of the Ad penton base proteins with cellular integrins which stimulates endocytosis (Meunier-Durmort et al., 1997; Huang et al., 1996). Presumably, Ad vectors are internalized into rat sympathetic neurons by similar mechanisms.

Secondly, when we infected SCG neurons with low Ad concentrations, we observed that the intensity of the X-gal stain (blue precipitate) or GFP fluorescence was significantly lower than in neurons infected with high Ad concentrations. One likely explanation for this difference in transgene expression is that at higher Ad concentrations,

neurons are infected with several viral particles, giving rise to more transgene expression while those infected with lower concentrations receive fewer virions per cell. This is supported by our experiments with AdHCMVsp1LacZ and AdGFP that clearly show that SCG neurons can be infected by more than one virion.

Thirdly, we found that neurons in culture for more than 2 weeks were less readily infected by Ads in comparison to neurons in culture for less than 1 week. As SCG neurons continue to grown in size and extend processes for many weeks in culture, this decreased infectability is not likely to be due to decreases in cell metabolism or cell viability. One possible explanation is that with time in culture, the expression of the receptor(s) such as integrins or others mechanisms involved in Ad adsorption and internalization are decreased.

Overall, the findings of our study demonstrate the effectiveness of Ad vectors as gene transfer agents in sympathetic neurons. Recombinant Ads provide a means to manipulate the expression of many different genes and can be used to investigate the intracellular mechanisms that operate in regulating normal nerve cell function. These results will allow researchers to perform many experiments that are currently not feasible with the existing technology.

In the next chapter, I describe my experiments and results on using recombinant Ad to manipulate the expression of nAChR subunits in neonatal sympathetic neurons.

Chapter 4

Overexpressing α3 nAChR Subunits Leads Directly to Increases in ACh-Evoked Current Densities

Introduction

Neonatal rat sympathetic neurons express five of the eleven known neuronal nAChR genes: α3, α5, α7, β2 and β4 (Mandelzys et al., 1994). Combined pharmacological and electrophysiological studies by Mandelzys et al. (1995) suggest that most, if not all, of the ACh-evoked current on SCG neurons is generated by receptors that contain α3, β2 and β4 in the same complex. Cooper and colleagues have previously shown that during the early postnatal development and the *in vitro* development of SCG neurons, α3 mRNA levels increase several fold while β2 and β4 mRNA levels do not change (Mandelzys et al., 1994; De Koninck and Cooper, 1995; see Chapter 1 Fig. 1.4). The increases in α3 mRNA levels correlate well with increases in ACh-evoked current densities on SCG neurons during both *in vivo* and *in vitro* development (Mandelzys et al., 1994; De Koninck and Cooper, 1995, see Chapter 1). One explanation for these observations is that α3 subunit expression is rate-limiting for the assembly and insertion of new nAChRs into the cell membrane. If so, then manipulating α3 mRNA levels should directly lead to changes in the number of functional nAChRs and the magnitude of ACh-evoked current densities on SCG neurons.

In this chapter, I test this prediction by altering α3 mRNA expression in SCG neurons. For these experiments, I use transient transfection procedures based replication-deficient adenovirus (Ad) vectors that I described in the previous chapter. Specifically, I am using two recombinant Ad vectors that I have built: one that expresses sense α3 mRNA and protein, and one that expresses antisense α3 mRNA. My results show that changes in the expression of α3 nAChR subunits lead to alterations in the magnitude of ACh-evoked currents on neonatal sympathetic neurons.

Materials and Methods

Construction of adenoviruses expressing sense and antisense α3

Recombinant Ads expressing either sense or antisense α3 nAChRs were built using the plasmid-based method described in Chapter 3. Briefly, both sense Adα3F and antisense Adα3AS were generated by *in vivo* homologous recombination between the shuttle plasmids described below and pJM17. The presence of the correct insert was confirmed by PCR analysis of viral DNA as described in Chapter 3.

Sense α3 adenovirus. To build the sense α3-containing Ad, we used a rat α3 cDNA that had been previously modified to include the sequence coding for the FLAG octapeptide DYKDDDDK (GATTACAAGGACGATGATGACAAG) (Kodak IBI) at the 3' end of the coding sequence but before the translation stop codon [α3FLAG in pcDNA1 (Invitrogen), gift from Dr. Philippe Séguéla, Montreal Neurological Institute]. The epitope FLAG, which is recognized by the Anti-FLAG M2 antibody (Kodak, IBI), was added to facilitate the detection of virally produced α3 proteins in transfected neurons. We subcloned the full length α3FLAG cDNA into the shuttle plasmid pCA13 in the sense orientation with respect to this plasmid's HCMV promoter. The orientation of the fragment was verified by DNA restriction fragment analysis and was confirmed by partial sequencing with primers specific for the regions flanking the polycloning site of pCA13 (see Chapter 3 for primer sequences).

To ensure that α3FLAG was correctly inserted into pCA13 and that the epitope FLAG did not interfere with the ability of α3 subunits to co-assemble with β subunits into functional receptors, we co-expressed pCA13α3FLAG with rat β4 nAChR cDNA in *X.* oocytes according to the methods described by Bertrand et al. (1991). We found that the physiology of α3FLAGβ4 receptors was identical to that of wild-type α3β4 receptors. We transfected separately the plasmids pCA13α3FLAG and α3FLAG-pcDNA1 into

HEK 293 cells by Ca^{2+}phosphate-DNA precipitation, and then fixed and immunostained the cells using the Anti-FLAG M2 antibody (see below for immunostaining procedures) to verify that the FLAG epitope was correctly expressed.

Antisense α3 adenovirus. To create an Ad expressing antisense α3 mRNA, we used a HindIII-BglII fragment of the rat α3 cDNA that encompassed 254 bp of the 5'UTR and the first 325 bp of the α3 coding region. This fragment was subcloned into the shuttle vector pCA13 in an antisense orientation with respect to the HCVM promoter. The orientation of the fragment was verified by DNA restriction fragment analysis and by sequencing (see Chapter 3 for primer sequences). The sequence of this portion of the α3 cDNA has low homology to other nAChR subunits at the nucleotide level; therefore, antisense mRNA produced from this fragment is unlikely to block the translation of other nAChR subunit mRNA species expressed by SCG neurons.

Neuronal Cultures

Primary cultures of postnatal day 1 (P1) rat SCG and nodose neurons were prepared according to the procedures described in Chapter 2. For all neuronal cultures, the media was supplemented with nerve growth factor (2.5S NGF, 25 ng/ml); NFG was added to nodose cultures to promote low level expression of nAChRs (De Koninck et al., 1993). SCG and nodose cultures were treated with cytosine arabinofuranoside (Ara-C, 10 μM), an anti-mitotic agent, for the first 2-3 days in culture. This treatment killed the faster growing satellite and Schwann cells, leaving only a few slowly dividing fibroblast-like cells in the neuronal cultures. The neurons were plated at densities of 4000-8000 cells/cm^2 in modified petri dishes with inner wells ranging in size from 0.5 to 1.5 cm in diameter (see Chapter 3). Cultures in 0.5 cm wells were preferentially used for immunocytochemistry experiments while cultures in 1.5 cm wells were used for

experiments involving electrophysiology, RNA or protein measurements. For some experiments, cultures of non-neuronal cells from SCG ganglia were prepared. Briefly, after dissociation of the ganglia into single cells (see Chapter 2), non-neuronal cells were recovered from the upper layer of the Percoll density gradients (see Chapter 2), washed 2X with Hanks Balanced Salt Solution (HBSS; 140 mM NaCl, 5.4 mM KCl, 0.33 mM NaH_2PO_4, 0.44 mM KH_2PO_4, 2.8 mM $CaCl_2$, 0.18 mM $MgCl_2$, 10 mM Hepes, 5.6 mM glucose, 5 μM/ml phenol red, pH 7.4), and plated at a low density in normal L15 culture media in the absence of NGF or Ara-C; in the absence of NGF, any remaining SCG neurons die.

Infection of SCG and nodose cultures

Stocks of recombinant Adα3F, Adα3AS, and AdGFP were prepared and titered as described in Chapter 3. SCG and nodose neurons in culture for 3-5 days were infected with different Ad concentrations by replacing the growth media with growth media containing Ad. The cells were placed at 37°C in a 5% CO_2 incubator, and the infection was allowed to proceed for 16-20 hr. The cells were then refed with regular growth media and allowed to grow for an additional 2-5 days prior to analysis of neuronal nAChR expression by the different methods described below. The number of days after infection refers to the number of days from the beginning of the virus application.

RNA preparation and RNase protection assays

Total cellular RNA was prepared from control and infected cultures of SCG and nodose neurons using the RNeasy total RNA kit (Qiagen) as described in Chapter 2. For certain experiments, RNA samples were treated with DNase I to degrade any remaining

viral DNA. Typically, RNA from four petri dishes was pooled together for each RNA sample. The yield of total RNA ranged from 2-3 μg.

RNase protection assays were performed as described in Chapter 2. Briefly, ^{32}P-UTP-labeled antisense RNA probes to α3 and GAPDH were transcribed *in vitro* using SP6 and T7 RNA polymerase respectively, from linearized plasmids containing portions of the cDNA clones. The α3 antisense riboprobe, 600 bases long, was synthesized to the 3' end of the normal rat α3 cDNA. This probe was used to detect both endogenous α3 and viral α3 transcripts (see Fig. 4.1A): it protected 540 bases of the endogenous α3 transcript (340 bases of coding region and 200 bases of 3' untranslated region (UTR) but protected only 340 bases of virally expressed α3 mRNA because this transcript contains the FLAG sequence in lieu of the 3' UTR. The GAPDH antisense riboprobe, synthesized from the mouse GAPDH cDNA (mouse pTRI-GAPDH, Ambion), was a shortened version of that described in Chapter 2: it was 209 bases in length and protected 150 bases of the rat GAPDH mRNA transcript. The thermal stabilities of both probes, based on their melting temperatures, were found to differ by less than 1°C.

Each hybridization reaction was performed with 1μg of total cellular RNA prepared from control and infected neurons and 200 000 cpms of α3 probe and 30 000 cpms of GAPDH probe. The acrylamide gels were dried and exposed to a phosphor imaging plate prior to being exposed to X-ray film (Kodak XAR). The hybridization intensities were quantified using a phosphor imager (Molecular Dynamics). The specific activity of each riboprobe was calculated from the number of adenine residues in the cDNA sequence equivalent to the protected RNA sequence. To compare hybridization intensities between different probes, the hybridization signals of a given probe were divided by the specific activity of that probe. Total α3 mRNA expression was calculated by adding the normalized hybridization signals for viral and endogenous α3.

Immunocytochemistry

Infected and control SCG neurons were fixed with freshly prepared 4% paraformaldehyde (PFA) in 0.1 M Na phosphate buffer (pH 7.4) for 10 min at room temperature and rinsed 3X for 5 min with PBS (14 mM NaCl, 3 mM KCl, 10 mM Na_2HPO_4, 1.8 mM KH_2PO_4, pH 7.4). For permeabilization, the cells were incubated in 0.1% Triton X-100 (Sigma) in PBS for 10 min. All samples were incubated for 1 hr in blocking buffer [PBS supplemented with 5% Carnation powdered skim milk and/or 5% normal goat serum (Jackson ImmunoReasearch Laboratories)]. All antibodies were diluted in blocking buffer. After blocking, the samples were incubated with the mouse monoclonal Anti-FLAG M2 antibody (Kodak, IBI) at 5 or 10 μg/ml for 1 hr, and then washed 3X in blocking buffer to remove unbound antibody. Next, the fixed neurons were incubated with biotin-sp-conjugated goat-anti-mouse IgG (1/200; Jackson ImmunoReasearch Laboratories) for 45 min, rinsed 3X with blocking buffer, then incubated in Cy3-conjugated streptavidin (1/200; Jackson ImmunoReasearch Laboratories) for 45 min, and finally rinsed 3X with PBS. For some experiments, instead of using biotin-sp-conjugated goat-anti-mouse IgG and Cy3-conjugated streptavidin, we used Alexa 546 conjugated goat-anti-mouse IgG (15 μg/ml; Molecular Probes) for 45 min followed by 3 rinses in PBS. The cells were examined by epifluorescense on a Zeiss Axiovert 35 microscope fitted with rhodamine filters using a either a 40X or a 63X objective.

Electrophysiology

ACh-evoked currents were measured on cultured SCG neurons infected with Adα3F using whole-cell patch-clamp recordings as described in Chapter 3. Briefly, the perfusion solution consisted of 140 mM NaCl, 5.4 mM KCl, 2.8 mM $CaCl_2$, 0.18 mM $MgCl_2$, 10 mM HEPES, 5.6 mM glucose, pH 7.4. ACh (100 μM in perfusion solution)

was pressure applied using the two agonist application methods described in Chapter 3. Both methods gave comparable results on peak ACh-evoked current densities. ACh-evoked current densities were calculated by dividing the mean peak amplitudes by the whole-cell capacitance as described in Chapter 3.

In Chapter 3, we show that in neurons infected with 2 different Ads, if a given neuron is infected with one virus there is an ≈ 80% likelihood that it is also infected with the other virus. Therefore to increase the probability of recording from Adα3F-infected neurons, we took advantage of this phenomenon and co-infected cultured SCG neurons with equal amounts of Adα3F and AdGFP (15 or 30 pfu/nl each). Controls were performed on sister cultures infected with AdGFP at concentrations equal to the total amount of virus applied in the experimental condition (30 or 60 pfu/nl). For both experimental and control conditions, we used GFP expression as a marker of infection: we recorded ACh-evoked currents from GFP expressing neurons that appeared healthy and had a clear nucleus and a distinct nucleolus. Identical procedures were performed for our preliminary experiment with the antisense Adα3AS.

Immunoprecipitation and SDS PAGE analysis

^{35}S-methionine labeling of cellular proteins. Three day old cultures of P1 SCG neurons were infected with 50 pfu/nl of Adα3F or AdGFP for 16-20 hr and allowed to grow for an additional 2 days prior to labeling. The cells first were washed 2X with methionine- and cysteine-free DMEM media (Gibco BRL) and placed into the incubator for 30 min to methionine starve the cells. The neurons were then incubated for 4 hr in methionine- and cysteine-free DMEM media supplemented with Trans^{35}S-Label (150 μCi/ml; ICN), 5% dialyzed calf serum (Gibco BRL), and NGF (25 ng/ml). After labeling, the cells were washed 2X with ice cold HBSS supplemented with 1 mM $CaCl_2$ and 1 mM $MgCl_2$, to remove unincorporated ^{35}S-methionine. The cells were then solubilized on ice

for 30 min in lysis buffer [1% Triton X-100, 0.5% NP40 (Boehringer Mannheim), 150 mM NaCl, 20 mM Tris-HCl pH 8.0, and protease inhibitors (1X Complete tablet, Boehringer Mannheim)].The lysates were harvested by pipetting and centrifuged briefly in a microcentrifuge to pellet cellular debris. The supernatants from 12-16 1.5 cm-well culture dishes were pooled together in a volume of 0.9-1.2 ml.

Immunoprecipitation. Non-specific protein binding to protein G Sepharose was eliminated by preclearing the lysates with equilibrated protein G Sepharose (20 μl, equilibrated with lysis buffer, Pharmacia) for 1 hr at 4°C on a rocking platform. The protein G Sepharose was pelleted by brief centrifugation, and the supernatant transferred to a clean tube. Anti-FLAG M2 antibody (5 μg) was added to the supernatant and the mixture was incubated for 16 hr at 4°C on a rocking platform. Protein G Sepharose equilibrated in lysis buffer (20 μl) was added to the cell extracts and allowed to mix for 2 hr at room temperature on a rocking platform. The protein G Sepharose beads were then washed 5X with lysis buffer to remove unbound proteins, and then resuspended in 1X sample buffer (62.5 mM Tris-HCl pH 6.8, 2% SDS, 0.00125% bromophenol blue, 10% glycerol, 5% β-mercaptoethanol) and boiled for 10 min. The protein samples were briefly centrifuged to pellet the Sepharose beads, and the supernatants were either frozen or loaded directly onto SDS polyacrylamide gels.

SDS-PAGE and fluorography. The immunoprecipitated proteins were separated by SDS-polyacrylamide gel electrophoresis (PAGE) (Laemmli, 1970). Briefly, the denatured protein samples were applied onto gels composed of a 10% separating polyacrylamide gel and a 4% stacking polyacrylamide gel. The proteins were electrophoresed at 175 V for 1.25 hr. Prestained SDS-PAGE proteins standards (broad range, Biorad) were used to estimate the molecular weight of visualized proteins. The proteins in the separating gel were then fixed in a solution of 10% glacial acetic acid and

30% methanol for 1 hr with gentle agitation, treated for 1 hr with Enhance (NEN Dupont), a fluorography enhancer, and then soaked for 30 min in water to precipitate the fluorescent material. Finally, the gels were dried and exposed to X-ray film at -80°C (Kodak X-AR).

Statistical analysis. The results are expressed as the mean ± standard error of the mean (SEM) and Student's *t* tests were used to assess statistical significance.

Results

α3 mRNA overexpression in neurons infected with Adα3F

We examined the level of α3 mRNA overexpression in cultured SCG neurons infected with various concentrations of Adα3F using RNase protection assays (Fig. 4.1). We used a single antisense riboprobe synthesized from the 3' end of the rat α3 cDNA to distinguish between endogenous α3 and viral α3 transcripts (Fig. 4.1A). This riboprobe protected 540 bases of the endogenous α3 transcript (340 bases of coding region and 200 bases of 3' UTR) but protected only 340 bases of the virally expressed α3 mRNA because this transcript contains the FLAG sequence instead of the 3' UTR. For each reaction, we assayed GAPDH mRNA levels as an internal control and quantified the hybridization signals with a phosphor imaging system.

To exclude the possibility that some of the hybridization signal arose from α3 cDNA contained viral DNA molecules, we treated several RNA samples with DNase I to verify that we were measuring only RNA and not viral DNA. We obtained identical results to those shown in figure 4.1B, and concluded that our RNA samples did not contain viral DNA.

Figure 4.1. Quantification of α3 mRNA expression in Adα3F-infected SCG neurons. ***A***, Illustration depicting the homology between the α3 riboprobe and endogenously and virally expressed α3 mRNA. Using a single ^{32}P-labeled riboprobe synthesized to the 3' end of normal α3 cDNA, we detected both endogenous and viral α3 transcripts. The 600 base riboprobe protected 540 bases of endogenous α3 mRNA and only 340 bases of viral α3 because this latter transcript contains the sequence for the FLAG epitope in lieu of the 3'UTR. ***B***, RNase protection assay for α3 and GAPDH mRNA expression in total RNA isolated from control and Adα3F-infected cultured SCG neurons. Briefly, 3 day old cultures of P1 SCG neurons were infected with different concentrations of Adα3F and then grown for 3 additional days prior to RNA harvesting. 1 μg of total RNA was used for each reaction. GAPDH mRNA expression was assessed to verify that equal amounts of total RNA were used in each reaction; the GAPDH probe is 209 bases in length and has a protected probe length of 150 bases. ***C***, Quantification of total α3 mRNA expression in infected SCG neurons expressed relative to endogenous α3 mRNA levels in cultured SCG neurons. Each point represents the mean of 3 or 4 experiments. The error bars which represent the SEM were smaller than the graph symbols and therefore cannot be seen.

A

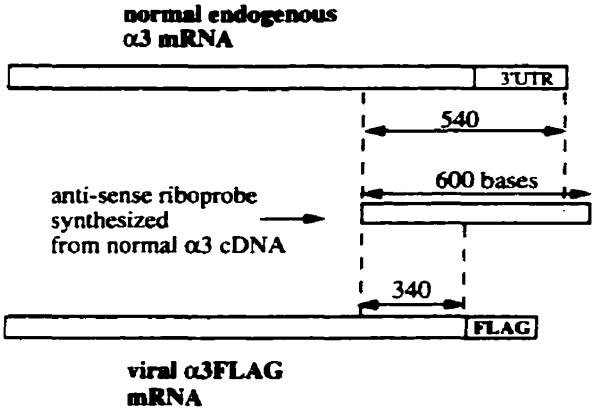
normal endogenous
α3 mRNA
3'UTR
540
600 bases
anti-sense riboprobe
synthesized
from normal α3 cDNA
340
FLAG
viral α3FLAG
mRNA

B

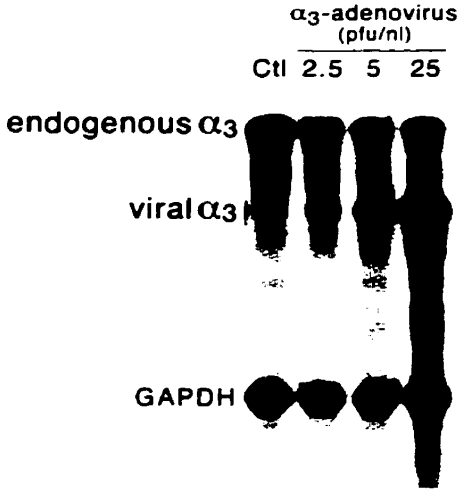
α3-adenovirus
(pfu/nl)
Ctl 2.5 5 25
endogenous α3
viral α3
GAPDH

C

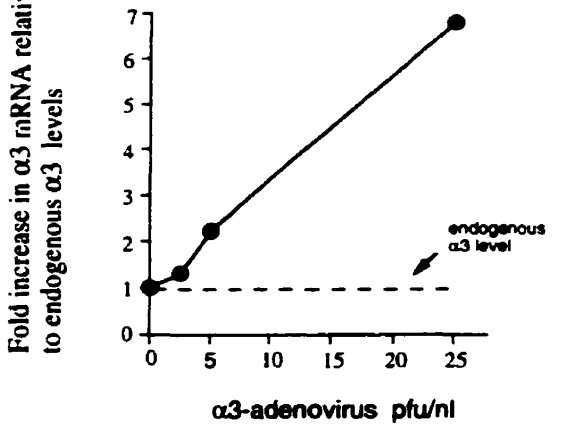
Fold increase in α3 mRNA relative
to endogenous α3 levels
0
1
2
3
4
5
6
7
0
5
10
15
20
25
endogenous
α3 level
α3-adenovirus pfu/nl

Figure 4.1C shows the level of α3 mRNA overexpression relative to normal endogenous α3 mRNA levels in SCG neurons that were infected with various concentrations of Adα3F. This figure show that a 6-7 fold overexpression of α3 transcripts can be easily achieved in SCG neurons using recombinant Ad vectors. We have not yet examined viral α3 mRNA levels in neurons infected with higher concentrations of Adα3F.

To determine if similar viral α3 mRNA levels could be expressed in other populations of peripheral neurons, we examined viral α3 transcript levels in cultured nodose neurons infected with Adα3F using RNase protection assays (Fig. 4.2). When we quantified the level of α3 mRNA expression, we found that an ≈30 fold increase above endogenous α3 mRNA levels was obtained using 25 pfu/nl of Adα3F (Fig. 4.2B). This apparent large increase arises from the fact that endogenous α3 transcript levels in nodose neurons are fairly low in comparison to those of SCG neurons (see Fig. 4.1B). However, when we compared the level of viral α3 mRNA between SCG and nodose neurons, we found that for a given viral concentrations, the quantity of viral α3 mRNA in SCG and nodose neurons were very similar. In addition, we found that the level of viral α3 mRNA expression is proportional to the concentration of virus applied (Fig. 4.3).

Immunocytochemical detection of virally expressed α3 proteins

To detect virally expressed α3 proteins, we used a mouse monoclonal antibody that recognizes the artificial epitope FLAG found at the C-terminus of virally encoded α3 proteins. Figure 4.4 shows examples of permeabilized SCG neurons exhibiting FLAG immunofluorescence: fluorescence is observed in the entire soma and in the thick processes that we presume are dendrites, but not in the nucleus. In addition, α3FLAG proteins appear to be expressed on the cell membrane.

Figure 4.2. Quantification of α3 mRNA expression in Adα3F-infected nodose neurons. ***A***, RNase protection assay for α3 and GAPDH mRNA expression in total RNA isolated from control and Adα3F-infected cultured nodose neurons performed as described in Fig. 4.1. Briefly, 3 day old cultures of P1 nodose neurons were infected with different concentrations of Adα3F and grown for 3 additional days prior to RNA harvesting. ***B***, Quantification of total α3 mRNA expression in Adα3F-infected nodose neurons as described in Figure 4.1C. Each point represents the mean of 2-3 experiments. The error bars which represent the SEM were smaller than the graph symbols and therefore cannot be seen.

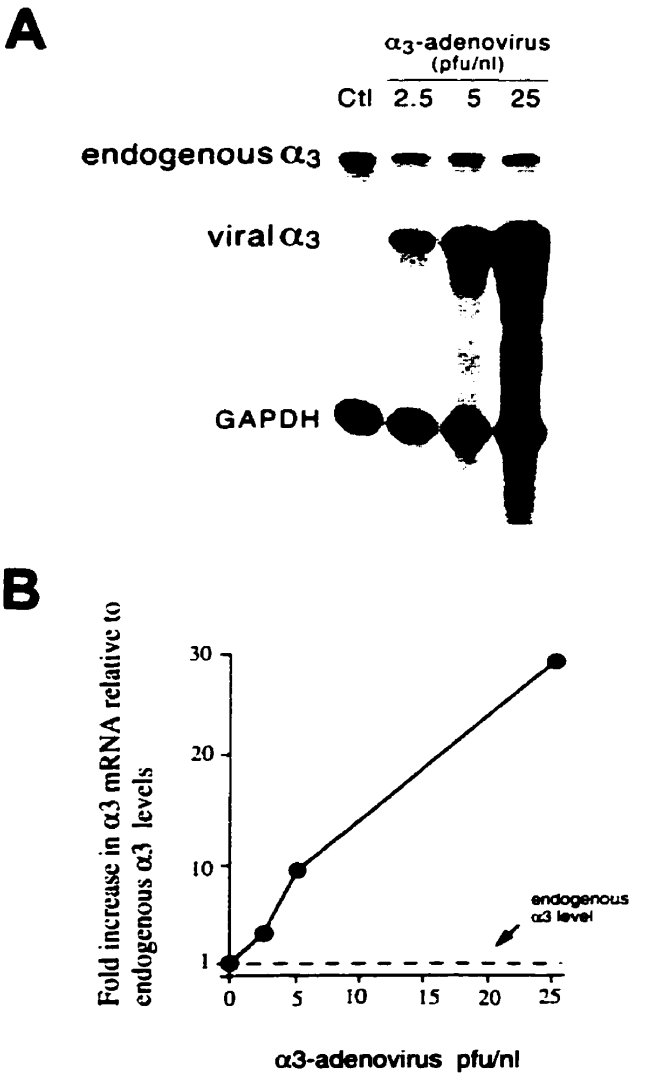
A
α3-adenovirus (pfu/nl)
Ctl 2.5 5 25
endogenous α3
viral α3
GAPDH
B
Fold increase in α3 mRNA relative to endogenous α3 levels
30
20
10
1
0 5 10 15 20 25
endogenous α3 level
α3-adenovirus pfu/nl

Figure 4.3. Viral α3 mRNA levels in neurons are proportional to virus concentration. Graph showing viral α3FLAG mRNA levels for several Adα3F concentrations applied onto SCG and nodose neurons. The hybridization signals for α3FLAG mRNA in infected SCG and nodose neurons were averaged for each viral concentration and are expressed relative to those at 2.5 pfu/nl. Each point represents the mean of 5-7 experiments and the error bars represent the SEM.

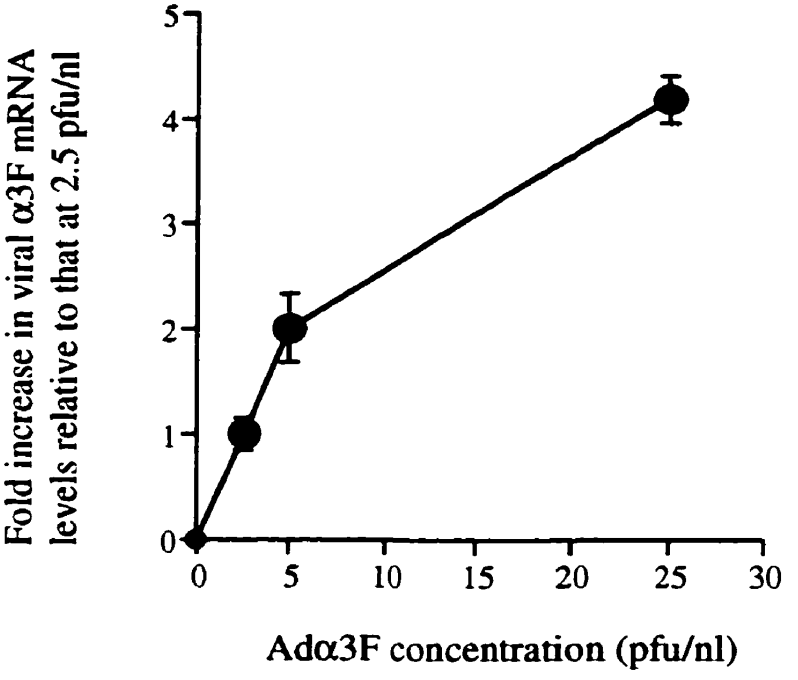
Fold increase in viral α3F mRNA levels relative to that at 2.5 pfu/nl
0
1
2
3
4
5
0
5
10
15
20
25
30
Adα3F concentration (pfu/nl)

Figure 4.4. Detection of α3FLAG proteins in Adα3F-infected SCG neurons. ***A***, Phase contrast photomicrographs of the fields shown below in ***B***. ***B***, Fluorescence photomicrographs of Adα3F-infected cultured SCG neurons showing FLAG immunoreactivity. The immunostaining procedures were performed using the Anti-FLAG M2 antibody and the Alexa 546 goat-anti-mouse IgG conjugated secondary antibody on fixed and permeabilized SCG neurons that we infected 3 days earlier with 50 pfu/nl of Adα3F. ***C***, Fluorescence photomicrographs showing low background fluorescence: Adα3F-infected SCG neurons were immunostained as in ***B*** except that the Anti FLAG M2 antibody was omitted. Scale bar, 25 μm.

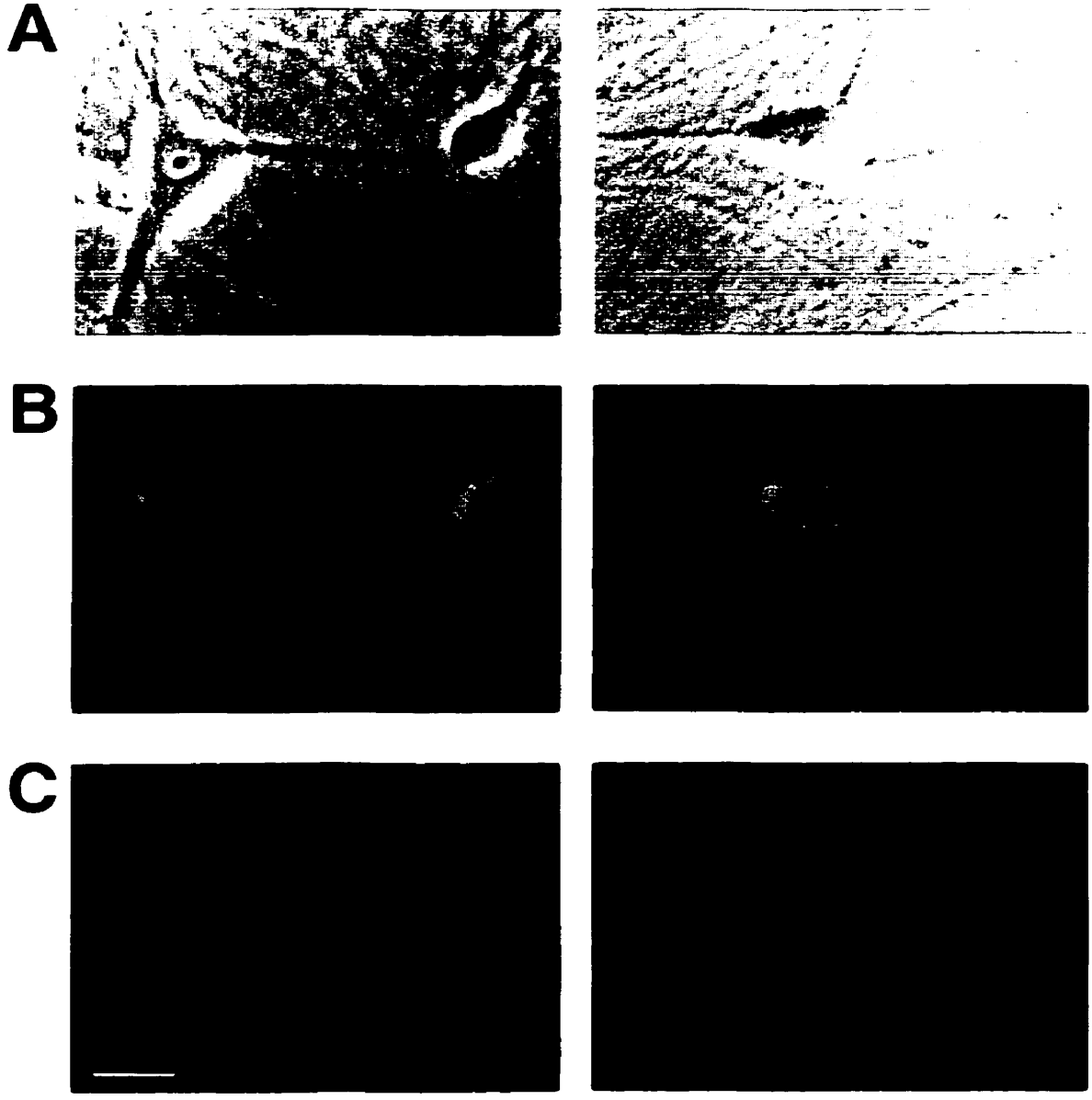
A
B
C

As the FLAG epitope is located on the extracellular C-terminal domain of the α3 subunit, we examined surface α3FLAG protein expression in non-permeabilized Adα3F-infected SCG neurons; however, we were unable to detect surface FLAG expression above background levels. To examine the possibility that surface α3FLAG-containing nAChRs are too few in number to be detected above background immunofluorescence, we tested several different methods of "blocking" non-specific antibody-binding in an attempt to reduce background immunofluorescence. However, in spite of reducing background fluorescence to levels similar to those shown in figure 4.4C, we were unable to detect FLAG specific immunofluorescence on non-permeabilized Adα3F-infected SCG neurons.

In these Adα3F-infected SCG cultures, we observed that a few non-neuronal cells exhibited marked FLAG fluorescence that was significantly higher than that detected in SCG neurons (Fig. 4.5). In these non-neuronal cells, we observed abundant intracellular FLAG immunoreactivity with high signals found mainly in perinuclear regions, possibly associated with the endoplasmic reticulum (ER) or Golgi network; this staining did not appear to be associated with the cell membrane. We immunostained Adα3F-infected cultures of non-neuronal cells prepared from SCG ganglia and observed similar FLAG immunoreactivity; no specific FLAG signals were detected in control uninfected non-neuronal cells. In addition, we did not observe any FLAG immunofluorescence above background levels in non-permeabilized Adα3F-infected non-neuronal cells, indicating that most FLAG immunoreactivity was located intracellularly. The possible explanations for the differences in FLAG immunostaining between neurons and non-neuronal cells are discussed below.

Figure 4.5. α3FLAG expression in non-neuronal cells from SCG cultures infected with Adα3F. The infection and immunostaining procedures were performed as described in Figure 4.4. ***A,*** Fluorescence photomicrograph showing a brightly fluorescent non-neuronal cell in a culture of SCG neurons. ***B,*** Phase contrast photomicrograph of the same field as in ***A***; the arrow indicates the nucleus of the fluorescent non-neuronal cell. Scale bar, 50 μm.

A

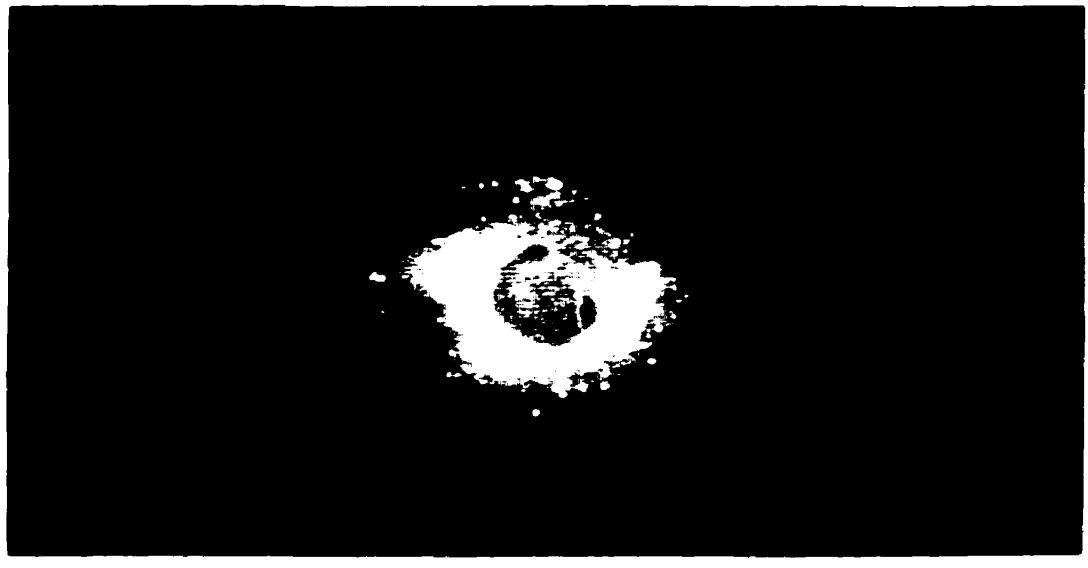

B

Overexpression of α3 increases ACh-evoked current densities

To determine whether the overexpression of α3 leads to changes in the number of functional nAChRs expressed at the cell surface, we measured ACh-evoked currents on Adα3F-infected SCG neurons (Fig. 4.6A). To identify infected neurons, we co-infected the cells with equal amounts of Adα3F and AdGFP, and then measured ACh-evoked currents on GPF positive neurons; in the previous chapter, I showed that when SCG neurons are co-infected with equal amounts of two different Ad vectors, the likelihood of a cell being infected by both viruses is ≈ 80%. In these experiments, we used 2 different concentrations of Adα3F: 15 and 30 pfu/nl that we predicted should give a ≈ 3-4 and a ≈ 7 fold overexpression in α3 mRNA respectively (see Figure 4.1). In cultures treated with 15 pfu/nl Adα3F, the mean ACh-evoked current density (± SEM) was 111.2 ± 10.5 (n=21), an ≈ 20% increase in comparison to control GFP-infected and uninfected cultured SCG neurons (Fig. 4.6C). The rate of activation or desensitization of ACh-evoked currents between Adα3F-infected neurons and uninfected and control AdGFP-infected neurons were similar. In addition, the ACh-evoked currents on Adα3F infected neurons showed strong inward rectification (Fig. 4.6B), similar to ACh-evoked currents on control SCG neurons (Fig. 3.9B). In cultures infected with 30 pfu/nl Adα3F, we found that the mean ACh-evoked current density was 128.3 ± 10.4 pA/pF (n=22), an ≈ 40% percent increase in comparison to controls (Fig. 4.6C). These results demonstrate that increases in α3 expression are sufficient to alter the expression of functional nAChRs. When we compare the distribution of ACh-evoked current densities on Adα3F neurons with that of controls (AdGFP-infected neurons and uninfected neurons), a shift in the magnitude of ACh-evoked current densities on individual neurons is observed in neurons overexpressing α3 mRNA (Fig. 4.6D).

Recently, I built a recombinant Ad, Adα3AS, that expresses antisense α3 mRNA but have not had time to fully characterize it. In our initial experiments on SCG neurons

Figure 4.6. ACh-evoked current densities are increased on Adα3F-infected SCG neurons. ACh-evoked currents were recorded from Adα3F-infected cultured SCG neurons. ***A***, Representative ACh-evoked current on an SCG neuron infected with 30 pfu/nl of each Adα3F and AdGFP. ***B***, The current-voltage relationship (*I-V*) relationship for the ACh-evoked current from an Adα3F-infected SCG neuron, obtained as described in Fig. 3.9. ***C***, Mean ACh-evoked current densities (pA/pF) on SCG neurons infected with either 15 pfu/nl (n=21) or 30 pfu/nl of each Adα3F and AdGFP (n=36), or with 30 pfu/nl of both Adα3**AS** and AdGFP (n=7). The control mean ACh-evoked current densities were calculated from both control uninfected SCG neurons or SCG neurons infected with AdGFP (30-60 pfu/nl)(n=35)(see Fig. 3.9). Mean ACh-evoked current densities on SCG neurons infected with 15 pfu/nl and 30 pfu/nl of Adα3F are significanly larger than those on controls ($p<0.01$; n=21 and $p<0.001$, n=36, respectively) while those on Adα3AS are significantly smaller than controls ($p<0.001$, n=7). The error bars represent the SEM. ***D***, Bar graph showing distribution of ACh-evoked current densities for Adα3F-infected cultured SCG neurons (30 pfu/nl; n=36)(black bars) and control SCG neurons (uninfected and AdGFP-infected; n=35)(white bars). This graph shows that the portion of SCG neurons with ACh-evoked current densities greater than 130 pA/pF is much larger in Adα3F infected SCG neurons than in control neurons.

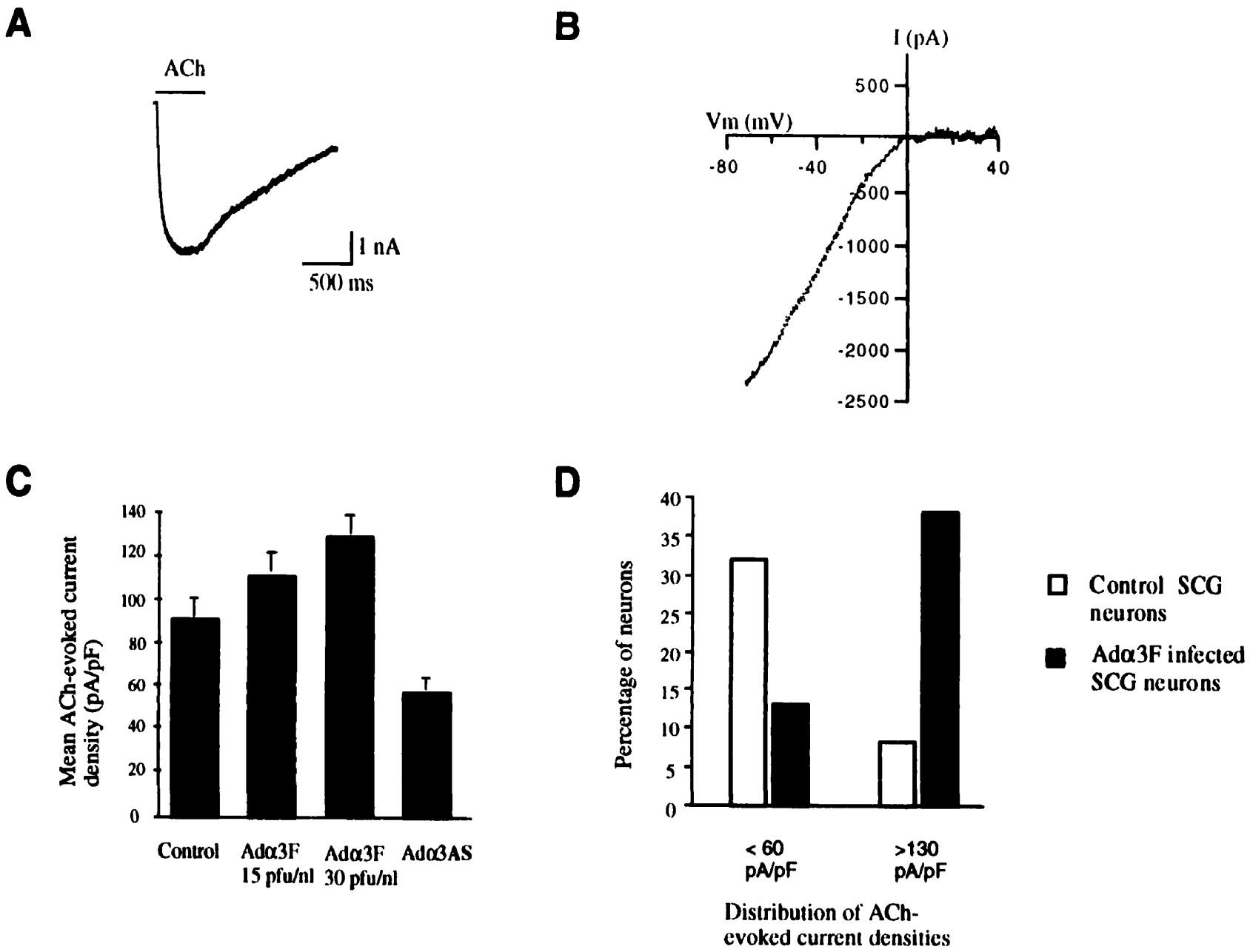
A
ACh
1 nA
500 ms
B
I (pA)
500
Vm (mV)
-80
-40
40
-500
-1000
-1500
-2000
-2500
C
Mean ACh-evoked current density (pA/pF)
140
120
100
80
60
40
20
0
Control
Adα3F 15 pfu/nl
Adα3F 30 pfu/nl
Adα3AS
D
Percentage of neurons
40
35
30
25
20
15
10
5
0
< 60 pA/pF
>130 pA/pF
Distribution of ACh-evoked current densities
Control SCG neurons
Adα3F infected SCG neurons

infected with this Ad (50 pfu/nl), we observed that the expression of antisense α3 mRNA reduced ACh-evoked current densities on SCG neurons by ≈ 35-40% (56.1 ± 6.7 pA/pF, n=7) 3 days after infection (Fig. 4.6C).

Measuring viral α3 protein expression in Adα3F-infected SCG neurons

One explanation for why we did not measure larger increases in ACh-evoked current densities when we overexpressed α3 mRNA by 6-7 fold in SCG neurons is that increases α3 mRNA may not lead to proportional increases in α3 proteins. To investigate this possibility, we have begun to measure α3FLAG protein expression in infected SCG neurons. As a first approach, we performed Western blot analyses on cell lysates prepared from Adα3F-infected SCG neurons using the Anti-FLAG M2 antibody and chemiluminescence to detect α3FLAG proteins. However, our results were inconclusive and require further investigation. One possibility is that the level of α3FLAG protein is too low to be detected with this approach.

Next, we attempted immunoprecipitation experiments. We metabolically-labeled Adα3F-infected SCG neurons with ^{35}S-methionine and used the anti-FLAG M2 antibody to immunoprecipitate α3FLAG proteins. The immunoprecipitated proteins were resolved by SDS PAGE and fluorography. A protein band of approximately 50-55 kDa was detected in immunoprecipitated proteins from Adα3F-infected neurons but not in those from controls (Fig. 4.7); this protein band is similar in molecular weight to the 54.8 kDa molecular weight of the rat α3 subunit (Sargent, 1993). These results suggest that we can detect α3FLAG proteins using immunoprecipitation.

Figure 4.7. Immunoprecipitation of α3FLAG proteins from Adα3F-infected SCG neurons. Cultured SCG neurons were infected 50 pfu/nl of Adα3F or AdGFP 3 days prior to metabolic-labeling with ^{35}S-methionine. α3FLAG proteins were immunoprecipitated with the Anti-FLAG M2 antibody and then separated by SDS-PAGE. Controls included immunoprecipitation of FLAG proteins from AdGFP-infected neurons, and "mock" immunoprecipitation (no Anti FLAG M2 antibody) of proteins from Adα3F-infected neurons. A protein band of ≈50-55 kDa, corresponding to the predicted size of α3 proteins, was detected in immunoprecipitated proteins from Adα3F-infected SCG neurons.

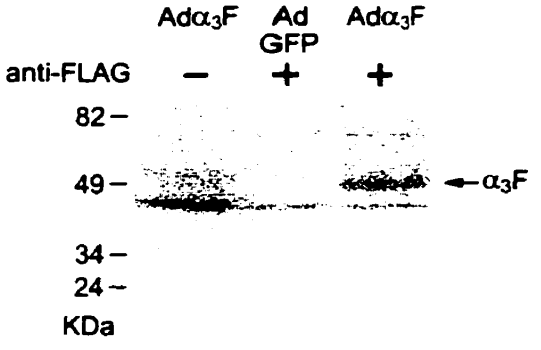

Figure 4.7. Immunoprecipitation of α3FLAG proteins from Adα3F-infected SCG neurons. Cultured SCG neurons, infected 3 days earlier with 50 pfu/nl of Adα3F, were metabolically-labeled with ^{35}S-methionine. α3FLAG proteins were immunoprecipitated with the anti-FLAG M2 antibody from lysates prepared from these cells and then separated by SDS-PAGE. Controls included immunoprecipitation of FLAG proteins from AdGFP infected neurons (50 pfu/nl), and mock immunoprecipitation (no M2 antibody) of proteins from Adα3F infected neurons. A protein band of ≈50-55 kDa, corresponding to the predicted size of α3 proteins was detected in immunoprecipitated proteins from Adα3F-infected SCG neurons.

Discussion

In this study, I investigate the role of α3 subunit gene expression in the appearance of functional nAChRs on cultured rat sympathetic neurons using Ad-mediated gene transfer to alter the expression of α3 subunits. I show that manipulating α3 expression alters the magnitude of ACh-evoked current densities on cultured SCG neurons. However, as many of my results are preliminary, in this discussion I also suggest further experiments to investigate the contributions of α3 subunits to ACh-evoked currents on SCG neurons.

Using Ad-mediated gene transfer, I show that α3 mRNA can be overexpressed by 6-7 fold in sympathetic neurons. I also demonstrate that viral α3 mRNA levels increase proportionally to the concentrations of virus applied in the range tested (0-25 pfu/nl). Presumably, at higher viral concentrations these mRNA levels will increase further and then plateau when either the cellular transcriptional machinery becomes saturated or when viral infection become toxic to the neurons (> 80-100 pfu/nl; see Chapter 3). Because endogenous α3 mRNA expression is not affected by Adα3F infection at the viral concentrations that I have tested, I do not anticipate to find any changes in α5, α7, β2 or β4 transcript levels. However, I have not yet verified whether the expression of these subunits is affected by either viral infection or changes in α3 expression.

Using whole-cell patch clamp techniques, we demonstrate that overexpression of α3 subunits leads to an increase in ACh-evoked current densities in comparison to age-matched controls. This finding supports my hypothesis that α3 subunit expression is rate-limiting for the assembly and insertion of functional nAChRs in the cell membrane.

When we measured ACh-evoked current densities on cultured SCG neurons infected with two different Adα3F concentrations, we found an ≈ 20% (15 pfu/nl) and an

≈ 40% (30 pfu/nl) increase in the ACh-evoked current densities in comparison to controls (see Fig. 4.6C). These concentrations are predicted to result in an ≈ 3-4 and ≈ 7 fold increase in α3 mRNA levels respectively, indicating that increases in α3 mRNA levels do not give rise to similarly large increases in ACh-evoked current densities. The modest increases in the ACh-evoked current densities suggest that an upper limit may exist for the number of functional α3-containing nAChRs that can be inserted into the cell membrane. This upper limit may result from an insufficient number of β subunits to co-assemble with virally expressed α3FLAG proteins. An alternative possibility is that the cellular machinery in the ER that folds and assembles nAChRs may be unable to efficiently assemble large quantities of nAChRs. These two possibilities could be examined by co-infecting SCG neurons with Adα3F and another Ad that expresses either β2 or β4 subunits. If this limit is due to a lack of β subunits, then one would expect to find substantially higher ACh-evoked current densities. If the limit is due a difficulty with folding and assembly, one would not expect to find higher ACh-evoked current densities.

An additional explanation is that α3FLAG-containing receptors may be stored intracellularly and not transported to the cell membrane. In chick CGN, the majority of assembled nAChRs appear to be stored in a large intracellular pool while only 1/5 to 1/10 of nAChRs are expressed on the neuronal cell surface (Jacob and Berg, 1987; Margiotta et al., 1987; Stollberg and Berg, 1987). If similar intracellular nAChR pools exist in SCG neurons, it is likely that in Adα3F-infected neurons most α3FLAG-containing nAChRs would be stored intracellularly rather than expressed on the cell surface. This could account for why ACh-evoked current densities are increased as much as α3 mRNA levels in Adα3F-infected SCG neurons.

To determine whether similar large intracellular pools of nAChRs exist in rat SCG neurons, one could examine surface and intracellular α3 protein expression using an antibody that recognizes all α3 proteins. At the moment, there are no specific antibody for rat α3. However, two monoclonal antibodies (mAbs) that recognize chick α3 subunits

exist and may be able to detect rat α3: mAb313 raised in rat (Whiting et al., 1991) and mAb A3-1 raised in mouse (Vernallis et al., 1993). Both mAbs were raised against the same chick α3 fusion protein containing the large cytoplasmic domain found between the membrane spanning domains M3 and M4, but recognize different epitopes on chick α3 subunits. These antibodies could be potentially used to characterize α3-containing nAChRs on rat SCG neurons.

If α3 subunit expression is rate-limiting for assembly of the nAChRs that mediate ACh-evoked currents on SCG neurons, I predict that repression of α3 protein expression would affect ACh-evoked current densities. Indeed, in one initial experiment, we found that overexpressing antisense α3 mRNA in SCG neurons, which presumably bound to and inhibited sense α3 mRNA translation, led to reduced ACh-evoked current densities. Therefore, this preliminary result lends further support to my hypothesis that the expression of α3 subunits is rate-limiting for the assembly and insertion of nAChRs on SCG neurons during early postnatal development.

I am in the process of building a recombinant Ad that expresses a dominant negative form of the α3 subunit. I have truncated the rat α3 cDNA to include the 1st half of α3 cDNA sequence, ending just after the sequences coding for M2. This polypeptide should be competent for receptor assembly, but because it lacks M3 and M4, it should disrupt receptor function; similar dominant negative constructs of muscle nAChR subunits disrupt muscle nAChR receptor function (Verrall and Hall 1992; Wang et al., 1996a). By co-expressing this truncated α3 subunit with both wild-type α3 and β4 subunits in *X.* oocytes, we have verified that truncation of α3 is sufficient to disrupt nAChR function. Because the dominant negative approach has proven to be very effective for studies on K channels where the presence of one dysfunctional subunit was sufficient to cripple receptor function (Kass and Davies, 1996; Spector et al., 1996; Johns et al., 1997), I anticipate that the dominant negative approach will significantly decrease functional α3 containing receptors. However, I do not know yet whether the antisense α3

or the dominant negative approach will be more effective at reducing functional α3-containing receptors.

By augmenting or repressing α3 protein expression, it is possible that I have altered the composition of nAChR subtypes expressed on SCG neurons. Mandelzys et al. (1995) have shown that, at the macroscopic level, most nAChRs on SCG neurons behave as a uniform population with respect to agonist activation and toxin blockade and are likely to be composed of α3, β2, and β4 subunits in the same receptor complex. It is conceivable that the overexpression of α3 subunits favors the assembly of receptors composed of only α3 and β4 subunits, as β4 mRNA levels are ≈ 4 higher than β2 levels in SCG neurons (Mandelzys et al., 1994; De Koninck and Cooper, 1995). Conversely, by repressing α3 expression, I may favor the assembly of receptors containing α3, β4, and α5. To determine whether overexpression or repression of α3 subunits affects the subunit composition of nAChRs, one would need to examine the pharmacology and the single channel properties of these nAChRs.

Previous experiments by Zigmond and colleagues demonstrate that nAChRs located at synaptic sites on SCG neurons are blocked by the snake toxin n-BTX but not by α-BTX (Loring and Zigmond, 1987; Sah et al., 1987; Loring et al., 1988). Because n-BTX also blocks α3-containing receptors expressed on *X.* oocytes (reviewed in Sargent, 1993) and nAChRs on the soma of SCG neurons (Mandelzys et al., 1995), these findings suggest that α3-containing receptors are targeted to synapses. To investigate the role of α3 subunits in synaptic transmission, one could examine synaptic interactions among infected cultured SCG neurons to determine whether the excitatory postsynaptic potentials (epscs) are significantly larger in neurons overexpressing α3 subunits and smaller in neurons treated with virus vectors expressing antisense α3 mRNA.

Using immunocytochemistry on permeabilized SCG neurons, I show that virally expressed α3FLAG proteins are found in the cell body and dendrites but not in the nuclei of SCG neurons (see Fig. 4.4). I was unable to determine if α3FLAG-containing

receptors are clustered or targeted to specific locations on the neuronal cell membrane because I could not detect surface FLAG expression in non-permeabilized Adα3F-infected SCG neurons. My inability to detect extracellular FLAG epitope expression may due to the fact that surface α3FLAG-containing nAChRs are too few in number to be detected above background immunofluorescence. Indeed, as mentioned above, there is good evidence that the majority of assembled nAChRs are stored intracellularly in chick CGNs, and that only a fraction of the total cellular nAChRs are found on the cell surface (Jacob and Berg, 1987; Margiotta et al., 1987; Stollberg and Berg, 1987). If similar intracellular pools exist in SCG neurons, most α3FLAG-containing nAChRs would be located intracellularly while only a fraction of these receptors would be found in the cell membrane, giving low surface α3FLAG expression.

I found significantly higher FLAG immunofluorescence in Adα3F-infected non-neuronal cells than in Adα3F-infected SCG neurons. One possible explanation for this unexpected finding is that non-neuronal cells are more readily infected by Ads than neurons and consequently express higher amounts of α3FLAG proteins. In my experiments with AdGFP and AdHCMVsp1LacZ infection of SCG cultures presented in the previous chapter, I did not observe any qualitative differences in the intensity of β-gal or GFP expression between infected non-neuronal cells and SCG neurons. Therefore, this possibility seems unlikely.

Alternatively, when α3FLAG subunits are assembled into nAChRs in SCG neurons, the FLAG epitope may be buried and therefore less accessible to the anti-FLAG antibody. The FLAG tagged C-terminus of rat α3 is located only 5 amino acids after the last membrane spanning domain (Boulter et al., 1986a); conceivably the FLAG epitope is imbedded within the assembled receptor, and therefore may not be detected by FLAG immunostaining. In contrast, non-neuronal cells do not express any β subunits (Mandelzys et al., 1994), and α3FLAG subunits are likely to remain unassembled, allowing the FLAG epitope in these α3FLAG proteins to be readily detected. There is

ample evidence that muscle nAChR subunits co-assemble very rapidly after translation and that unassembled and misfolded subunits are rapidly degraded in the endoplasmic reticulum (Green and Millar, 1995). If neuronal nAChRs are assembled in a similar manner, and if the FLAG epitope is buried within the receptor complex, then it follows that in Adα3F-infected neurons the majority of virally expressed FLAG epitopes would be either hidden in assembled nAChRs while unassembled α3FLAG proteins would be degraded, and therefore less FLAG immunoreactivity would be found than expected.

An alternative approach to investigate α3FLAG protein expression would be immunostain control and Adα3F-infected SCG neurons with an antibody that recognizes both endogenous and viral α3 subunits and then examine the differences in α3 protein immunostaining. If either of the two chick α3 mAbs described above recognizes rat α3 subunits, they may useful to characterize total α3 protein expression. However, because these mAbs recognize intracellular α3 epitopes they could not be used to characterize surface α3 protein expression. Nevertheless, these antibodies may be useful to characterize total α3 protein expression by Western and/or immunoprecipitation analyses (see below).

I have not used mAb35, the monoclonal antibody that has been used extensively to study nAChRs on chick CGN neurons, in my immunostaining experiments because this antibody recognizes the α5 subunit (Vernallis et al., 1993) and SCG neurons express very low levels of α5 mRNA. In addition, results of previous experiments by Cooper and colleagues with this antibody did not detect any mAb35-specific immunostaining on cultured SCG neurons.

A good approach to resolve these complex issues about α3FLAG protein expression is to quantify α3FLAG protein levels. My preliminary results with immunoprecipitation experiments indicate that it is possible to detect α3FLAG proteins in primary cultures of neurons. Further work is needed, however, to quantify α3FLAG protein levels and to correlate them with α3FLAG mRNA levels. If one of the two chick

α3 mAbs described above detects rat α3 proteins, we could compare total α3 protein expression with viral α3 protein expression.

Using ^{35}S-methionine pulse-chase labeling experiments with the anti FLAG antibody, one should be able to determine the turnover rate for virally expressed α3 subunits. If either of the two chick α3 mAbs detects rat α3 proteins, one could also evaluated the turnover rate of endogenous α3 proteins. This would indicate whether viral α3 subunits are rapidly degraded or if their half life similar to endogenous α3 subunits; the estimated half life of α3-containing nAChRs found on chick CGNs and chick sympathetic neurons is ≈ 1 day (Stollberg and Berg, 1987; Listerud et al., 1991).

In summary, my results demonstrate that recombinant Ad vectors are an effective tool for investigating ion channel function in primary cultures of sympathetic neurons. The development of Ad vectors opens new avenues for the study of numerous aspects of neuronal function.

Chapter 5

General Discussion

General discussion

For my doctoral research, I have investigated different aspects of gene expression that are important for the expression of neurotransmitter gated-ion channels on developing rat peripheral neurons. In one series of experiments, I examined the factors and mechanisms that regulate the expression of 5-HT_3Rs on neonatal sympathetic and sensory neurons. My results demonstrate that 5-HT_3R transcript expression is differentially regulated in vagal sensory nodose neurons and sympathetic neurons *in vivo* and in culture. In addition, I show that 5-HT_3R expression in nodose neurons depends, in part, on neurotrophic factors and target innervation. In a second series of experiments, I investigated the role of nAChR subunit expression in the appearance of functional nAChRs on neonatal sympathetic neurons. Specifically, I demonstrate that changes in α3 mRNA levels lead directly to changes in the magnitude of ACh-evoked current densities. To do this, I first modified and optimized novel gene transfer procedures based on recombinant adenovirus (Ad) vectors, and then used these vectors to manipulate α3 mRNA levels.

As these results have already been discussed in detail in the preceding chapters, here, I discuss the implications of my work for further studies on the various cellular mechanisms that control the expression of neuronal nAChRs and 5-HT_3Rs on peripheral neurons. In Chapters 3 and 4, I show that recombinant adenovirus vectors (a) are efficient gene transfer agents for sympathetic neurons and (b) can be used to overexpress ion channels on neurons. In this chapter, I emphasize how adenovirus vectors can be used to investigate a variety of other issues related to the biology of neuronal nAChRs and 5-HT_3Rs.

In this discussion, I address several topics related to the regulation of neuronal nAChR and 5-HT_3R expression. These include: the contribution of the different nAChR

subunits to sympathetic neuron excitability; the cellular mechanisms that direct the assembly of neuronal nAChRs; the targeting and anchoring of neurotransmitter-gated ion channels to synaptic sites; and the molecular signals that direct neuronal nAChR expression during synapse formation.

Adenovirus vectors in neurobiology research

The development of efficient gene transfer techniques for neurons has opened new avenues for the investigation of numerous cellular processes, such as signal transduction cascades, synapse formation, and apoptosis. Prior to the development of viral vectors, it was not possible to overexpress foreign proteins in neurons without resorting to building transgenic animals. A major advantage of viral vectors is that they can be used to overexpress either sense or antisense mRNA, as I show in Chapter 4. In addition, with viral vectors, it is possible to introduce into neurons dominant negative mutants that can disrupt normal wild-type protein function, allowing researchers to study the contributions of diverse proteins to normal cellular function (Herskowitz, 1987).

Recently, Ad-mediated gene transfer has been used to overexpress a variety of proteins in both central and peripheral neurons. For example, recombinant Ads have been used to overexpress G protein-gated inward rectifier K channels in hippocampal neurons (Ehrengruber et al., 1997) and 5-HT_3Rs in dorsal root ganglion neurons (Smith et al., 1997). Ad vectors have also been used to overexpress ciliary neurotrophic factor (CNTF) and B-50/GAP43 in CNS neurons *in vivo* (Holtmaat et al., 1997; Lisovoski et al., 1997). In addition, Ad vectors have been successfully employed to suppress protein expression in neurons: Kammesheidt et al. (1997) used Ads to express antisense mRNA for the NMDA receptor NR1 to decrease NMDA receptor-mediated synaptic currents in hippocampal neurons while Johns et al. (1997) used Ads to introduce a dominant

negative mutant of the voltage-gated K channel gene Kv4.2 into rat cerebellar granule cells to examine the contribution of this K channel to neuronal excitability. Over the last two years, recombinant Ads have gained tremendous popularity as gene delivery vehicles for neurons as well many other postmitotic cell types because they allow researchers to examine many cell biology issues that could not be addressed before.

However, a major limitation of using Ad vectors is that the current methods for building these vectors are inefficient and time consuming. Specifically, the frequency of successful recombination is low and, therefore, it is often necessary to repeat the procedures several times in order to obtain recombinant Ads. Recently, two new methods have been developed that increase the frequency of recombination. Hardy et al. (1997) have devised a procedure that uses Cre recombinase from bacteriophage P1 to catalyze the recombination between loxP sites in the shuttle plasmid and the donor Ad DNA. Because Cre recombinase is very efficient at recombination, virus rescue by this method is greatly enhanced. Vogelstein and colleagues have developed a method in which the homologous recombination events are done in *E.* coli bacteria rather than in HEK 293 cells (He et al., 1998). This method takes advantage of the highly efficient homologous recombination machinery present in bacteria and also markedly increases the recovery of recombinant Ads (He et al., 1998).

Using adenovirus vectors to investigate different aspects of nAChR expression on sympathetic neurons

My results presented in Chapter 4 indicate that α3 subunits are an important component of the receptors that mediate ACh-evoked currents on rat sympathetic neurons. However, sympathetic neurons also express α5, α7, β2 and β4 nAChR subunits, and therefore it is necessary to evaluate the physiological contribution of these subunits to

nAChRs expressed on these neurons. In addition, very little is known about the regulation of nAChR assembly or the mechanisms that direct the targeting and anchoring of the different nAChR subtypes to specific membrane domains. Many of these questions can be investigated using recombinant Ads to selectively overexpress or repress different nAChR subunits or to overexpress mutated or modified subunit constructs.

Role of α3, β2 and β4 subunits

As a first approach, the contribution of β subunits to ACh-evoked currents on sympathetic neurons can be investigated by perturbing the expression of β2 and β4 with sense or antisense adenovirus constructs, in much the same way as I have done for α3 subunits in Chapter 4. It is not known whether the overexpression or the repression of these β subunits will affect the assembly, targeting or anchoring of nAChRs on SCG neurons. I speculate that the overexpression of β2 will favor the formation of receptors containing only α3 and β2 while repression of β2 may favor the assembly of nAChRs composed of only α3 and β4. Presumably similar predictions can also be made about β4 overexpression and repression. Because α3β2 and α3β4 receptors expressed in *X.* oocytes differ in their sensitivities to the agonists cytisine, 1,1-dimethyl-4-phenyl-piperazinium iodide (DMPP), and nicotine (Luetje and Patrick, 1991; McGehee and Role, 1995; Sivilotti et al., 1997), it should be possible to determine whether the differential expression of β subunits affects the subunit composition of nAChRs by comparing the pharmacologies of ACh-evoked currents on cultured sympathetic neurons infected with different β Ad constructs.

As mentioned previously, pharmacological and electrophysiological data indicate that most nAChRs on SCG neurons are composed of α3, β2, and β4 subunits (Mandelzys et al., 1995). My results presented in Chapter 4 provide additional evidence that α3 subunits are part of the nAChRs that mediate ACh-evoked currents on SCG neurons. The

presence of both β2 and β4 subunits in this major nAChR species could be further investigated using adenoviruses to express dominant negative forms of these two subunits. Dominant negative constructs for β2 and β4 could be made by truncating each cDNA just after the sequences coding for the second membrane spanning domain, similar to the dominant negative α3 construct described in the discussion of Chapter 4. These truncated subunits should be capable of assembling normally, but because they lack M3 and M4, they should disrupt receptor function. If the expression of β2 and β4 dominant negative constructs each reduces the ACh-evoked current densities on SCG neurons, this would indicate that both β2 and β4 subunits assemble into the receptors that mediate ACh-evoked currents on SCG neurons. Together, these experiments on perturbing the expression of β2 and β4 should clarify the physiological roles of β subunits on SCG neurons.

Role of α5 subunits

The contributions of α5 subunits to ACh-evoked currents on rat sympathetic neurons are not known. α5 mRNA levels are very low in comparison to those of other nAChR subunits in neonatal rat sympathetic neurons and do not increase over time *in vivo* or in culture when ACh-evoked current densities increase (Mandelzys et al., 1994; De Koninck and Cooper, 1995). However, there is evidence that α5 co-assembles with α3 and β4 in chick ciliary ganglion neurons and with α4 and β2 in chick brain (Conroy et al., 1993;Vernallis et al., 1993; Wang et al., 1996b; Conroy and Berg, 1998). If α5 mRNA levels correlate with protein expression in SCG neurons, then presumably a small portion of nAChRs would contain α5 subunits. When heterologously expressed in *X.* oocytes and mammalian cells, receptors incorporating α3, α5, and β4 exhibit distinct agonist sensitivities (Fucile et al., 1997) and have higher single channel conductances than receptors containing α3β4 or α3β2β4 (Sivilotti et al., 1997). This suggests that α5-

containing nAChRs on SCG neurons, while few in number, may have a distinct physiological function. By overexpressing α5 subunits with recombinant adenoviruses in cultured sympathetic neurons and measuring ACh-evoked current densities and the kinetics of single channel openings, it should be possible to determine whether α5 subunits are incorporated into the receptors that mediate ACh-evoked currents.

Alternatively, the contribution of α5 subunits to ACh-evoked currents on SCG neurons could be examined using an adenovirus that expresses a dominant negative form of the α5 subunit. If the expression of dominant negative α5 subunits reduces ACh-evoked current densities, this would suggest that α5 subunits contribute to the generation of ACh-evoked currents on SCG neurons. Conversely, if the expression of dominant negative α5 subunits does not alter ACh-evoked current densities, this would indicate that α5 subunits are not major contributors to the ACh-evoked currents on these neurons.

If α5-containing nAChRs have a distinct physiological role on SCG neurons, it is possible that they may be targeted to specific membrane domains that may differ from α3β2β4 receptors. The localization of α5-containing receptors could be examined with immunocytochemistry experiments using an α5-specific antibody. As endogenous α5 subunit expression is low on SCG neurons, it would be best to examine the localization of α5 subunits on SCG neurons infected with an α5 expressing Ad construct. Alternatively, if no suitable antibodies for α5 are available, the α5 subunit could be modified to include an epitope tag such as FLAG or c-myc either at its C-terminal end or within the large cytoplasmic domain found between M3 and M4. Such epitope tagged α5 subunits could be introduced into SCG neurons using Ad vectors, and the targeting of these subunits could be examined by immunostaining for the expression of the epitope. Together, these experiment should shed some light on the physiological function(s) of α5 subunits in SCG neurons.

Role of α7 subunits

In chick ciliary ganglion neurons, α7-containing receptors mediate an α-BTX sensitive rapidly-activating and -inactivating component of ACh-evoked currents (Zhang et al., 1994). Similar currents have not been detected on rat sympathetic neurons in spite of the fact that SCG neurons express both α7 mRNA and α-BTX-binding proteins (Trouslard, et al., 1993; De Koninck and Cooper, 1995). I speculate that α7 currents may be too small to be resolved. To test this possibility, one could overexpress α7 subunits and quantitatively correlate mRNA levels with α7 current.

In addition, by examining α-BTX-binding on neurons overexpressing α7 subunits, it should be possible to determine if α7 receptors are localized to perisynaptic sites in sympathetic neurons, as has been shown in chick ciliary ganglion neurons (Wilson Horch and Sargent, 1995), or if they are uniformly distributed over the cell body as previous ^{125}I-α-BTX-binding studies on rat SCG neurons suggest (Fumagali and DeRenzis, 1984).

Folding and assembly of neuronal nAChRs

Signals that specify subunit association

The mechanisms that govern the assembly of neuronal nAChRs are an important cellular means of regulating nAChR subtype diversity. Little is known about the mechanisms that determine which nAChR subunits can co-assemble together. For example, what are the signals that allow the co-assembly of α3 with β4 subunits but prevent α3 from assembling with α7 or 5-HT$_3$R subunits. Strong evidence indicates that the extracellular N-terminal domains of the muscle nAChR subunits contain the necessary signals that specify muscle nAChR subunit associations (Green and Millar, 1995). Similarly, the N-terminal domain of glycine receptor subunits are implicated in

determining subunit assembly (Kuhse et al., 1993). I speculate that the N-terminal domains of neuronal nAChR and 5-HT_3R subunits also specify subunit associations.

One approach to examine this possibility would be to identify specific N-terminal regions or sequences that are involved in receptor assembly. To do this, one could use adenovirus vectors to overexpress in SCG neurons nAChR subunits with deletions or mutations of the N-terminal sequences and examine whether receptor assembly occurs normally. Similar experiments could be performed to examine 5-HT_3R assembly. An understanding of the mechanisms that specify which subunits can co-assemble will help determine how neurons control and limit the expression of diverse nAChR subtypes.

Role of molecular chaperones in neuronal nAChR assembly

The assembly of neuronal nAChRs in the endoplasmic reticulum (ER) is a complex process that must involve multiple folding and subunit association events. Studies on muscle nAChR assembly show that a large percentage of newly synthesized protein subunits do not assemble into functional receptors but are misfolded and rapidly degraded (Green and Millar, 1995). It is not known whether similarly large amounts of neosynthesized neuronal nAChR subunits are also improperly folded and degraded. To examine this possibility, one could label cellular proteins in Adα3F-infected SCG neurons with a pulse of ^{35}S-methionine and then immunoprecipitate both non-assembled α3FLAG subunits and assembled α3FLAG-containing receptors using the Anti FLAG M2 antibody (Ross et al., 1991). By comparing the radioactive intensity of the pulsed α3FLAG subunits with that of the other labeled nAChR subunits immunoprecipitated from the assembled α3FLAG receptors, one should be able to establish the proportion of α3FLAG subunits that are incorporated into assembled neuronal nAChRs. This determination would help to understand the relationship between mRNA levels and subunit protein expression.

The folding events during nAChR subunit assembly presumably involve the help of molecular chaperones, proteins that guide the folding of nascent polypetides (Ou et al, 1993; Gelman et al., 1995). One candidate chaperone is calnexin, a transmembrane molecular chaperone found in the ER that participates in the folding and oligomerization of many multisubunit glycoproteins complexes including muscle nAChRs (Ou et al., 1993; Gelman et al., 1995; Keller et al., 1996). Another ER chaperone, BiP, has been shown to interact with muscle nAChR subunits that are misfolded and unable to assemble (Blount and Merlie, 1991; Forsayeth et al., 1992). Therefore, I speculate that calnexin and BiP may also participate in the assembly of neuronal nAChRs and 5-HT_3Rs. One could perform immunoprecipitation experiments using antibodies for calnexin, Bip, and nAChR and/or 5-HT_3R subunits, to determine if these chaperones are associated with these receptor subunits. If the levels of any of these proteins are too low to be detected, a logical alternative approach would be to overexpress these proteins in sympathetic neurons using adenovirus vectors and then examine whether these proteins are associated *in vivo*.

Targeting of neurotransmitter-gated ion channel to synaptic sites

An additional regulatory step in the expression neuronal nAChRs is the transport of these receptors to the appropriate sites within the neuron's complex architecture. It is not known whether newly synthesized neuronal nAChRs are first transported to the cell surface and then redirected to their target sites by lateral diffusion in the plasma membrane, or if they are transported intracellularly and then translocated to the membrane once they arrive at their destination. Support for the first possibility come from the observation that nAChRs on the surface of muscle cells are recruited into clusters at the neuromuscular junction by the diffusion in the plasma membrane (Anderson and

Cohen,1977; Fallon and Hall, 1994). In addition, evidence from experiments on the targeting of *Drosophila* Shaker K channels to neuromuscular synapses suggests that K channels are first translocated to the cell surface and then transported to synapses (Zito et al., 1997). Perhaps similar protein trafficking mechanisms are common to all ion channels?

Neuronal nAChRs. There is good evidence that different neuronal nAChR subtypes are targeted to different locations within neurons. For example, $\alpha 3\beta 4$-containing receptors appear to be targeted to synaptic domains in autonomic neurons while $\alpha 7$- and $\alpha 4\beta 2$-containing receptors are targeted to nerve terminals of central neurons (Wilson Horch and Sargent, 1996; Role and Berg, 1996; Wonnacott, 1997). It is very likely that the different neuronal nAChR subunits contain specific sites or regions that interact with targeting molecules. One candidate region is the long intracellular domain between the M3 and M4 transmembrane domains. This intracellular region shows considerable sequence and size variability among all neuronal nAChR subunits and is postulated to interact with intracellular proteins. Therefore, I speculate that this region may specify the targeting of different nAChR subtypes. The role of the large intracellular domain between M3 and M4 in receptor targeting in SCG neurons could be examined by expressing nAChR subunits in which this regions has been mutated or even swapped with that of another subunit. Preliminary evidence indicates that deletion of the large intracellular loop of $\alpha 4$ does not impair its ability to assemble and form pharmacologically and physiologically normal nAChRs in *X.* oocytes (E. Cooper, unpublished results), and therefore mutations or deletions of the large intracellular loop are unlikely to perturb receptor function.

In contrast to chick ciliary ganglion neurons, the localization of different nAChR subunits on rat sympathetic neurons has not yet been thoroughly examined. It should be possible to determine whether the different subunits are localized to synaptic sites using

immunostaining techniques on sections of sympathetic ganglia as well as on SCG neurons that have developed in culture. Alternatively, if suitable antibodies are not available or if the receptor levels are too low to be resolved by immunostaining, the localization of nAChRs on SCG neurons could be determined by overexpressing epitope tagged subunits using either adenovirus vectors or other viral vectors that express high levels of transgenes, such as the Semliki Forest Virus (Liljestrom and Garoff, 1991; see also Chapter 1).

Because $\alpha4\beta2$ receptors appear to targeted to presynaptic sites while $\alpha3$-containing receptors are destined to postsynaptic sites, one can use this differential distribution to determine whether the α or β component governs the targeting of nAChRs. This could be done by overexpressing different pair-wise combinations of nAChR subunits in cultured SCG neurons and comparing (a) the localization of $\alpha4\beta2$ and $\alpha3\beta2$ receptors to determine if α subunits dictate targeting, and (b) the localization of $\alpha3\beta2$ and $\alpha3\beta4$ to evaluate if β subunits determine receptor targeting.

5-HT_3Rs. There is good evidence that the majority of 5-HT_3Rs in the CNS and PNS are targeted to presynaptic nerve terminals (Lambert et al., 1995). For example, 5-HT_3Rs are located on the central and peripheral terminals of nodose neurons (Lambert et al., 1995). In contrast, very little is known about the localization of 5-HT_3Rs on sympathetic neurons. One could examine the localization of this receptor in sympathetic neurons by immunostaining with a specific antibody for this receptor. Alternatively, if a suitable antibody is not available or if receptor levels are too low, again one could overexpress epitope tagged 5-HT_3R subunits in cultured sympathetic neurons and examine their targeting. If 5-HT_3Rs are found to be concentrated to presynaptic terminals on sympathetic neurons, this would suggest a role for 5-HT_3Rs in neurotransmitter release. In addition, sympathetic neurons could serve as an interesting model for the comparison of the mechanisms that target neuronal nAChRs to postsynaptic sites and 5-HT_3Rs to

nerve terminals. In contrast, if 5-HT_3Rs are found to be associated with postsynaptic membranes, this would suggest that these receptors may play a role in sympathetic neuron excitability. Moreover, this would indicate that the targeting mechanisms differ in sympathetic and nodose neurons and would provide a system in which one could investigate cell-specific targeting mechanisms.

Synapse Formation

Very little is known about the molecular mechanisms that promote the formation of interneuronal synapses. Recent advances have been made in understanding glutaminergic synaptogenesis. NMDA receptors appear to be linked to the cytoskeleton through PDZ domain interactions with membrane associated proteins such as PSD-95 (Craven and Bredt, 1998).

Two recent findings, however, have shed some light into the mechanisms that direct cholinergic synapse formation on autonomic neurons. The first finding is the recent discovery by Role and colleagues of several neuregulin isoforms that are expressed by the presynaptic inputs of chick sympathetic neurons (Yang et al., 1998). During neuromuscular synapse formation, neuregulins augment muscle nAChR expression: neuregulins are secreted by the motor nerve terminal and bind to the receptor tyrosine kinases erbB2, erbB3 and erbB4 found on the muscle cell surface; this binding initiates a cascade of intracellular signaling events that lead to increased nAChR expression by the nuclei near the new synapse (Fischbach and Rosen, 1997). Role and colleagues have demonstrated that chick neuronal neuregulins can also promote the expression of nAChR subunits and ACh-evoked currents on cultured chick sympathetic neurons. These results suggest that neuregulins may regulate neuronal nAChR expression during synaptogenesis (Yang et al., 1998).

The second finding is the recent identification of several rapsyn-like proteins that may anchor neuronal nAChRs to synaptic membranes in chick brain and CGN (Burns et al., 1997). Muscle rapsyn, also known as the 43 kDa protein, is responsible for the clustering and anchoring of muscle nAChRs to postsynaptic sites (Apel and Merlie, 1995). Rapsyn appears to link muscle nAChRs to a large complex of proteins known as the dystrophin-receptor complex which in turn is linked to the cytoskeleton (Apel et al., 1995). The identification of rapsyn-like molecules in the chick nervous system suggests that rapsyn may mediate the clustering and anchoring of neuronal nAChRs at interneuronal synapses (Burns et al., 1997).

The recent discovery of rapsyn-like molecules and neuregulins at interneuronal synapses suggests that the events involved in cholinergic synapse formation in the PNS may be similar to those that direct synaptogenesis at the neuromuscular junction.

Adenovirus vectors for *in vivo* applications

A logical extension of our work and that of others will to be investigate the mechanisms that regulate the expression of neuronal nAChRs *in vivo*. Indeed, several research groups have used transgenic and gene "knockout" approaches to study nAChR expression and function *in vivo* (Daubas et al., 1993; Picciotto et al., 1995; Bessis et al., 1997; Orr-Urtreger et al., 1997). An alternative, and perhaps simpler and less costly approach may be to use Ad vectors to investigate specific questions about nAChR expression *in vivo*. For example, to examine whether α3 subunits contribute to synaptic transmission *in vivo*, by injecting Adα3F into sympathetic ganglia one should be able to determine if the overexpression of α3 subunits increases synaptic efficacy. In addition to their usefullness in neurobiological research *in vivo*, Ad vectors have attracted much

attention for their potential use in the gene therapy of various cancers and inherited genetic diseases such as Duchennes muscular dystrophy and cystic fibrosis.

One difficulty in using recombinant Ad vectors for *in vivo* applications is that they are highly immunogenic (Wood et al., 1996; Christ et al., 1997). In spite of the deletion of E1 genes that control the expression of most other viral genes, first generation recombinant Ads still express low levels of early and late viral proteins that can provoke cellular and humoral immune responses (Christ et al., 1997). In animal studies, the host immune responses were shown to limit the duration of vector expression and prevent repeated administration of viruses (Douglas and Curiel, 1997). Similar host immune responses were found in preclinical gene therapy trials for cystic fibrosis using Ad expressing the cystic fibrosis transmembrane regulator (CFTR) channel which prevented the readministration of Ad vectors (Shenk, 1995; Wilson, 1995).

Second-generation Ad vectors are currently being engineered to overcome some of these problems. One approach has been to create recombinant Ads with deletions in the early genes E2, E3, and/or E4 which markedly reduce the expression of viral proteins (Christ et al., 1997; Amalfitano et al., 1998; Dedieu et al., 1998). Another approach has been to build recombinant Ads that are essentially devoid of viral coding sequences (Hardy et al., 1997; Schiedner et al., 1998). Such "gutless" Ad vectors do not express viral proteins and are, therefore, much less toxic and immunogenic and can express their transgenes for long periods of time *in vivo* (Schiedner et al., 1988). In addition, these vectors have very large capacities for foreign DNA, allowing for the transfer of large DNA regulatory elements, genomic DNA or multiple expression cassettes (Schiedner et al., 1998). One limitation of the using first generation adenovirus vectors for promoter analysis experiments is that they can express low levels of their foreign genes even in the absence of a promoter. Because these new "gutless" adenoviruses lack most viral sequences, they can be used to investigate transcriptional regulation. For example, using

these new "gutless" adenoviruses, it is now possible to introduce promoter constructs into neurons to investigate the regulation of nAChR gene transcription.

Conclusion

Over the last decade, much has been learned about the structure, function and expression of neuronal nAChRs, 5-HT_3Rs, and other neurotransmitter-gated ion channels. Future challenges will include the investigation of the molecular signals that govern interneuronal synapse formation and the mechanisms that regulate the transcription, assembly and targeting of neurotransmitter-gated ion channels on neurons. It is tempting to speculate that mechanisms similar to those that operate in the formation of the neuromuscular junction will also be found for synaptogenesis among neurons. Lastly, the development of viral vectors facilitates the investigation of the regulation of neurotransmitter-gated ion channel expression and opens new avenues for the study of multiple cellular and molecular aspects of neuronal function.

BIBLIOGRAPHY

Akabas MH, Karlin A (1995) Identification of acetylcholine receptor channel-lining residues in the M1 subunit of the α subunit. Biochemistry 34:12496-12500.

Akabas MH, Kaufmann C, Archdeacon P, Karlin A (1994) Identification of acetylcholine receptor channel-lining residues in the entire M2 segment of the α subunit. Neuron 13:919-927.

Akli S, Caillaud C, Vigne E, Stratford-Perricaudet L, Perricaudet M, Peschanski MR (1993) Transfer of a foreign gene into the brain using adenovirus vectors. Nature Genet 3:223-228.

Alkondon M, Rocha ES, Maelicke A, Albuquerque EX (1996) Diversity of nicotinic acetylcholine receptors in the rat brain.V. α-Bungarotoxin-sensitive nicotinic receptors in olfactory bulb neurons and presynaptic modulation of glutamate release. J. Pharmacol Exp Ther 278:1460:1471.

Altman-Hamamdzic S, Groseclose C, Ma JX, Hamamdzic D, Vrindavanam NS, Middaught LD, Parratto NP, Sallee FR (1997) Expression of beta-galactosidase in mouse brain: utilization of a novel nonreplicative Sindbis virus vector as a neuronal gene delivery system. Gene Therapy 4:815-822.

Amalfitano A, Hauser MA, Hu H, Serra D, Begy CR, Chamberlain JS (1998) Production and characterization of improved adenovirus vectors with the E1, E2b, and E3 genes deleted. J Virol 72:926-933.

Anand R, Conroy WG, Schoepfer R, Whiting P, Lindstrom J (1991) Neuronal nicotinic acetylcholine receptors expressed in *Xenopus* oocytes have a pentameric quaternary structure. J Biol Chem 266:11192-11198.

Anand R, Lindstrom J (1992) Chromosomal localization of seven neuronal nicotinic acetylcholine receptor subunit genes in humans. Genomics 13:962-967.

Andresen M, Kunze D (1994) Nucleus tractus solitarius-gateway to neural circulatory control. Ann Rev Physiol 56:93-116.

Anderson MJ, Cohen MW (1997) Nerve-induced and spontaneous redistribution of acetylcholine receptors on cultured muscle cells. J Physiol 268:757-773.

Arenella LS, Oliva JM, Jacob MH (1993) Reduced levels of acetylcholine receptor expression in chick ciliary ganglion neurons developing in the absence of innervation. J Neurosci 13:4525-4537.

Apel ED and Merlie JP (1995) Assembly of the postsynaptic apparatus. Curr Opin Neurobiol 5:62-67.

Apel E, Roberds SL, Campbell KP, Merlie JP (1995) Rapsyn may function as a link between the acetylcholine receptor and the agrin binding dystrophin-associated glycoprotein complex. Neuron 15:115-126.

Apud JA (1993) The 5-HT_3 receptor in mammalian brain: a new target for the development of psychotropic drugs? Neuropsychopharm 8:117-130.

Bailey MJ, Possee RD (1991) Manipulation of baculovirus vectors. *In:* Murray, EJ ed., "Gene Transfer and Expression Protocols", Methods in Molecular Biology, Vol 7, Humana Press, Clifton, NJ, pp 147-168.

Bannerji R (1995) Genetics and biology of retroviral vectors. *In* Kaplitt, MG, Loewy, AD, ed., "Viral vectors: gene therapy and neuroscience applications", Academic Press, San Diego, CA, pp. 75-88.

Bartlett JS, Samulski RJ (1995) Genetics and Biology of Adeno-associated virus. *In*: Kaplitt, MG and Loewy AR eds., "Viral vectors: gene therapy and neuroscience applications" Academic Press, San Diego, CA, pp.55-73.

Barthel L, Raymond P (1993) Subcellular localization of α-tubulin and opsin mRNA in the goldfish retina using digoxigenin-labeled cRNA probes detected by alkaline phosphatase and HRP histochemistry. J Neurosci Meth 50:145-152.

Baumgartner BJ, Shine HD (1997) Targeted transduction of CNS neurons with adenoviral vectors carrying neurotrophic factor genes confers neuroprotection that exceeds the transduced population. J Neurosci 17:6504-6511.

Beeson D, Bryson M, Betty M, Jeremiah S, Povey S, Vincent A, Newsom-Davis J (1993) Primary structure of the human muscle acetylcholine receptor. cDNA cloning of the gamma and epsilon subunits. Eur J Biochem 215:229-238.

Bertrand D, Cooper E, Valera S, Rungger D, Ballivet M (1991) *In:* Conn PM "Electrophysiology and microinjection: Methods in Neuroscience", Academic, New York.

Bett AJ, Haddara W, Prevec L, Graham FL (1994) An efficient and flexible system for construction of adenovirus vectors with insertion or deletions in early regions 1 and 3. Proc Natl Acad Sci 91:8802-8806.

Bett AJ, Prevec L, Graham FL (1993) Packaging capacity and stability of human adenovirus type 5 vectors. J Virol 67:5911-5921.

Bessis A, Simon-Chazottes D, Devillers-Thiery A, Guenet JL, Changeux JP (1990) Chromosomal localization of the mouse genes coding for α2, α3, α4, and β2 subunits of neuronal nicotinic acetylcholine receptor. FEBS Lett 264:48-52.

Bessis A, Savatier N, Devillers-Thiery A, Bejanin S, Changeux JP (1993) Negative regulatory elements upstream of a novel exon of the neuronal nicotinic acetylcholine receptor α2 subunit gene. Nucleic Acids Res 21:2185-2192.

Bessis A, Salmon AM, Zoli M, Le Novere N, Picciotto M, Changeux JP (1995) Promoter elements conferring neuron-specific expression of the β2-subunit of the neuronal nicotinic acetylcholine receptor studied in vitro and in transgenic mice. Neuroscience 69:807-819.

Bessis A, Champitaux N, Chatelin L, Changeux JP 91997) The neuron-restrictive silencer element: a dual enhancer/silencer crucial for patterned expression of a nicotinic receptor gene in the brain. Proc Natl Acad Sci 94:5906-5911.

Bigger CB, Casanova EA, Gardner PD (1996) Transcriptional regulation of neuronal nicotinic acetylcholine receptor genes. Functional interactions between Sp1 and the rat beta4 subunit gene promoter. J Biol Chem 271:32842-32848.

Bigger CB, Melnikova IN, Gardner PD (1997) Sp1 and Sp3 regulate expression of the neuronal nicotinic acetylcholine receptor β4 subunit gene. J Biol Chem 272:25976-25982.

Black I B (1978) Regulation of autonomic development. Ann Rev Neurosci 1:183-214.

Blount P, Merlie JP (1991) BIP associates with newly synthesized subunits of the mouse muscle nicotinic receptor. J Cell Biol 113:1125-1132.

Bondi A, Chieregatti G, Eusebi V, Fulcheri E, Bussolati G (1982) The use of β-galactosidase as a tracer in immunocytochemistry. Histochemistry 76:153-158.

Boulter J, Luyten W, Evans K, Mason P, Ballivet M, Goldman D, Stengelin S, Martin G, Heinemann S, Patrick J (1985) Isolation of a clone coding for the α-subunit of a mouse acetylcholine receptor. J Neurosci. 5:2545-2552.

Boulter J, Evans K, Goldman K, Martin G, Treco D, Heinemann S, Patrick J (1986a) Isolation of a cDNA clone coding for a possible neural nicotinic acetylcholine receptor α-subunit. Nature 319:386-374.

Boulter J, Evans K, Martin G, Mason P, Stengelin S, Goldman D, Heinemann S, Patrick J (1986b) Isolation and sequence of cDNA clones coding for the precursor of the γ subunit of mouse muscle nicotinic acetylcholine receptor. J Neurosci Res 16:37-49.

Boulter J, O'Shea-Greenfield A, Duvoisin RM, Connolly JG, Wada E, Jensen A, Gardner PD, Ballivet M, Deneris ES, McKinnon D, Heinemann S, Patrick J (1990). α3, α5 and β4: three members of the rat neuronal nicotinic acetylcholine receptor-related gene family for a gene cluster. J Biol Chem 265:4472-4482.

Boyd RT, Jacob MH, Couturier S, Ballivet M, Berg DK (1988) Expression and regulation of neuronal acetylcholine receptor mRNA in chick ciliary ganglia. Neuron 1:495-502.

Boyd RT, Jacob MH, McEachern AE, Caron S, Berg DK (1991) Nicotinic acetylcholine receptor mRNA in dorsal root ganglion neurons. J Neurobiol 22:1-14.

Boyd RT (1994) Sequencing and promoter analysis of the genomic region between the rat neuronal nicotinic acetylcholine receptor β4 and α3 genes. J Neurobiol 8:960-973.

Britto LR, Keyser KT, Lindstrom JM, karten HJ (1992) Immunohistochemical localization of α-BTX-binding proteins in the chick brain. J Comp Neurol 317:325-340.

Buoanno A, Mudd J, Merlie JP (1989) Isolation and characterization of the β and ε subunit genes of mouse muscle acetylcholine receptor. J Biol Chem 13:7611-7616.

Burns AL, Benson D, Howard MJ, Margiotta JF (1997) Chick ciliary ganglion neurons contain transcripts coding for acetylcholine receptor-associated protein at synapses (Rapsyn). J Neurosci 17:5016-5026.

Campos-Caro A, Smillie FI, Dominguez del Toro E, Rovira JC, Vicente-Agullo F, Chapuli J, Juiz JM, Sala S, Sala F, Ballesta JJ, Criado M (1997) Neuronal nicotinic acetylcholine receptors on bovine chromaffin cells: cloning, expression, and genomic organization receptor subunits. J Neurochem 68:488-497.

Castro MG, Rowe J, Morrison E, Tomasec P, Murray CA, Shering AF, Lowenstein PR (1996) Calcium-phosphate, DEAE-dextran coprecipitation, and electroporation to transfer genes into neuronal and glial cell lines. *In:* Lowenstein PR and Enquist LW eds., "Protocols for gene transfer in neuroscience: towards gene therapy of neurological disorders", Wiley, West Sussex, England, pp 9-23.

Chalfie M, Tu Y, Euskirchen G, Ward WW, Prasher DC (1994) Green fluorescent protein as a marker for gene expression. Science 263:802-805.

Changeux JP (1993) Chemical signaling in the brain. Scientific American, Nov., 58-62.

Changeux JP, Devillers-Thiery A, Chemouilli P (1984) Acetylcholine receptor: an allosteric protein. Science 225:1335-1345.

Chomczynski P, Sacchi N (1987) Single-step method of RNA isolation by acid guanidium thiocyanate-phenol-chloroform extraction. Anal Biochem 162:156-159.

Christ M, Lusky M, Stoeckel F, Dreyer D, Dieterle, A, Michou A-I, Pavirani A, Mehtali M (1997) Gene therapy with recombinant adenovirus vectors: evaluation of the host immune response. Immunology Letters 57:19-25.

Clarke PBS, Schwartz RD, Paul SM, Pert CB, Pert A (1985) Nicotinic-binding in rat brain: autoradiographic comparison of [3H] acetylcholine, [3H] nicotine, and [125I]-α-bugarotoxin. J Neurosci 5:1307-1315.

Clarke PBS (1993) Nicotinic receptors in mammalian brain: localization and relation to cholinergic innervation. Prog Brain Res 98:77-83.

Clarke PBS (1995) Nicotinic receptors and cholinergic neruotransmission in the central nervous system. Annals NY Acad Sci 757:73-83.

Coggan JS, Paysan J, Conroy WG, Berg DK (1997) Direct recording of nicotinic responses in presynaptic nerve terminals. J Neurosci 17: 5798-5806.

Colquhoun L, Dineley K, Patrick J (1993) A hetero-beta neuronal nicotinic acetylcholine receptor expressed in *Xenopus* oocytes. Soc Neurosci Abst 19:1533.

Cooper E, Couturier S, Ballivet M (1991) Pentameric structure and subunit stoichiometry of a neuronal nicotinic acetylcholine receptor. Nature 350:235-238.

Conroy WG, Vernallis AB, Berg DK (1992) The α5 gene product assembles with multiple acetylcholine receptor subunits to form distinctive subtypes in the brain. Neuron 9:679-691.

Conroy WG, Berg DK (1995) Neurons can maintain multiple classes of nicotinic acetylcholine receptors distinguished by different subunit compositions. J Biol Chem 270:4424-4431.

Conroy WG, Berg DK (1998) Nicotinic receptor subtypes in the developing chick brain: appearance of a species containing alpha4, beta2, and alpha5 gene products. Mol Pharm 53:392-401.

Corriveau RA, Berg DK (1993) Coexpression of multiple acetylcholine receptor genes in neurons: quantification of transcripts during development. J Neurosci 13:2662-2671.

Corriveau RA, Berg DK (1994) Neurons in culture maintain acetylcholine receptor levels with far fewer transcripts than *in vivo*. J Neurobiol 25:1579-1592.

Corsini J, Traul DL, Wilcox CL, Gaines P, Carlson JO (1996) Efficiency of transduction by recombinant Sindbis replicon virus varies among cell lines, including mosquito cells and rat sensory neurons. Biotechniques 21:492-497.

Couturier S, Bertrand D, Matter JM, Hernandez MC, Bertrand S, Millar N, Valera S, Barkas T, Ballivet M (1990a) A neuronal nicotinic acetylcholine receptor subunit (α7) is developmentally regulated and forms a homo-oligomeric channel blocked by α-BTX. Neuron 5:847-856.

Couturier S, Erkman L, Valera S, Rungger D, Bertrand S, Boulter J, Ballivet M, Bertrand D (1990b) α5, α3, and non-α3: three clustered avian genes encoding neuronal nicotinic acetylcholine receptor-related subunits. J Biol Chem 265:17560-17567.

Craven SE, Bredt DS (1998) PDZ proteins organize synaptic signaling pathways. Cell 93:495-498.

Criado M, del Toro ED, Carrasco-serrano C, Smillie FI, Juiz JM, Viniegra S, Ballesta JJ (1997) Differential expression of α-bungarotoxin-sensitive neuronal nicotinic receptors in adrenergic chromaffin cells: a role for transcription factor Egr-1. J Neurosci 17:6554-6564.

Czajkowski C, Karlin A (1991) Agonist-binding site of Torpedo electric tissue nicotinic acetylcholine receptor. J Biol Chem 266:22603-22612.

Dale HH (1954) The beginnings and the prospects of neuro-humoral transmission. Pharmacol Rev 6:7-13.

Daubas P, Devillers-Thiery A, Geoffroy B, Martinez S, Bessis A, Changeux JP (1990) Differential expression of the neuronal acetylcholine receptor α2 subunit gene during chick brain development. Neuron 5:49-60.

Daubas P, Salmon AM, Zoli M, Geoffroy B, Devillers-Thiery A, Bessis A, Medeville F, Changeux JP (1993) Chicken neuronal acetylcholine receptor α2-subunit gene exhibits neuron-specific expression in the brain and spinal chord of transgenic mice. Proc Natl Acad Sci USA 90:2237-2241.

Davidson B, Allen E, Kozarsky K, Wilson K, Roessler B (1993) A model system for in vivo gene transfer into the central nervous system using adenoviral vector. Nature Genet 3:219-223.

Dedieu JF, Vigne E, Torrent C, Jullien C, Mahfouz I, Caillaud JM, Aubailly N, Orsini C, Perricaudet M, Yeh P (1998) Long-term gene delivery into the livers of immunocompetent mice with E1/E4-defective adenoviruses. J Virol 71: 4626-4637.

de Hoop MJ, Huber LA, Stenmark H, Wiliamson E, Zerial M, Parton RG, Dotti G (1994) The involvement of the small GTP-binding protein Rab5a in neuronal endocytosis. Neuron 13:1-12.

De Koninck P, Carbonetto S, Cooper E (1993) NGF induces neonatal rat sensory neurons to extend dendrites in culture after removal of satellites cells. J Neurosci 13:577-585.

De Koninck P, Cooper E (1995) Differential regulation of neuronal nicotinic ACh receptor subunit genes in cultured neonatal rat sympathetic neurons: specific induction of alpha 7 by membrane depolarization through a Ca^{2+}/calmodulin-dependent kinase pathway. J Neurosci 15:7966-7978.

Del Toro ED, Juiz JM, Peng X, Lindstrom J, Criado M (1994) Immunocytochemical localization of the α7 subunit of the nicotinic acetylcholine receptor in the rat central nervous system. J Compara Neurol 349:325-342.

Derkach V, Suprenant A, North RA (1989) 5-HT_3 receptors are membrane ion channels. Nature 339:706-709.

Donoghue S, Garcia M, Jordan D, Spyer KM (1982) Identification and brain-stem projections of aortic baroreceptor afferent neurones in nodose ganglia of cats and rabbits. J. Physiol, 322:337-352.

Douglas JT, Curiel DT (1997) Adenoviruses as vectors for gene therapy. Science and Medicine, Scientific American, March-April, 44-53.

Douglas W (1975) Histamines and antihistamines; 5-hydroxytryptamine and antagonists. In: The pharmacological basis of therapeutics, 5th ed., (Goodman L, Gilman A, eds), pp 590-624. New York: Macmillan.

Downie DL, Hope AG, Lambert JJ, Peters JA, Blackburn TP, Jones BJ (1994) Pharmacological characterization of the apparent splice variants of the murine 5-HT_3R-A subunit expressed in Xenopus laevis oocytes. Neuropharm 33:473-482.

Du Q, Tomkinson AE, Gardner PD (1997) Transcriptional regulation of neuronal nicotinic acetylcholine receptor genes. J Biol Chem 272:14990-14995.

Dubensky TW, Driver DA, Polo JM, Belli BA, Latham EM, Ibanez CE, Chada S, Brumm D, Banks TA, Mento SJ, Jolly DJ, Chang SM (1996) Sindbis virus DNA-based expression vectors: utility for in vitro and in vivo gene transfer. J Virol 70:508-519.

Elgoyhen AB, Johnson DS, Boulter J, Vetter, Heinemann (1994) α9: an acetylcholine receptor with novel pharmacological properties expressed in rat cochlear hair cells. Cell 79:705-715.

Eng CM, Kozak CA, Beaudet AL, Zoghbi HY (1991) Mapping of multiple subunits of the neuronal nicotinic acetylcholine receptor to chromosome 15 in man and chromosome 9 in mouse. Genomics 9:278-282.

Engisch KL, Fishbach GD (1990) The development of ACh- and GABA-activated currents in normal and target-deprived embryonic chick ciliary ganglia. Dev Biol 139:417-426.

Ehrengruber MU, Doupnik CA, Xu Y, Garvery J, Jasek M, Lester H, Davidson N (1997) Activation of heteromeric G protein-gated inward rectifier K^+ channels overexpressed by adenovirus gene transfer inhibits the excitability of hippocampal neurons. PNAS 94:7070-7075.

Federoff HJ, Geschwind MD, Geller AI, Kessler JA (1992) Expression of nerve growth factor *in vivo*, from a defective HSV-1 vector, prevents effects of axotomy on sympathetic ganglia. Proc Natl Acad Sci USA 89:1636-1640.

Federoff HJ (1995) The use of defective herpes simplex virus amplicon vectors to modify neural cells and the nervous system. *In*: Kaplitt, MG and Loewy AR eds., "Viral vectors: gene therapy and neuroscience applications" Academic Press, San Diego, CA, pp 109-118.

Felgner PL (1991) Cationic liposome-mediated transfection with lipofectin reagent. In: Murray EJ ed. "Methods in molecular biology: gene transfer and expression protocols". Humana press, Clifton New Jersey, pp 81-90.

Fink DJ, Glorioso JC (1997) Engineering herpes simplex virus vectors for gene transfer to neurons. Nature Medicine 3:357-359.

Fischbach GD, Rosen KM (1997) Aria: a neuromuscular junction neuregulin. Ann Rev Neurosci 20:429-458.

Flores CM, Rogers SW, Pabreze LA, Wolfe BB, Kellar KJ, (1992) A subtype of nicotinic cholinergic receptor in rat brain is composed of α4 and β2 subunits and is up-regulated by chronic nicotine treatment. J Pharmacol Exp Ther 41:31-37.

Forsayeth JR, Gu Y, Hall ZW (1992) Bip forms stable complexes with unassembled subunits of the acetylcholine receptor in transfected COS cells and in C2 muscle cells. J Cell Biol 117:841-847.

Forsayeth JR, Kobrin E (1997) Formation of oligomers containing the β3 and β4 subunits of the rat nicotinic receptor. J Neurosci 17:1531-1538.

Fozard JR (1984) Neuronal 5-HT receptors in the periphery. Neuropharm 23:1473-1486.

Fucile S, Barabino B, Palma E, Grassi F, Limatola C, Mileo AM, Alema S, Ballivet M, Eusebi F (1997) α5 subunit forms functional α3β4α5 nAChRs in transfected human cells. Neuroreport 8:2433-2436.

Fumagali L, DeRenzis G, Miani N (1976) Acetylcholine receptors: number and distribution in intact and deafferented superior cervical ganglion of the rat. J Neurochem 27:47-52.

Fumagali L, DeRenzis G (1984) Extrasynaptic localization of α-bungarotoxin receptors in the rat superior cervical ganglia. Neurchem Int 6:355-364.

Furukawa K, Akaike N, Onodera H, Kogure K (1992) Expression of 5-HT3 receptors in PC12 cells treated with NGF and 8-Br-cAMP. J Neurophys 67:812-819.

Furshpan, E., Potter, D. and Landis, S. (1980-81) On the transmitter repertoire of sympathetic neurons in culture. Harvey Lectures 76:149-91.

Gaddum JH, Picarelli A (1957) Two kinds of tryptamine receptors. Br J Pharmacol 12:323-328.

Geller AI, During MJ, Neve RL (1991) Molecular analysis of neuronal physiology by gene transfer into neurons using herpes simplex virus vectors. Trends Neurosci 14:428-432.

Gelman MS, Chang W, Thomas DY, Bergeron JJM, Prives JM (1995) Role of the endoplasmic reticulum chaperone calnexin in subunit folding and assembly of nicotinic acetylcholine receptors. J Biol Chem 270:15085-150-92.

Gerzanich V, Kuryatov A, Anand R, Lindstrom J (1997) "Orphan" α6 nicotinic AChR subunit can form a functional heteromeric acetylcholine receptor. Mol Pharmacol 51:320-327.

Ginsberg HS (1988) Adenoviruses. *In:* Dulbecco R, Ginsberg HS "Virology", 2nd ed., JB Lippincott Co, Philadelphia, pp 147-60.

Glorioso JC, Bender MA, Goins WF, DeLucca N, Fink D (1995) Herpes simplex virus as a gene-delivery vector to the central nervous system. *In*: Kaplitt, MG and Loewy AR eds., "Viral vectors: gene therapy and neuroscience applications" Academic Press, San Diego, CA, pp 1-23.

Gordon JC, Rowland HC (1990) Nerve growth factor induces 5-HT_3 recognition sites in rat pheochromocytoma (PC12) cells. Life Sci 46:1435-1442.

Görne-Tschelnokow U, Stecker A, Kaduk C, Naumann D, Hucho F (1994) The transmembrane domains of the nicotinic acetylcholine receptor contain α-helical and β structures. EMBO J 13:338-341.

Gotti C, Hanke W, Maury K, Moretti M, Ballivet M, Clementi F, Bertrand D (1994) Pharmacology and biophysical properties of α7 and α7-α8 α-bungarotoxin receptor subtypes immunopurified from the chick optic lobe. Eur J Neurosci 6:1281-1291.

Graham FL, van der Ebb AJ (1973) A new technique for the assay of infectivity of human Adenovirus 5 DNA. Virol 52:456-467.

Graham FL, Prevec L (1991) Manipulation of adenovirus vectors. *In:* Murray EJ, ed. "Methods in Molecular Biology: Gene transfer and expression protocols" Volume 7, Humana Press, Clifton, New Jersey, pp. 109-128.

Gray R, Rajan As, Radcliffe KA, Yakehiro M, Dani JA (1996) Hippocampal synaptic transmission enhanced by low concentrations of nicotine. Nature 383:713:716

Green WN, Claudio T (1993) Acetylcholine receptor assembly: subunit folding and oligomerization occur sequentially. Cell 74:57-69.

Green WN, Milllar NS (1995) Ion channel assembly. Trends in Neurosci 18:280-287.

Greenshaw AJ (1993) Behavioral pharmacology of 5-HT_3 receptor antagonists: a critical update on therapeutic potential. Trends Pharmacol Sci 14:265-270.

Guy HR, Hucho F (1987) The ion channel of the nicotinic acetylcholine receptor. Trends Neurosci 8:318-321.

Hall ZW, Sanes JR (1993) Synaptic structure and development: the neuromuscular junction. Cell72/Neuron 10 99-121.

Hall ZW, Hildebrand, J. and Kravitz, E. Eds. (1974) Chemistry if Synaptic Transmission: Essays and Sources Chiron Press, Newton, MA, USA.

Halvorsen SW, Berg DK (1986) Identification of a nicotinic acetylcholine receptor on neurons using an a-neurotoxin that blocks receptor function. J Neurosci 6:3405-3412.

Hamil OP, Marty A, Neher E, Sakmann B, Sigworth F (1981) Improved patch clamp techniques for high resolution current recording from cells and cell-free membrane patches. Pfluegers Arch 391:85-100.

Hardy S, Kitamura M, Harris-Stansil T, Dai Y, Phipps ML (1997) Construction of adenovirus vectors through Cre-lox recombination. J Virol 71:1842-1849.

Hawrot E, Patterson P (1979) Long-term culture of dissociated sympathetic neurons. Methods Enzymol 58:574-584.

He TC, Zhou S, Da Costa LT, Yu J, Kinzler KW, Vogelstein K (1998) A simplified system for generating recombinant adenoviruses. Proc Natl Acad Sci USA 95:2509-2514.

Herdegen T, Zimmerman M (1994) Expression of c-Jun and JunD transcription factors represent specific changes in neuronal gene expression following axotomy. Progress Brain Res 103:153-171.

Hernandez MC, Erkman L, Matter-Sadzinski L, Roztocil T, Ballivet M, Matter JM (1995) Characterization of the nicotinic acetylcholine receptor b3 gene: its regulation with the avian nervous system effected by a promoter 143bp in length. J Biol Chem 270:3225-3233.

Herskowitz I (1987) Functional inactivation of genes by dominant negative mutations. Nature 329:219-222.

Heumann R, Lindholm D, Bandtlow C, Meyer M, Radeke MJ, Misko TP, Shooter E, Thoenen H (1987) Differential regulation of mRNA encoding nerve growth factor and receptor in rat sciatic nerve during development, degeneration, and regeneration: role of macrophages. Proc Natl Acad Sci USA 84: 8735-8739.

Hill JA, Zoli M, Bourgeois JP, Changeux JP (1993) Immunocytochemical localization of a neuronal nicotinic receptor: the β2 subunit. J Neurosci 13:1551-1568.

Hitt M, Bett AJ, Addison CL, Prevec L, Graham FL (1995) Techniques for human adenovirus vector construction and characterization. Methods in Molecular Genetics, Vol 7, Academic Press, San Diego, CA, pp 13-30.

Ho DY, Mokarski ES (1988) Beta-galactosidase as a marker in the peripheral and nervous tissues of the herpes-simplex virus-infected mouse. Virology 174:279-283.

Ho D, Mocarski ES (1989) Herpes simplex virus latent RNA (LAT) is not required for late infection in the mouse. Proc Natl Acad Sci USA 86:7596-7600.

Hökfelt T, Ceccatelli S, Gustafsson L, Hulting A-L, Verge V, Villar M, Xu X-J, Xu Z-Q, Zhang X, Wiesenfeld-Hallin Z, Zhang X (1994a) Plasticity of NO synthase expression in the nervous and endocrine system. Neuropharm 33:1221-1227.

Hökfelt T, Zhang X, Wiesenfeld-Hallin Z (1994b) Messenger plasticity in primary sensory neurons following axotomy and its functional implications. Trends Neurosci 17:22-30.

Holtmatt A, Hermens W, Sonnemans M, Giger R, Van Leeuwen F, Kaplitt MG, Oestreicher A, Gispen WH, Verhaagen J (1997) Adenoviral vector-mediated expression of B-50/GAP-43 induces alterations in the membrane organization of olfactory axon terminals in vivo. J Neurosci 17:6575-6586.

Hope AG, Downie DL, Sutherland L, Lambert JJ, Peters JA, Burchell B (1993) Cloning and functional expression of an apparent splice variant of the murine 5-HT_3 A subunit. Eur J Pharmacol 245:187-192.

Hong SS, Karayan L, Tournier J, Curiel DT, Boulanger PA (1997) Adenovirus type 5 fiber knob binds to MHC class I $\alpha 2$ domain at the surface of human epithelial and B lymphoblastoid cells. EMBO J 16:2294-2306.

Huang S, Kamata T, Takada Y, Ruggeri ZM, Nemrow GR (1996) Adenovirus interaction with distinct integrins mediates separate events in cell entry and gene delivery to hematopoietic cells. J Virol 70:4502-4508.

Imoto K, Busch C, Sakmann B, Mishina M, Konno T, Nakai J, Bujo H, Mori Y, Fukuda K, Numa s (1988) Rings of negatively charged amino acids determine the acetylcholine receptor channel conductance. Nature 335:645-648.

Isenberg KE, Ukhun IA, Holstad SG, Jafri S, Uchida U, Zorumski CF, Yang J (1993) Partial cDNA cloning and NGF regulation of a rat 5-HT_3 receptor subunit. Neuroreport 5:121-124.

Jackson MB, Yakel JL (1995) The 5-HT_3 receptor channel. Ann Rev Physiol 57:447-468.

Jacob MH (1991) Acetylcholine receptor expression in developing chick ciliary ganglion neurons. J Neurosci 11:1701-1712.

Jacob MW, Berg DK (1983) The ultrastructural localization of α-bungarotoxin-binding sites in relation to synapses on chick ciliary ganglion neurons. J Neurosci 3:260-271.

Jacob MW, Berg DK, Lindstrom JM (1984) A shared antigenic determinant between the Electrophorus acetylcholine receptor and a synaptic component on chick ciliary ganglion neurons. Pro Natl Acad Sci USA 81:3223-3227.

Jacob M, Berg D (1987) Effects of preganglionic denervation and postganglionic axotomy on acetylcholine receptors in the chick ciliary ganglion. J Cell Biol 105:1847-1854.

Johns DC, Nuss HB, Marban E (1997) Suppression of neuronal and cardiac transient outward currents by viral gene transfer of dominant-negative Kv4.2 constructs. J Biol Chem 272:31598-31603.

Johnson D, Heinemann S (1995) Embryonic expression of the 5-HT_3 receptor subunit, 5-HT_3R-A, in the rat: an in situ hybridization study. Mol Cell Neurosci 6:122-133.

Johnson D, Heinemann SF (1995) Detection of 5-HT_3R-A, a 5-HT_3 receptor subunit in submucosal and myenteric ganglia of rat small intestine using in situ hybridization. Neurosci Lett 184:67-70.

Johnson PA, Miyanohara A, Levine F, Cahill T, FiredmanT (1992a) Cytotoxicity of replication-defective mutant of herpes simplex virus type 1. J Virol 66:2952-2965.

Johnson PA, Yoshida K, Gage FH, Friedmann T (1992b) Effects of gene transfer into cultured CNS neurons with a replication defective herpes simplex virus type 1 vector. Mol Brain Res 12:95-102.

Kammesheidt A, Kata K, Ken-Ichi I, Sumikawa K (1997) Adenovirus-mediated NMDA receptor knockouts in the rat hippocampal CA1 region. Neuroreport. 8:635-638.

Kandel ER, Schwartz JH, Jessel TM (1991) Principles of neurosicence, 3rd ed. New York, Elsevier.

Kaplitt MG, During MJ (1995) Transfer and expression of potentially therapeutic genes into the mammalian central nervous system in vivo using adeno-associated viral vectors. *In*: Kaplitt, MG and Loewy AR eds., "Viral vectors: gene therapy and neuroscience applications" Academic Press, San Diego, CA, pp193-210.

Karlin A, Akabas MH (1995) Toward a structural basis for the function of nicotinic acetylcholine receptors and their cousins. Neuron 15:1231-1244.

Kass RS, Davies MP (1996) The roles of ion channels in an inherited heart disease: molecular genetics of the long QT syndrome. Cardiovasc Res 32:443-454.

Kawa K (1994) Distribution and functional properties of 5-HT_3 receptors in the rat hippocampal dentate gyrus: a patch-clamp study. J Neurophysiol 71:1935-1947.

Keller SH, Lindstrom J, Taylor P (1996) Involvement of the chaperone protein calnexin and the acetylcholine receptor β-subunit in the assembly and cell surface expression of the receptor. J Biol Chem 271:22871-22877.

Koob GF (1992) Drugs of abuse: anatomy, pharmacology and function of reward pathways. Trends Pharmacol 13:177-184.

Krieg PA, Melton DA (1987) In vitro RNA synthesis with SP6 RNA polymerase. Methods Enzymol 155:397-415.

Kuhse J, Laube B, Magalei D, Betz H (1993) Assembly of the inhibitory glycine receptor: identification of amino acid sequence motifs governing subunit stoichiometry. Neuron 11:1049-1056.

Kwong AD, Frenkel N (1995) Biology of herpes simplex virus (HSV) defective viruses and development of the amplicon system. *In*: Kaplitt, MG and Loewy AR eds., "Viral vectors: gene therapy and neuroscience applications" Academic Press, San Diego, CA, pp193-210.

Laemmli, UK. Cleavage of structural proteins during the assembly of the head of bacteriophage T4. Nature 227:680-685.

Lake RA, Owen MJ (1991) Transfection of Chloramphenicol-acetyltransferase gene into eukaryotic cells using dietyl-aminoethyl (DEAE)-dextran. *In:* Murray, EJ ed., "Gene Transfer and Expression Protocols", Methods in Molecular Biology Vol 7, Humana Press, Clifton, NJ, pp 23-33.

Lamar E, Miller K, Patrick J (1990) Amplification of genomic sequences identifies a new gene, α6, in the nicotinic acetylcholine receptor gene family. Soc Neurosci Abstr 16:285.2.

Lambert JL, Peters JA, Hope AG (1995) 5-HT_3 receptors. *In:* North, RA ed., "Ligand- and voltage-gated ion channels", CRC Handbook of receptors and channels CRC Press Inc., Boca Raton, Florida, pp 177-211.

Landmesser L, Pilar G (1972) The onset and development of transmission in the chick ciliary ganglion. J Physiol 222:691-713.

Langley JN, Anderson HK (1892). The actions of nicotine on the ciliary ganglion and on endings of the third cranial nerve. J Physiol (London) 13:460-468.

Le Gal La Salle G, Robert JJ, Berrard, S, Vidoux V, Stratford-Perricaudet L, Perricaudet M, Mallet J (1993) An adenovirus vector for gene transfer into neurons and glia in the brain. Science 259:988-990.

Leib DA, Oliva PD (1993) Gene delivery into neurons: is herpes simplex virus the right tool for the job? Bioessays 15:547-554.

Léna C, Chaugeux JP (1997) Role of Ca^{2+} ions in nicotinic facilitations of $GABA_A$ release in mouse thalamus. J Neurosci 17:576-585.

Le Novère N, Changeux JP (1995) Molecular evolution of the nicotinic acetylcholine receptor: an example of multigene family in excitable cells. J Mol Evol 40:155-172.

Le Novère N, Changeux JP (1997). Website: http/www.pasteur.fr/units/neurobiol/

Levey MS, Brumwell CL, Dryer SE, Jacob M (1995) Innervation and target tissue interactions differentially regulate acetylcholine receptor subunit mRNA levels in developing neurons *in situ.* Neuron 14:153-162.

Levey MS, Jacob MH (1996) Changes in the regulatory effects of cell-cell interactions on neuronal AChR subunit transcript levels after synapse formation. J Neurosci 16:6878-6885.

Liljestrom P, Garoff H (1991) A new generation of animal cell expression vectors based on the Semliki forest virus replication. Biotechnology 9:1356-1361.

Lindstrom J, Anand R, Peng X, Gerzanich V, Wang F, Li Y (1995) Neuronal nicotinic receptor subtypes. Annals NY Acad Sci 757:100-116.

Lindstrom JM (1995) Nicotinic Acetylcholine Receptors. *In:* North, RA ed., "Ligand-and voltage-gated ion channels", CRC Handbook of receptors and channels CRC Press Inc., Boca Raton, Florida, pp 153-175.

Loring RH, Zigmond RE (1987) Ultrastructural distribution of 125I-toxin F-binding sites on chick ciliary ganglion neurons: synaptic localization of a toxin that blocks ganglionic nicotinic receptors. J Neurosci 7:2153-2162.

Loring RH, Sah DWY, Landis SC, Zigmond RE (1988) The ultrastructural distribution of putative nicotinic receptors on cultured neurons from the rat superior cervical ganglion. Neurosci 24:1071-1080.

Loring RH, Zigmond RE (1988) Characterization of neuronal nicotinic receptors by snake venom toxins. Trends Neurosci 11:73-78.

Lisovoski F, Akli S, Peltekian E, Vigne E, Haase G, Perricaudet M, Dreyfus P, Kahn A, Peschanski M (1997) Phenotypic alteration of astrocytes induced by ciliary neurotrophic factor in the intact adult brain, as revealed by adenovirus-mediated gene transfer. J Neurosci 17:7228-7236.

Listerud M, Brussard AB, Devay P, Colman DR, Role LW (1991) Functional contribution of neuronal AChR subunits revealed by antisense oligonucleotides. Science 254:1518-1521.

Litman P, Barg J, Rindzoonski L, Ginzburg I (1993) Subcellular localization of Tau mRNA in differentiating neuronal cell cultures: implications for neuronal polarity. Neuron 10:627-638.

Luetje CW, Wada K, Rogers S, Abramson SN, Tsuji K, Heinemann S, Patrick J (1990) Neurotoxins distinguish between different neuronal nicotinic acetylcholine receptor subunit combinations. J Neurochem 55:632-640.

Luetje CW, Patrick J (1991) Both α- and β-subunits contribute to the agonist sensitivity of neuronal nicotinic acetylcholine receptors. J Neurosci 11:837-845.

Lukas R (1995) Diversity and patterns of regulation of nicotinic receptor subtypes. Annals NY Acad Sci 757:153-168.

Mackett M (1991) Manipulating vaccinia virus vectors. *In:* Murray, EJ ed., "Gene Transfer and Expression Protocols", Methods in Molecular Biology Vol 7, Humana Press, Clifton, NJ, pp 129-146.

Mandelzys A, Cooper E, Verge VMK, Richardson PM (1990) Nerve growth factor induces functional nicotinic acetylcholine receptors on rat sensory neurons in culture. Neuroscience 37:523-530.

Mandelzys A, Cooper E (1992) Effects of ganglionic satellite cells and NGF on the expression of nicotinic acetylcholine currents by rat sensory neurons. J Neurophysiol 67:1213-1221.

Mandelzys A, Pié B, Deneris E, Cooper E (1994) The developmental increase in ACh current densities on rat sympathetic neurons correlates with changes in nicotinic ACh receptor α-subunit gene expression and occurs independent of innervation. J Neurosci 14:2357-2364.

Mandelzys A, De Koninck P, Cooper E (1995) Agonist and toxin sensitivities of ACh-evoked currents on neurons expressing multiple nicotinic ACh receptor subunits. J Neurophysiol 74:1212-1221.

Maricq A, Peterson A, Brake A, Myers R, Julius D (1991) Primary structure and functional expression of the $5HT_3$ receptor, a serotonin-gated ion channel. Science 254:432-437.

Margiotta JF, Berg DK, Dionne VE (1987) The properties and regulation of functional acetylcholine receptors on chick ciliary ganglion neurons. J Neurosci 7:3612-3622.

Margiotta JF, Gurantz D (1989) Changes in the number, function, and regulation of nicotinic acetylcholine receptors during neuronal development. Dev Biol 135:326-339.

Marks MJ, Pauly JR, Gross SD, Deneris ES, Hermana-Borgmeyer I, Heinemann SF, Collins AC (1992) Nicotine-binding and nicotinic receptor subunit RNA after chronic nicotine treatment. J Neurosci 12:2765-2784.

Martin D, Schmidt R, DiStefano P, Lowry O, Carter J, Johnson EM (1988) Inhibitors of protein synthesis and RNA synthesis prevent neuronal death caused by nerve growth factor deprivation. J Cell Biol 106:829-844.

McDonough J, Deneris E (1997) β43': an enhancer displaying neural-restricted activity is located in the 3'-untranslated exon of the rat nicotinic acetylcholine receptor β4 gene. J Neurosci 17:2273-2283.

McEachern AE, Jacob MH, Berg DK (1989) Differential effects of nerve transection on the ACh and GABA receptors of chick ciliary ganglion neurons. J Neurosci 9:3899-3907.

McFarlane S, Cooper E (1992) Postnatal development of voltage-gated K currents on rat sympathetic neurons. J Neurosci 67:1291-1300.

McFarlane S, Cooper E (1993) Extrinsic factors influence the expression of voltage-gated K currents on neonatal rat sympathetic neurons. J Neurosci 13:2591-2600.

McGehee DS, Heath MJS, Gelber S, Devay P, Role LW (1995) Nicotinic enhancement of fast excitatory synaptic transmission in CNS by presynaptic receptors. Science 269: 1692-1696.

McGehee DS, Role LW (1995) Physiological diversity of nicotinic acetylcholine receptors expressed by vertebrate neurons. Ann Rev Physiol 57:521-546.

Mei N (1970) Disposition anatomique et propriétés électrophysiologiques des neurones sensitifs vagaux chez le chat. Exp Brain Res 11: 465-479.

Meunier-Durmort C, Picard R, Ragot T, Perricaudet M, Hanique B, Forest C (1997) Mechanisms of adenovirus improvement of cationic liposome-mediated gene transfer. Biochi Biophys Acta 1330:8-16.

Milton NGN, Bessis A, Changeux JP, Latchman DS (1995) The neuronal nicotinic acetylcholine receptor α2 subunit gene promoter is activated by the Brn-3b POU family transcription factor and not by Brn-3a or Brn-3c. J Biol Chem 270:15143-15147.

Milton NG, Bessis A, Changeux JP, Latchman DS (1996) Differential regulation of neuronal nicotinic acetylcholine receptor subunit gene promoters by Brn-3 POU family of transcription factors. Biochemical Journal 317:419-423.

Miquel M-C, Emerit M, Gingrich J, Nosjean A, Hamon M, El Mestikawy S (1995) Developmental changes in the differential expression of two serotonin 5-HT_3 receptor splice variants in the rat. J Neurochem 65:475-483.

Miyake A, Mochizuki S, Takemoto Y, and Akuzawa S (1995) Molecular cloning of human 5-hydroxytryapmine$_3$ receptor: heterogeneity in distribution and function among species. Mol Pharmacol 48:407-416.

Morales M, Battenberg E, de Lecea L, Sanna PP, Bloom FE (1996) Cellular and subcellular immunolocalization of the type3 serotonin receptor in the rat central nervous system. Mol Brain Res 36:251-260.

Morgenstern JP, Land H (1991) Choice and manipulation of retroviral vectors. *In:* Murray, EJ ed., "Gene Transfer and Expression Protocols", Methods in Molecular Biology Vol 7, Humana Press, Clifton, NJ, pp 181-208.

Moriyoshi K, Richards L, Akazawa C, O'Leary DDM, Nakanishi S (1996) Labeling neural cells using adenoviral gene transfer of membrane-targeted GFP. Neuron 16:255-260.

Morley BJ, Happes HK (1995) An in situ hybridization study of mRNA expression for α5 and α6 in the nicotinic acetylcholine receptor gene family. Soc Neurosci Abstr 21:527.15.

Moss B (1996) Genetically engineered poxviruses for recombinant gene expression, vaccination, and safety. Proc Natl Acad Sci USA 93:11341-11348.

Murray N, Zheng YC, Mandel G, Brehm P, Bolinger R, Reuer Q, Kullberg R (1995) A single site on the ε sbunit is responsible for the change in ACh receptor channel conductance during skeletal muscle development. Neuron 14:865-870.

Neve RL (1993) Adenovirus vectors enter the brain. Trends Neurosci 16:251-253.

Nichols RA, Mollard P (1996) Direct observation of serotonin 5-HT3 receptor induced increases in calcium levels in individual brain nerve terminals. J Neurochem 67:581-592.

Noda M, Takahashi H, Tanabe T, Toyosato M, Furutani Y, Hirose T, Asai M, Inayama S, Miyata T, Numa S (1982) Primary structure of the α-subunit precursor of *Torpedo californica* acetylcholine receptor deduced from cDNA sequence. Nature 299;793-797.

Noda M, Takahashi H, Tanabe T, Toyosato M, Kikyotani S, Hirose T, Asai M, Inayama S, Takshima H, Miyata T, Numa S (1983a) Primary structure of β- and δ-subunits precursors of *Torpedo californica* acetylcholine receptor deduced from cDNA sequences. Nature 301:251-255.

Noda M, Takahashi H, Tanabe T, Toyosato M, Kikyotani S, Furutani Y, Hirose T, Takshima H, Inayama S, Miyata T, Numa S (1983b) Structural homology of *Torpedo californica* acetylcholine receptor subunits. Nature 302:528-532.

Okayama H, Chen C (1991) Calcium phosphate mediated gene transfer into established cell lines. *In:* Murray, EJ ed., "Gene Transfer and Expression Protocols", Methods in Molecular Biology Vol 7, Humana Press, Clifton, NJ, pp 15-21.

Ohuoha DC, Knable MB, Wolf SS, Kleinmann JE, Hyde TM (1994) The subnuclear distribution of 5-HT_3 receptors in the human nucleus of the solitary tract and other structures of the caudal medullla. Brain Res 637:222-226.

Orr-Urtreger A, Göldner FM, Saeki M, Lorenzo I, Goldberg L, De Biasi M, Dani JA, Patrick JW, Beaudet AR (1997) Mice deficient in the α7 neuronal nicotinic acetylcholine receptor lack α-bungarotoxin binding sites and hippocampal fast nicotinic currents. J Neurosci 17:9165-9171.

Ortells M, Lunt G (1995) The transmembrane region of the nicotinic acetylcholine receptor: is it a all-helix bundle? Receptors Channels2:53-59.

Ortells M, Lunt G (1995) Evolutionary history of the ligand-gated ion channel superfamily of receptors. Trends in Neurosci. 18: 121-127.

Ou WJ, Cameron PH, Thomas DY, Bergeron JJM (1993) Association of folding intermediates of glycoproteins with calnexin during protein maturation. Nature 364:771-776.

Parks DS, Levine B, Ferrari G, Greene LA (1997) Cyclin dependent kinase inhibitors and dominant negative cyclin dependent kinase 4 and 6 promote survival of NGF-deprived sympathetic neurons. J Neurosci 17:8975-8983.

Paton WDM, Zaimis EJ (1952) The methonium compounds. Pharmacol Rev 4:219-253.

Patrick J, Stallcup B (1977a) α-Bungarotoxin binding and cholinergic receptor function on a sympathetic nerve line. J Biol Chem 252:8629-8633.

Patrick J, Stallcup B (1977b) Immunological distinction between acetylcholine receptor and the α-bungarotoxin-binding component on sympathetic neurons. Proc Natl Acad Sci USA 74:4689-46-92.

Peng X, Gerzanich V, Anad R, Whiting P, Lindstrom J (1994) Nicotine-induced upregulation of neuronal nicotinic receptors results from a decrease in the rate of turnover. Mol Pharmacol 46:523-530.

Peroutka SJ (1995) 5-HT receptors: past, present and future. Trends Neurosci 18:68-69.

Peters JA, Malone HM, Lambert JJ (1993) An electrophysiological investigation of the properties of 5-HT_3 receptors of rabbit nodose ganglion neurones in culture. Br J Pharmacol 110:665-676.

Philips MI (1997) Antisense inhibition and adeno-associated viral vector delivery for reducing hypertension. Hypertension 29:177-187.

Picciotto MR, Zoli M, Rimondini R, Léna C, Marubio LM, Pich EM, Fuxe K, Changeux JP (1998) Acetylcholine receptors containing the β subunit are involved in the reinforcing properties of nicotine. Nature 391:173-177.

Portalier P, Vigier D (1979) Localization of aortic cells in the nodose ganglion by HRP retrograde transport in the cat. Neurosci Let 11:7.

Pratt G, Bowery N (1989) The 5-HT3 receptor ligand [3H] BRL 43694 bind to presynaptic sites in the nucleus tractus solitarius of the rat. Neuropharmacol 28:1367-1376.

Purves, D. and Lichtman, J. (1984) Principles of Neural Development Sinaur Associates, Inc. Sunderland MA, USA.

Raftery MA, Hunkapiller M, Strader C, Hood LE (1980) Acetylcholine receptor: complex of homologous subunits. Science 208:1454.

Rajendra S, Lynch JW, Schofield PR (1997) The glycine receptor. Pharmacol Ther. 73:121-146.

Raivich G, Hellweg R, Kreutzberg GW (1991) NGF receptor-mediated reduction in axonal NGF uptake and retrograde transport following sciatic nerve injury and during regeneration. Neuron 7:151-164.

Ramirez-Latorre J, Yu CR, Qu X, Perin F, Karlin A, Role L (1996) Functional contribution of α5 subunit to neuronal nicotinic acetylcholine receptor channel. Nature 380:347-351.

Reiner A, Brecha NC, Karten HJ (1982) Basal ganglia pathways to the tectum: the afferent and efferent connections of the lateral spiriform nucleus of pigeon. J Comp Neurol 208:16-36.

Roerig B, Nelson DA, Katz LC (1997) Fast synaptic signaling by nicotinic acetylcholine and serotonin 5-HT_3 receptors in developing visual cortex. J Neurosci 17:8353-8362.

Roizman B, Jenkins F (1985) Genetic engineering of novel genomes of large DNA viruses. Science 229:1208-1214.

Role LW, Berg DK (1996) Nicotinic receptors in the development and modulation of CNS synapses. Neuron 16:1077-1085.

Rosenberg M, Séguéla P, Cooper E (1994) Developmental expression of 5-HT_3 receptor mRNA in rat sympathetic and sensory neurons. Soc for Neurosci abstract 474.2.

Ross AF, Green WN, Hartman DS, Claudio T (1991) Efficiency of acetylcholine receptor subunit assembly and its regulation by cAMP. J Cell Biol 113:623-636.

Sambrook J, Fritsch EF, Maniatis T (1989) *Molecular Cloning: A laboratory Manual.* Cold Spring Harbour Laboratory, 2nd ed.

Sanders-Bush E, Mayer S (1996) 5-hydroxytryptamine (serotonin) receptor agonists and antagonists. *In:* Hardmann J, Limbird L, Molinoff P, Ruddon R, Goodman A, Gilman A, eds, "The pharmacological basis of therapeutics", 9th ed, McGraw Hill, New York, pp 249-257.

Sargent P (1993) The diversity of neuronal nicotinic acetylcholine receptors. Ann Rev Neurosci 16:403-443.

Schiedner G, Morral N, Parks RJ, Wu Y, Kooprmans SC, Langston C, Graham FL, Beaudet AL, Kochanek S (1998) Genomic DNA transfer with a high-capacity adenovirus vector results in improved *in vivo* gene expression and decreased toxicity. Nature Genetics 18:180-183.

Schuetze SM, Role LW (1987) Developmental regulation of nicotinic acetylcholine receptors. Ann Rev Neurosci 10:403:457.

Sepùlveda MI, Lummis SCR (1994) 5-HT_3 agonists can distinguish cloned 5-HT_3 receptors from NCB20 and NG108-15 cell lines. Br J Pharmacol 112:316P.

Séguéla P, Wadiche J, Dineley-Miller K, Dani J, Patrick J (1993) Molecular cloning, functional properties and distribution of rat brain α7: a nicotinic cation channel highly permeable to calcium. J Neurosci. 13:596-604.

Schoepfer R, Conroy W, Whiting P, Gore M, Lindstrom J (1990) Brain α-bungarotoxin binding protein cDNAs and mAbs reveal subtypes of this branch of the ligand-gated ion channel superfamily. Neuron 5:35-48.

Shenk T (1995) Group C adenoviruses as vectors for gene therapy. *In*: Kaplitt, MG and Loewy AR eds., "Viral vectors: gene therapy and neuroscience applications" Academic Press, San Diego, CA, pp 43-54.

Sivilotti L, Colquhoun D (1995) Acetylcholine receptor: too many channels, too few functions. Science 269:1681-1682.

Sivilotti LG, McNeil DK, Lewis TM, Nassar MA, Schoepfer R, Colquhoun D (1997) Recombinant nicotinic receptors, expressed in *Xenopus* oocytes, do not resemble native rat sympathetic ganglion receptors in single-channel behavior. J Physiol London 500.1:123-138.

Slack RS, Belliveau DJ, Rosenberg M, Atwal J, Lochmuller H, Aloyz R, Haghighi A, Lach B, Seth P, Cooper E, Miller FD (1996) Adenovirus-mediated gene transfer of the tumor suppressor, p53, induces apoptosis in postmitotic neurons. J Cell Biol 135:1085-1096.

Smith GM, Berry RL, Yang J, Tanelian D (1997) Electrophysiological analysis of dorsal root ganglion neurons pre- and post-coexpression of green fluorescent protein and functional 5-HT3 receptor. J Neurophyiol 77:3115-3121.

Smith MA, Stolberg J, Lindstrom JM, Berg DK (1985) Characterization of a component in chick ciliary ganglia that cross reacts with monoclonal antibodies in muscle and electric organ acetylcholine receptors J Neurosci 5:2726-27-31.

Smith MA, Margiotta JF, Franco A, Lindstrom JM, Berg DK (1986) Cholinergic modulation of an acetylcholine receptor-like antigen on the surface of chick ciliary ganglion neurons in cell culture. J Neurosci 6;946-953.

Smolen A, Raisman G (1980) Synapse formation in the rat superior cervical ganglion during normal development and after neonatal deafferentiation. Brain Res 181:315-323.

Sorenson EM, Parkinson D, Dahl JL, Chiapanelli VA (1989) Immunohistochemical localization of choline acetyltransferase in the chicken mesencephalon. J Comp Neurol 281:641657.

Spaete R, Frenkel N (1985) The herpes simplex virus amplicon: analyses of cis-acting replication functions. Proc Natl Acad Sci USA 82:694-698.

Spector PS, Curm ME, Zou A, Keating MT, Sanguinetti MC (1996) Fast inactivation causes rectification of the IKr channel. J Gen Physiol 107 611-619.

Spencer SC (1991) Electroporation technique of DNA transfection. *In:* Murray, EJ ed., "Gene Transfer and Expression Protocols", Methods in Molecular Biology Vol 7, Humana Press, Clifton, NJ, pp 45-52.

Sprengel R, Seeburg PH (1995) Ionotropic Glutamate Receptors. *In:* North, RA ed., "Ligand-and voltage-gated ion channels", CRC Handbook of receptors and channels CRC Press Inc., Boca Raton, Florida, pp 213-263.

Stevenson SC, Rollence M, Marshall-Neff J, McClelland A (1997) Selective targeting of human cells by a chimeric adenovirus vector containing a modified fiber protein. J Virol 71:4782-4790.

Stollberg J, Berg DK (1987) Neuronal nicotinic acetylcholine receptors: fate of surface and internal pools in cell culture. J Neurosci 7:1809-1815.

Sugita S, Shen KZ, North RA (1992) 5-hydroxytrypamine is a fast excitatory transmitter at 5-HT_3 receptors in the rat amygdala. Neuron 8:199-203.

Tecott LH, Maricq AV, Julius D (1993) Nervous system distribution of the serotonin 5-HT3 receptor mRNA. Proc Natl Acad Sci USA 90:1430-1434.

Tecott L, Shtrom S, Julius D (1995) Expression of a serotonin-gated ion channel in embryonic neural and nonneural tissues. Mol Cell Neurosci 6:43-55.

Tomasec P, Bain D, Castro M, Preston CM, Lowenstein PR (1996) Herpes simplex virus temperature sensitive mutant tsK as a vector for neuronal gene transfer. *In:* Lowenstein PR, Enquist LW eds. "Protocols for gene transfer in neuroscience: towards gene therapy of neurological disorders" Wiley, New York, pp 169-186.

Trouslard J, Marsh SJ, Brown DA (1993) Calcium entry through nicotinic and calcium channels in cultured rat superior cervical ganglion cells. J Physiol (London) 468: 53-71.

Tyers MB (1992) Pharmacology and preclinical antiemetic properties of ondansetron. Seminars Oncology 19(4):1-8.

Tyndale RF, Olsen RW, Tobin AJ (1995) $GABA_A$ receptors. *In:* North, RA ed. (1994) "Ligand-and voltage-gated ion channels", CRC Handbook of receptors and channels, CRC Press Inc., Boca Raton, Florida, pp 265-290.

Tzartos SJ, Rand DE, Einarson BL, Lindstrom JM (1981) Mapping of surface structure of Electrophorus acetylcholine receptors using monoclonal antibodies. J Biol Chem 256:8635-8645.

Ullian EM, Sargent PB (1995) Pronounced cellular diversity and extrasynaptic location of nicotinic acetylcholine receptor subunit immunoreactivities in the chicken pretectum. J Neurosci 15:7012-7023.

Ullian EM, McIntosh JM, Sargent PB (1997) Rapid synaptic transmission in the avian ciliary ganglion is mediated by two distinct classes of nicotinic receptors. J Neurosci 17:7210-7219.

Unwin N (1989) The structure of ion channels in membranes of excitable cells. Neuron 3:655-676.

Unwin N (1993a) Neurotransmitter action: opening of ligand-gated ion channels. Cell 72 /Neuron 10 (Review Supplement) 31-41.

Unwin N (1993b) Nicotinic acetylcholine receptor at 9 A Resolution. J Mol Biol 229:1101-1121.

Unwin N (1995) Acetylcholine receptor channel imaged in the open state. Nature 373:37-43.

Vanier C, Triller A (1997) Biology of the postsynaptic glycine receptor. Int Rev Cytol 176:201-244.

Vernallis AN, Conroy WG, Berg DK (1993) Neurons assemble acetylcholine receptors with as many as three kinds of subunits while maintaining subunit segregation among receptor subtypes. Neuron 10: 451-464.

Verrall S, Hall ZW (1992) The N-terminal domains of acetylcholine receptor subunits contain recognition signals for the initial steps of receptor assembly. Cell 68:23-31.

Vijayaraghavan S, Schmid HA, Halvorsen SW, Berg DK (1990) Cyclic AMP-dependent phosphorylation of a neuronal acetylcholine receptor α-type subunit. J Neurosci 10:3255-3262.

Voyvodic J (1987) Development and regulation of dendrites in the rat superior cervical ganglion. J Neurosci 7:904-912.

Wada E, Wada K, Boulter J, Deneris E, Heinemann S, Patrick J, Swanson LW (1989) Distribution of alpha2, alpha3, alpha4, and beta2 neuronal nicotinic receptor subunit mRNAs in the central nervous system: a hybridization histochemical study in the rat. J Comp Neurol 284:314-335.

Wallis DI, North RA (1978) The action of 5-hydroxytryptamine on single neurones of the rabbit superior cervical ganglion. Neuropharm 17:1023-1028.

Watson JD, Gilman M, Witkowski J, Zoller M (1992) Recombinant DNA, 2nd ed., Scientific American Books, New York, NY, chapter 12, pp 213-234.

Wang ZZ, Hardy SF, Hall ZW (1996a) Membrane tethering enables an extracellular domain of the acetylcholine receptor α subunit to form a heterodimeric-ligand binding site. J Cell Biol 135:809-817.

Wang F, Gerzanich V, Wells, GB, Anand R, Peng X, Keyser K, Linstrom J (1996b) Assembly of human neuronal nicotinic receptor α5 subunits with α3, β2, and β4 subunits. J Biol Chem 271:17656-17665.

Wagner RW (1994) Gene inhibition using oligonucleotides. Nature 372:333-335.

Wei MX, Tamiya T, Breakfield XO, Chiocca EA (1995) Virus vector-mediated transfer of drug-sensitivity genes for experimental brain tumor therapy. *In*: Kaplitt, MG and Loewy AR eds., "Viral vectors: gene therapy and neuroscience applications" Academic Press, San Diego, CA, pp 239-257.

Whiting PJ, Schoepfer R, Conroy WG, Gore MJ, Keyser KT, Shimasaki S, Esch F, Lindstrom JM (1991) Expression of nicotinic acetylcholine receptor subtypes in brain and retina. Mol Brain Res 10:61-70.

Wilson Horch HL, Sargent PB (1995) Perisynaptic distribution of multiple classes of nicotinic acetylcholine receptors on neurons in the chicken ciliary neurons. J Neurosci 15:7778-7795.

Wilson JM (1995) Gene therapy for cystic fibrosis: challenges and future directions. J Clin Invest 96:2547-2554.

Wirtshafter D (1981) The role of interpenduncular connections with the tegumentum in avoidance learning. Physiol Behav 26:985-989.

Wood MJA, Charlton HM, Wood KJ, Kajiwara K, Byrnes AP (1996) Immune responses to adenovirus vectors in the nervous system. Trends in Neurosci 19:497-501.

Wonnacott S, Irons J, Rapier C, Thorne B, Lunt GG (1989) Presynaptic modulation of transmitter release by nicotinic receptors. Prog Brain Res 79:157-163.

Wonnacott S (1997) Presynaptic nicotinic ACh receptors. Trends Neurosci 20:92-98.

Xiao X, Li J, McCown TJ, Samulski RJ (1997) Gene transfer by adeno-associated virus vectors into the central nervous system. Exp Neurol 144:113-124.

Xu H, Federoff HJ, Marogos J, Parada L, Kessle J (1994) Viral transduction of trkA into cultured nodose and spinal motor neurons conveys NGF responsiveness. Dev Biol 163:152-161.

Yakel J, Jackson M (1988) 5-HT_3 receptors mediate rapid responses in cultured hippocampus and a clonal cell line. Neuron 1:615-621.

Yang J, Mathie A, Hille B (1992) 5-HT_3 receptor channels in dissociated rat superior cervical ganglion neurons. J Physiol (Lond) 448:237-256.

Yang X, McDonough J, Fyodorov D, Morris M, Wang F, Deneris ES (1994) Characterization of an acetylcholine receptor α gene promoter and its activation by the POU domain factor SCIP/Tst-1. J Biol Chem 269:10252-10264.

Yang X, Fyodorov D, Deneris ES (1995) Transcriptional analysis of acetylcholine receptor α3 gene promoter motifs that bind Sp1 and AP2. J Biol Chem 270:8514-8520.

Yang X, Kuo Y, Devay P, Yu C, Role L (1998) A cysteine-rich isoform of neuregulin controls the level of expression of neuronal nicotinic receptor channels during synaptogenesis. Neuron 20: 255-270.

Yoshioka M, Goda Y, Ikeda T, Togashi H, Ushiki T, Saito H (1994) Involvement of 5-HT_3 receptors in the initiation of pharyngeal reflex. Am J Physiol 266:R1652-R1658.

Zhang L, Oz M, Weight F (1995) Potentiation of 5-HT_3 receptor-mediated responses by protein kinase C activation. Neuroreport 6:1336-1340.

Zhang M, Wang YT, Vyas DM, Neuman RS, Bieger D (1993) Nicotinic cholinoceptor-mediated excitatory postsynaptic potentials in rat nucleus amibiguus. Exp Brain Res 96:83-88.

Zhang ZW, Vijayaraghavan S, Berg DK (1994) Neuronal nicotinic acetylcholine receptors that bind α-bungarotoxin with high affinity function as ligand-gated ion channels. Neurons 12:167-177.

Zhang ZW, Coggan JS, Berg DK (1996) Synaptic currents generated by neuronal acetylcholine receptors sensitive to alpha-bungarotoxin. Neuron 17:1231-1240.

Zito K, Fetter, RD, Goodman CS, Isacoff, EY. Synaptic clustering of Fascilin II and Shaker: essential targeting sequnes and role of Dlg. Neuron 19:1007-1016.